AFWAL-TR-84-2014

12

IMPROVEMENT OF THE CORROSION RESISTANCE OF TURBINE ENGINE BEARINGS

J. H. Mohn
H. M. Hodgens II
H. E. Munson*
W. E. Poole

United Technologies Corporation
Pratt & Whitney Aircraft
Engineering Division
P.O. Box 2691, West Palm Beach, Florida 33402

* TRW, Bearings Division, Jamestown, New York

February 1984

Interim Report for Period August 1981 — July 1983

Aero Propulsion Laboratory
Air Force Wright Aeronautical Laboratories
Air Force Systems Command
Wright-Patterson AFB, Ohio 45433

NOTICE

When Government drawings, specifications, or other data are used for any purpose other than in connection with a definitely related Government procurement operation, the United States Government thereby incurs no responsibility nor any obligation whatsoever; and the fact that the government may have formulated, furnished, or in any way supplied the said drawings, specifications, or other data, is not to be regarded by implication or otherwise as in any manner licensing the holder or any other person or corporation, or conveying any rights or permission to manufacture use, or sell any patented invention that may in any way be related thereto.

This report has been reviewed by the Office of Public Affairs (ASD/PA) and is releasable to the National Technical Information Service (NTIS). At NTIS, it will be available to the general public, including foreign nations.

This technical report has been reviewed and is approved for publication.

John W. Artuso

JOHN W. ARTUSO
Project Engineer

Howard F. Jones

HOWARD F. JONES
Chief, Lubrication Branch
Fuels and Lubrication Division

FOR THE COMMANDER

Robert D. Sherrill

ROBERT D. SHERRILL, Chief,
Fuels and Lubrication Division
Aero Propulsion Laboratory

3531C

UNCLASSIFIED

SECURITY CLASSIFICATION OF THIS PAGE (When Data Entered)

REPORT DOCUMENTATION PAGE		READ INSTRUCTIONS BEFORE COMPLETING FORM
1. REPORT NUMBER AFWAL-TR-84-2014	2. GOVT ACCESSION NO. A144430	3. RECIPIENT'S CATALOG NUMBER
4. TITLE (and Subtitle) Improvement of the Corrosion Resistance of Turbine Engine Bearings		5. TYPE OF REPORT & PERIOD COVERED Interim Report for Period August 1981 — July 1983
		6. PERFORMING ORG. REPORT NUMBER P&WA/GPD/FR-17952
7. AUTHOR(s) J. H. Mohn H. E. Munson* W. E. Poole H. M. Hodgens II *TRW Bearings Div.		8. CONTRACT OR GRANT NUMBER(s) F33615-81-C-2023
9. PERFORMING ORGANIZATION NAME AND ADDRESS United Technologies Corporation Pratt & Whitney Aircraft Engineering Division P.O. Box 2691, West Palm Beach, FL 33402		10. PROGRAM ELEMENT, PROJECT, TASK AREA & WORK UNIT NUMBERS 3048-06-12
11. CONTROLLING OFFICE NAME AND ADDRESS Aero Propulsion Laboratory (POSL) AF Wright Aeronautical Laboratories (AFSC) Wright-Patterson AFB, Ohio 45433		12. REPORT DATE February 1984
		13. NUMBER OF PAGES 163
14. MONITORING AGENCY NAME & ADDRESS(if different from Controlling Office)		15. SECURITY CLASS. (of this report) Unclassified
		15a. DECLASSIFICATION/DOWNGRADING SCHEDULE

16. DISTRIBUTION STATEMENT (of this Report)

Approved for public release; distribution unlimited

17. DISTRIBUTION STATEMENT (of the abstract entered in Block 20, if different from Report)

18. SUPPLEMENTARY NOTES

19. KEY WORDS (Continue on reverse side if necessary and identify by block number)

Corrosion Resistance Test	M50	Nickel Sputter Coating
Wear Resistance Test	CRB7	Corrosion Resistant Bearings
Rolling Contact Fatigue Test	MRC2001	Corrosion Resistant Alloys
Hot Hardness Test	RSR565	Corrosion Resistant Coatings
Rolling Contact Bearings	Armoloy	Corrosion Resistant Surface Treatments

20. ABSTRACT (Continue on reverse side if necessary and identify by block number)

20. Abstract

This technical report encompasses the work accomplished in the first phase of a two-phase program aimed at developing an alternate material, fabrication technique, or material treatment for turbine engine mainshaft bearings with improved corrosion resistance compared to state of the art VIM-VAR M50.

DD FORM 1 JAN 73 1473 EDITION OF 1 NOV 65 IS OBSOLETE
S/N 0102-014-6601

UNCLASSIFIED

SECURITY CLASSIFICATION OF THIS PAGE (When Data Entered)

During Phase I, five corrosion-resistant bearing candidates (armoloy-coated M50, nickel sputter-coated M50, wrought CRB7, RSR565 and MRC2001) identified as the most promising were subjected to rolling contact fatigue, corrosion, hot hardness and wear screening tests. The phase concluded with selection of MCR2001 as the single most promising candidate for full-scale bearing fabrication and testing. In Phase II that candidate will be subjected to further full-scale bearing life and performance tests and a corrosion-resistant verification test.

FOREWORD

This interim technical report describes exploratory development work performed by the Pratt & Whitney Engineering Division under United States Air Force (USAF) Contract F33615-81-C-2023, improvement of the Corrosion Resistance of Turbine Engine Bearings. P&WA was assisted in this effort by TRW Bearings Division of TRW, Inc. The report covers the period from August 1981 to July 1983.

This program is sponsored by the Aero Propulsion Laboratory of the Air Force Wright Aeronautical Laboratories (AFWAL), Wright-Patterson Air Force Base, Ohio 45433 under project 3048, "Fuels, Lubrication and Fire Protection," Task 304806, "Aerospace Lubrication," work unit 30480612, "Improvement of the Corrosion Resistance of Turbine Engine Bearings." Mr. J. W. Artuso is the USAF AFWAL/POSL Project Engineer. The Pratt & Whitney Program Manager and Principal Investigator are J. H. Mohn and W. E. Poole, respectively. Test specimen preparation and material testing was conducted at TRW Bearings Division under the direction of Mr. A. T. Galbato, Manager of Research and Development.

This document is submitted in compliance with CLIN 0002 and CDRL Sequence Number 5.

Appreciation is extended to the following for their valuable assistance in this program: P. Allard (P&WA), J. W. Broch (P&WA), J. N. Fleck (TRW), B. McCoy (TRW), J. R. Miner (P&WA), D. Popgoshev (NAPC), and R. F. Spitzer (TRW).

4116C

TABLE OF CONTENTS

LIST OF ILLUSTRATIONS

4206C

LIST OF ILLUSTRATIONS (Continued)

4206C

LIST OF ILLUSTRATIONS (Continued)

LIST OF ILLUSTRATIONS (Continued)

4206C

LIST OF ILLUSTRATIONS (Continued)

4206C

LIST OF ILLUSTRATIONS (Continued)

LIST OF ILLUSTRATIONS (Continued)

LIST OF TABLES

LIST OF TABLES (Continued)

SECTION I

INTRODUCTION AND SUMMARY

The objective of this "Improvement of the Corrosion Resistance of Turbine Engine Bearings Program" is to provide a bearing which is significantly more corrosion resistant than VIM-VAR (vacuum induction melt, vacuum arc remelt) M50 state of the art bearings.

Improved bearing corrosion resistance can be achieved with either the use of a new corrosion resistant alloy, or by surface treating, or coating state of the art M50 with a protective covering. This 37-month, two-phase program will investigate all three methods: alloys, coatings and surface treatments. In Phase I, appropriate bearing materials, surface treatments, and coatings were identified. Screening tests were performed on the most promising candidates. The single most promising candidate was selected for full-scale bearing fabrication and testing to be accomplished in Phase II.

The Phase I effort was broken into five tasks which will be discussed in detail in this report. Task I began with a study of the corrosion mechanism which was a continuation of an ongoing effort at P&WA. In Task II, 17 candidates with potential for improving bearing corrosion resistance were identified for consideration. The 17 candidates included corrosion resistant alloys such as CRB7 (AMS5900) and BG42 (AMS5749), coatings such as the proprietary chrome plating process called Armoloy, and surface treatments such as nickel sputter-coated M50. Of these, the five most promising were selected based on available data and perceived material properties. The five highest potential candidates were Armoloy-coated M50, nickel sputter-coated M50, wrought CRB7 and powder metallurgy RSR565 and MRC2001. Task III ranked the five candidates based on rolling contact fatigue and corrosion resistance tests. From these test results, the three best candidates, Armoloy-coated M50, CRB7 and MRC2001 were selected for further evaluation. In Task IV, these three candidates were evaluated for wear resistance and hot hardness characteristics. Based on the property test results and criteria established in Task II, the most promising candidate MRC2001 was selected in Task V for full-scale bearing development and testing.

Phase II which will be included in the final report will consist of Task VI through IX. Task VI will consist of bearing fabrication. Twenty 35 millimeter bore size MRC207S endurance test bearings will be fabricated from the MRC2001 material and baseline VIM-VAR M50. Full engine size MRC2001 demonstration bearings will be fabricated. These performance demonstration bearings will duplicate the in-service 110 millimeter size TF30 No. 4 high-rotor thrust bearing which is the same geometry as the P&WA Joint Technology Demonstrator Engine (JTDE) No. 3 high-rotor thrust bearing. Bearing rolling contact fatigue (RCF) life tests will be conducted in Task VII. Task VIII will evaluate the performance characteristics of the full-scale bearing in a rig at 16,000 rpm (1.76 million DN*) and other conditions simulating actual engine operation. Although the speed exceeds normal TF30 high rotor operation, the testing will be used as partial substantiation for Bill-of-Material approval of the MRC2001, provided satisfactory RCF and performance are demonstrated. The used endurance test bearings will be subjected to corrosion tests in Task IX, using various oil formulations to be supplied by the USAF. The purpose of these tests is to provide confirmation that improved corrosion resistance will be retained even after extensive operation.

*DN = Bore diameter in millimeters × rpm

4145C

SECTION II

TECHNICAL DISCUSSION

A. BACKGROUND

Current engine bearings have proven to be reliable and durable but are often rejected for further use and discarded upon engine overhaul inspection long before their durability limits have been reached. This is due to environmental effects which degrade the bearing condition. Corrosion has been found to be the major cause of this premature bearing rejection (References 1 and 2). The expense and increased bearing usage caused by these rejections is unacceptable due to escalating labor and material costs and the increasing manufacturing lead time required to meet the higher overall bearing demand.

Current turbine engine bearings are made from AISI M50 steel. This material, originally developed as a tool steel, was selected for turbine engine bearing use because of its good rolling contact fatigue life and high hot hardness. In its current form, VIM-VAR M50 performs well but is sensitive to corrosion. The corrosion problem can be addressed in two ways: (1) development of corrosion resistant bearings or (2) development of corrosion inhibitors for lubrication systems and storage preservatives. Two recent investigations have addressed corrosion inhibitors for lubrication systems (References 3 and 4). The goal of the "Improvement of Corrosion Resistance of Turbine Engine Bearings" program is to provide a bearing which is significantly more corrosion resistant than M50 state of the art bearings.

B. CORROSION INVESTIGATION

1. Technical Approach

Corrosion is the most significant cause of gas turbine engine bearing field service rejection. Bearings rejected for corrosion have not expended their theoretical fatigue life. This effective reduction in bearing life results in higher maintenance costs associated with the inspection, repair and premature replacement of bearings.

The purpose of the corrosion mechanism investigation was to determine:

a) The requisite conditions for the corrosion of stored and service bearings
b) The main sources of corrosion contaminants
c) The predominant corrosion mechanism.

During the corrosion investigation, representative samples from bearings rejected from both storage and service environments for corrosion were studied. The rejected bearings were analyzed for the morphology of the corrosive attack and for the chemical species present in the corrosion products. Bearing preservatives and used engine oils were also analyzed for contaminants that might cause or accelerate corrosion of the various bearing materials.

The possibility of corrosion by galvanic attack was also explored. A galvanic cell could greatly increase the rate of corrosion. It consists of two dissimilar metals immersed in a conductive solution. To address this possibility, the galvanic potential of silver M50 and silver AISI 4340 couples in an aqueous sodium chloride solution were measured and the bearing environments were analyzed for reactive chemical species which readily dissociate in water solution.

Accelerated corrosion tests of bearing materials in contaminated oils were also conducted to support hypotheses generated during the investigation.

2. Analyses of Corroded Bearings

Representative storage and service corrosion-rejected turbine engine bearings from two advanced turbofan engine types in the current USAF inventory were selected as candidates for study. A wide sampling of bearings from storage was possible due to a related P&WA study which was in process at the time of this investigation. Conversations with P&WA field representatives and other knowledgeable personnel led to the conclusion that the field samples received, though few in number, are typical of the majority of field rejects for corrosion.

1) Stored Bearings

Main and accessory bearings which were rejected from storage due to corrosion were analyzed for the morphology of the corrosive attack and chemical species present in corrosion products by scanning electron microscopy (SEM), X-ray emission spectroscopy (XES), microprobe, metallography (MET), and Auger electron spectroscopy (AES) methods. Bearings examined included:

Bearing	*Condition*	*Preservative*	*Type*
A	New	MIL-C-11796B	Mainshaft
B	New	MIL-C-11796B	Mainshaft
C	New	MIL-C-11796B	Mainshaft
D	Used	NA	Mainshaft
E	New	MIL-C-11796B	Accessory
F	New	MIL-C-11796B	Accessory
G	Used	MIL-C-15074C	Accessory
H	Used	MIL-C-15074C	Accessory

All of the above bearings were of identical construction in terms of materials; balls and races being composed of M50 steel with silver-plated AISI 4340 cages. Used bearings exhibited characteristics of both storage and service environments, and provided valuable information in establishing differences and similarities of corrosion morphology and mechanisms. They are discussed further in Section IIB.2.3).

Corrosive attack of the silver-plated cages (AISI 4340 steel) during storage was manifested as stains affecting relatively large areas and ranging from very light violet to dark black in color. The morphologies of the stains generally correspond to rolling element cage contact loci and thick-thin preservative contours shown in Figures 1 and 2.

Light and dark areas (staining) associated with the thick-thin preservative contours probably only reflect the varying quantities of reactive species being made available from the corresponding volume of preservative to the silver surface. Similar logic can be applied to the rolling element cage contact loci where a thicker meniscus of preservative is often formed.

4146C

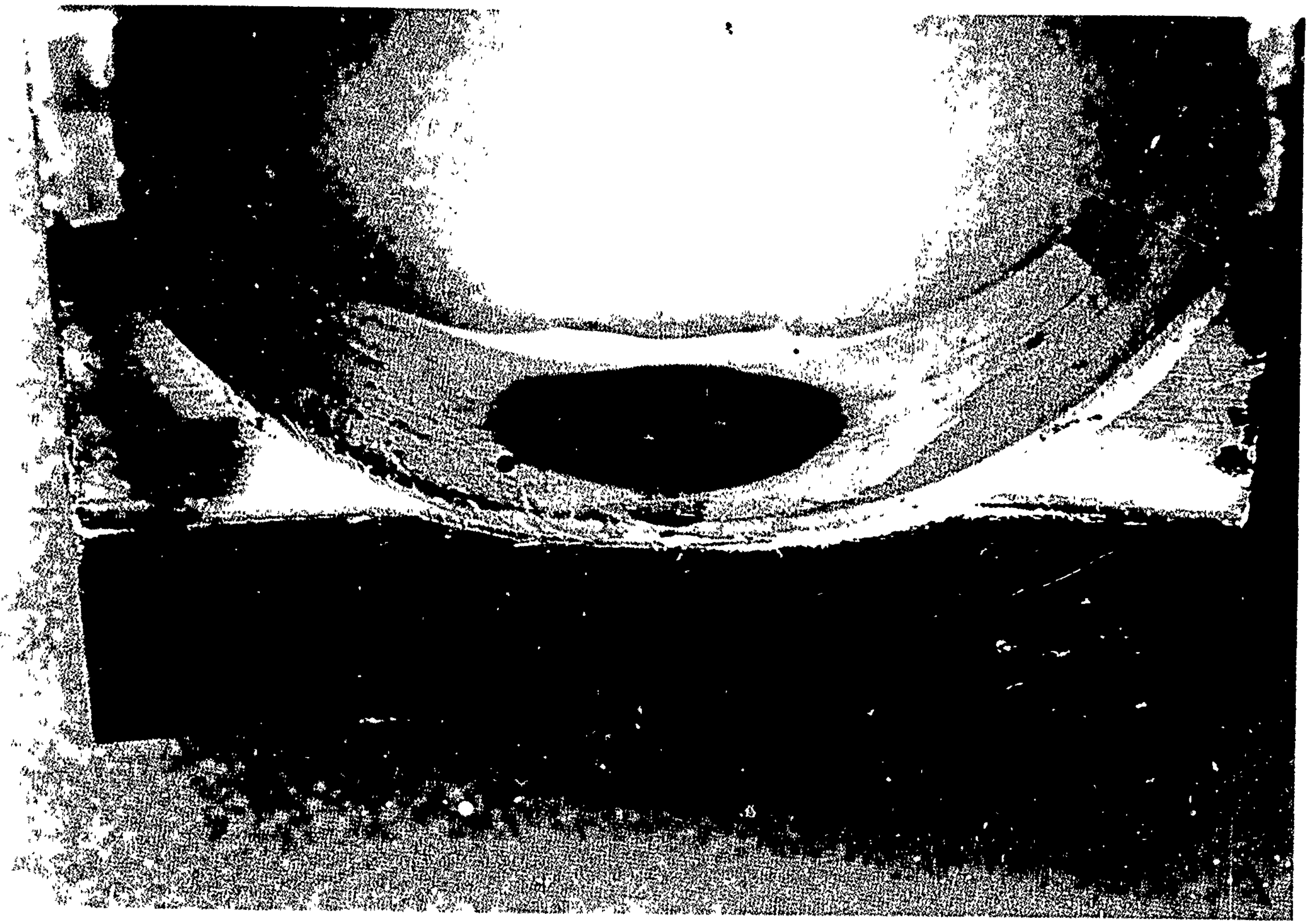

FE 352879

Figure 1. Dark Staining of Silver-Plated AISI 4340 Cage at Rolling Element-Cage and Race-Cage Contact Loci (Main Shaft Bearing C, Stored in MIL-C-11796B Preservative)

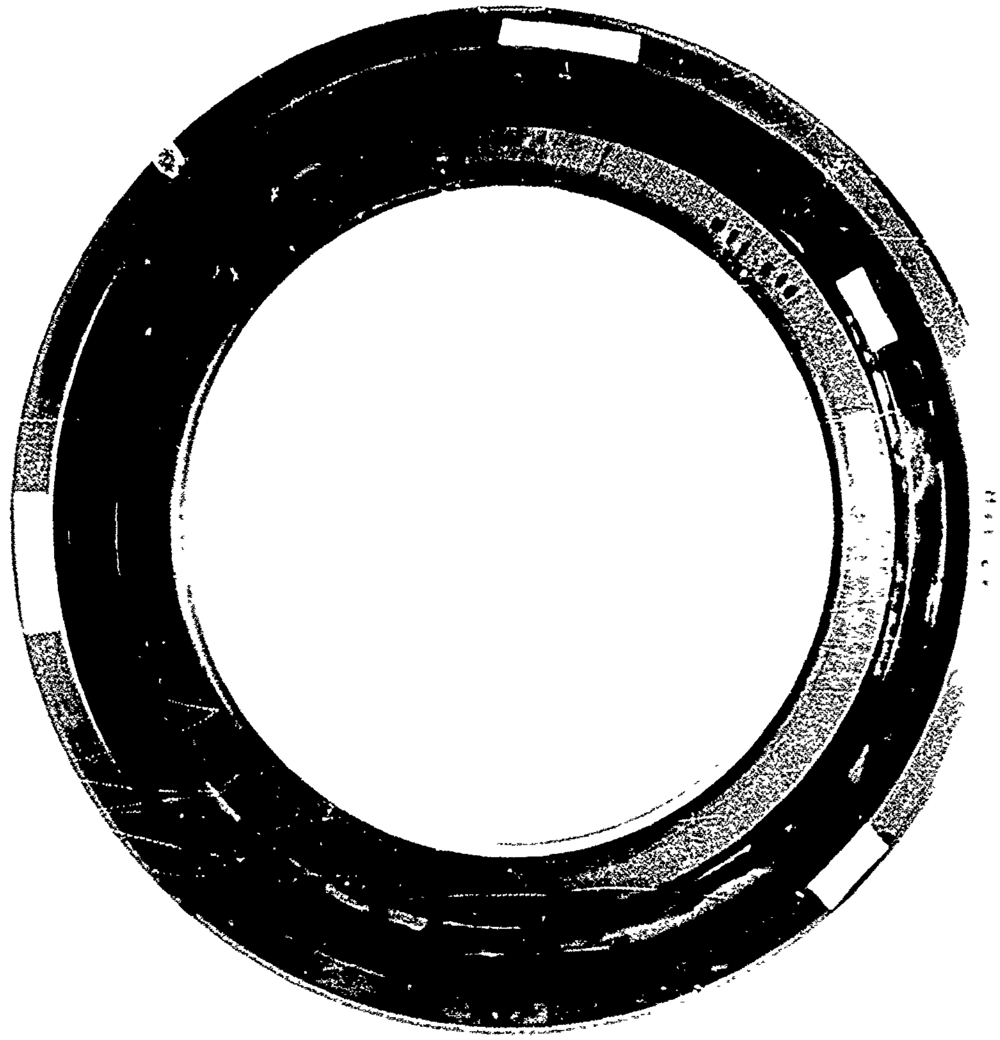

FE 352760

Figure 2. Heavy, Dark Staining of Silver-Plated AISI 4340 Cage Generally Conforming to Thick-Thin Preservative Boundary Morphology (Accessory Bearing, Similar to Accessory Bearing E Stored in MIL-C-11796B Preservative)

The lightest stains observed exhibited a violet tint (Figure 3) and SEM and XES analyses (Figure 4) identifed only silver and chlorine suggesting a silver halide compound. Similar analyses of slightly darker stains, light brown in color, revealed sulfur and chlorine contamination. The light brown color is attributed to the presence of sulfur as silver sulfide shown in Figure 5. Still darker, almost black stains, sometimes with a purple tint, were characterized by much higher XES spectra for sulfur shown in Figures 6 and 7.

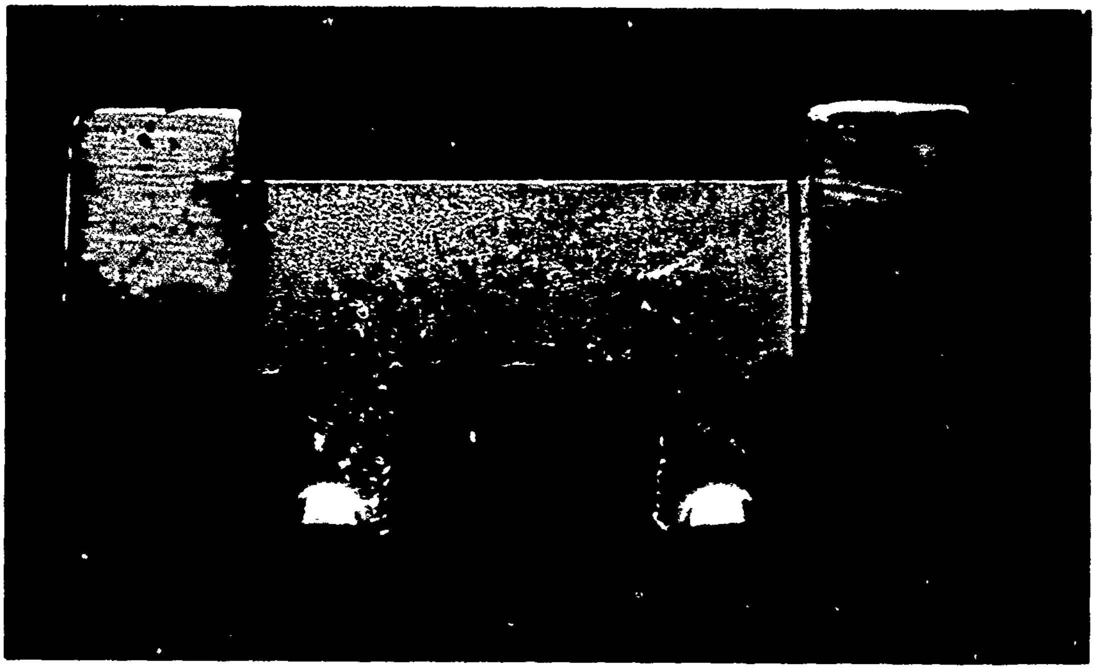

FE 352814

Figure 3. Light Violet Staining of Silver-Plated AISI 4340 Cage at Rolling Element-Cage Ccntact Loci (Accessory Bearing F, Stored in MIL-C-11796B Preservative)

Mag 10X

XES Spectra of Stained Region F

SEM Photomicrograph of Cage

XES Spectra of Unstained Region G

FD 230893

Figure 4 SEM Photomicrograph and XES Spectra of Light Violet-Stained Region (Area F) and Unstained Region (Area G) of Silver-Plated AISI 4340 Steel Cage Material (Accessory Bearing F)

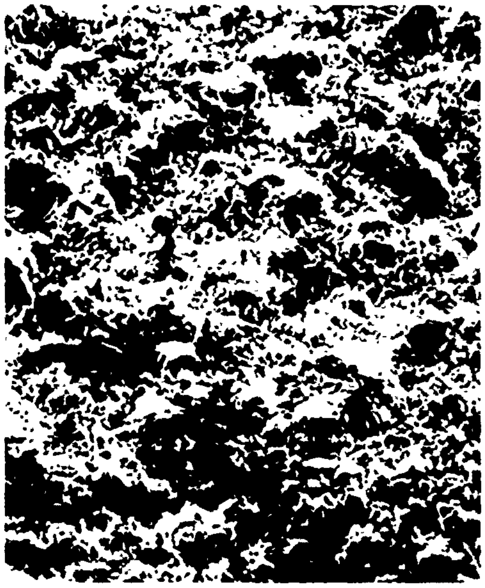

Mag 800X

Stained Silver Plate

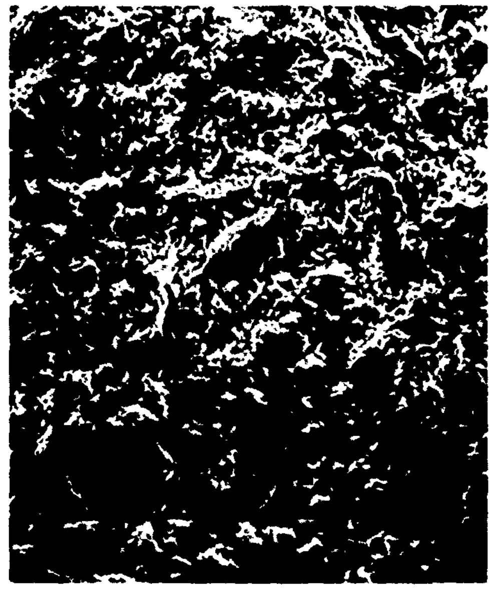

Mag 800X

Unstained Silver Plate

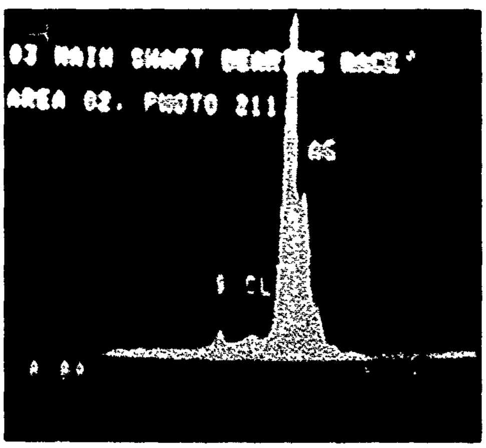

XES Spectra of Stained Silver Plate

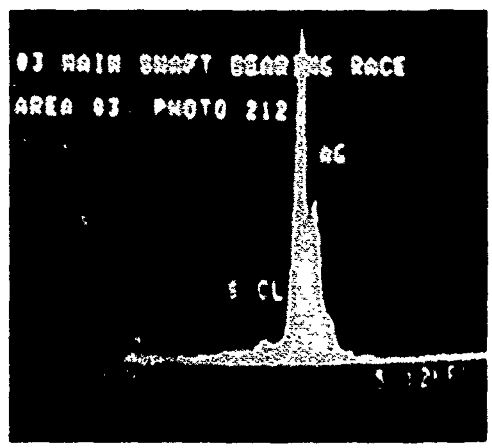

XES Spectra of Unstained Silver Plate
Note Absence of S

FD 230894

Figure 5. SEM Photomicrographs and XES Spectra of Light Brown Stained and Unstained Areas of Silver Plating on AISI 4340 Cage Material (Main Shaft Bearing C)

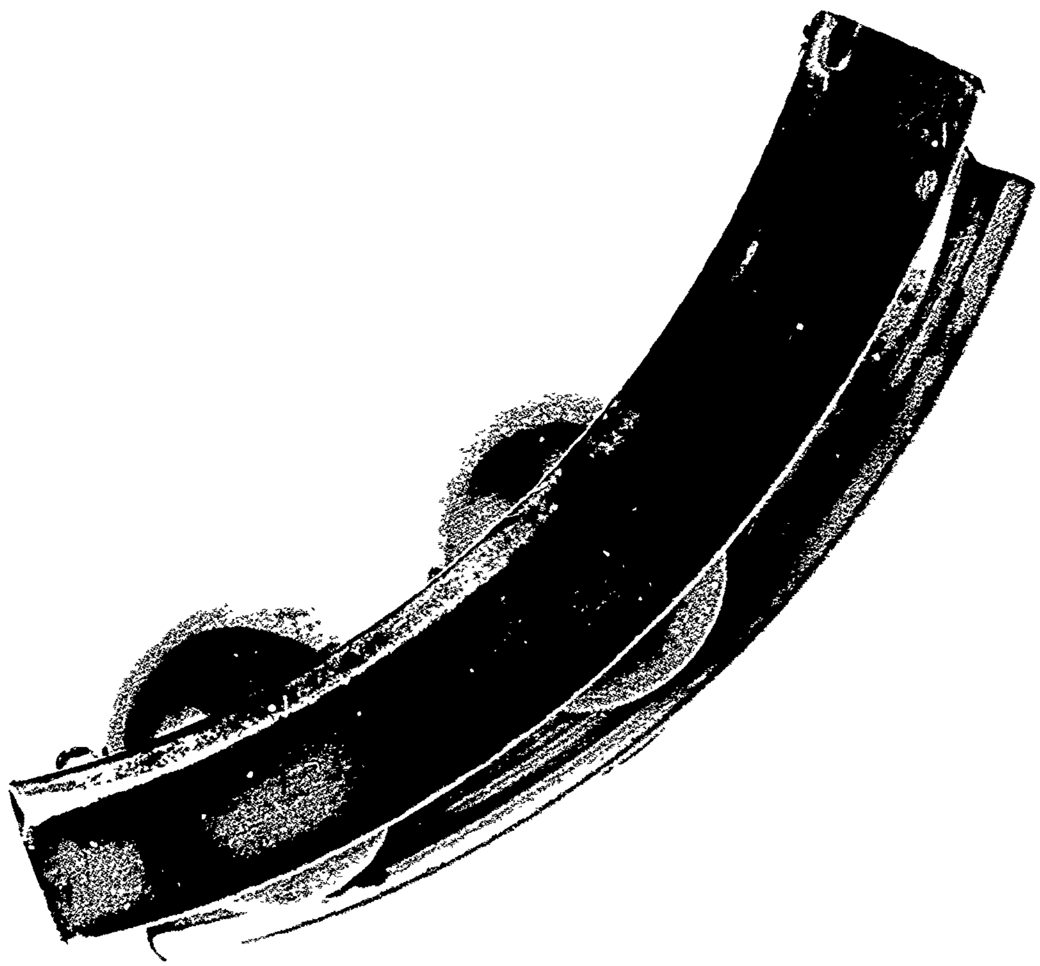

FE 352758

Figure 6. Heavy, Dark Staining of Silver-Plated AISI 4340 Cage Analyzed Via SEM, XES, Figure 7 (Accessory Bearing E, Stored in MIL-C-11796B Preservative)

4146C

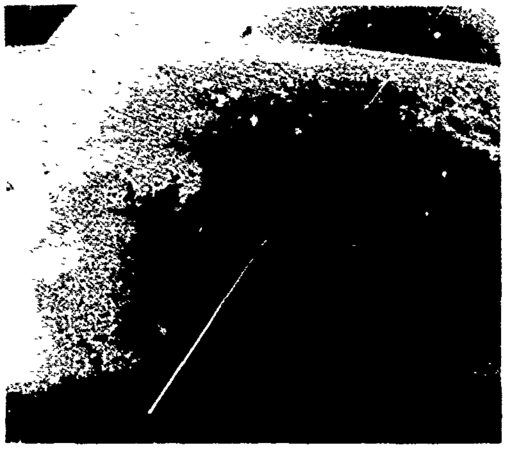

Mag 10×
SEM Photomicrograph of Stained Cage

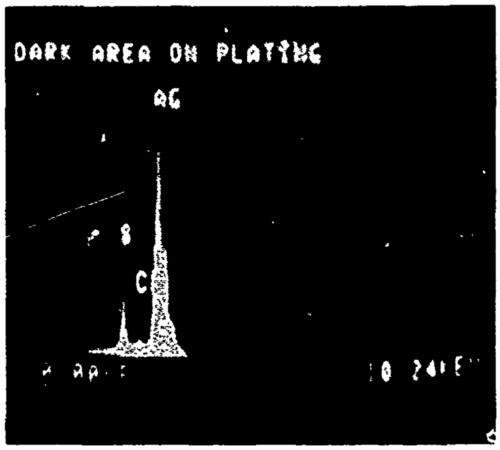

XES Spectra of Stained Region
Denoted at Left

FD 230895

Figure 7. SEM Photomicrograph and XES Spectra of Dark Stain on Silver-Plated AISI 4340 Cage Material (Accessory Bearing E)

AES analysis of medium to dark stains formed at ball-cage contact points (Figure 1) revealed sulfur to be the contaminant present in highest concentration, followed by chlorine, oxygen, carbon, iron and possibly calcium. Ion sputtering of the stained surface rapidly reduced the intensities of all contaminants, restoring a bright, virtually contaminant free silver surface as shown in Figure 8. The high intensity for sulfur relative to oxygen and the rapidity with which the contaminants were removed by ion sputtering indicates the stain to be a thin film of silver sulfide, approximately 1000 to 2000 angstroms thick.

A comparison of the free energies of formation for oxides and sulfides at 25°C reveals silver sulfide to be more stable than silver oxide (protective film on bright, unstained silver), a characteristic that becomes more pronounced at elevated temperatures. Thermodynamics, therefore, favors the substitution of sulfur for the oxygen in the protective silver oxide film if sulfur is available in a reactive state (not SO_4^{-2}). Reactive organic sulfur (as organic thiols, sulfides, disulfide, etc.) and inorganic sulfur (SO_3^{-2}, SO_2, S^o, H_2S, HS^-, S^{-2}), if water is present in solution with the preservative, are the primary corrodents responsible for staining and corrosion of the silver-plated components of stored bearings. Their presence in preservative media is probably due to the failure of refining techniques to remove these petroleum impurities down to the levels which would preclude visible staining of silver.

The next most important contaminant in terms of corrosive attack of stored silver-plated bearing components is chlorine, present in preservatives as chlorinated hydrocarbons, solvated chloride ions (if water is present in solution with the preservative), and chloride ions and compounds adsorbed to metal surfaces (improper handling).

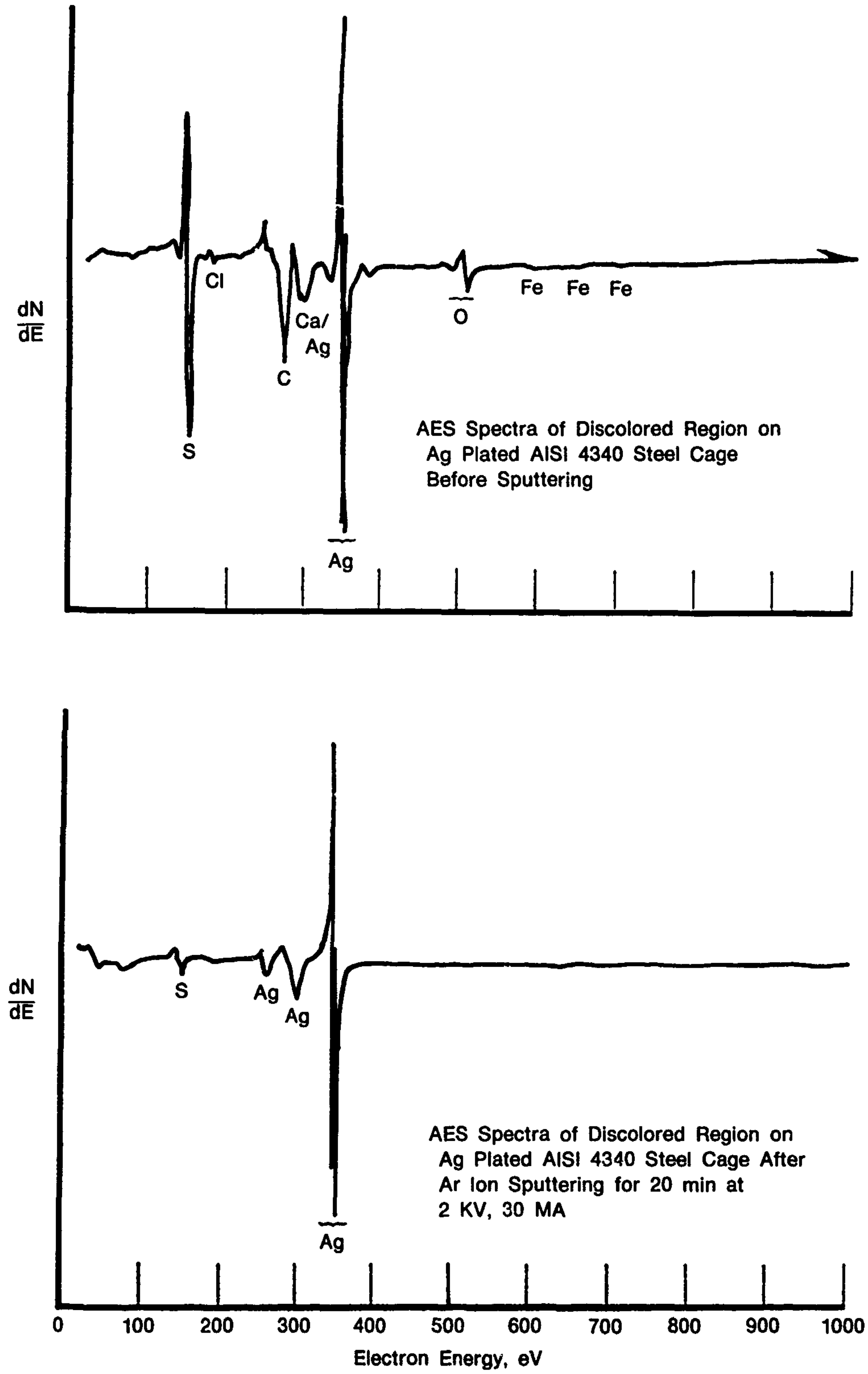

FD 230887

Figure 8. AES Spectra of Stained Region of Silver-Plated AISI 4340 Steel Cage Material from Main Shaft Bearing C, Stored in MIL-C-11796B Preservative, Showing Variation of Chemical Composition With Depth

4146C

Silver chloride, like silver sulfide, is more stable than the oxide at room temperatures which favors the substitution of the chloride for the protective oxide and results in staining.

Sources of chloride contamination are believed to include standard petroleum contaminants (as chlorinated hydrocarbons and solvated chloride ions) and improper handling procedures such as failure to use gloves or protective film when handling bearings.

Carbon and calcium contaminants are probably due to entrapment of the saponified (agents: sodium, potassium, calcium, magnesium, lithium, and/or aluminum) hydrocarbon preservative in the corrosion product. Carbon might also have migrated the short distance from an adjacent corroding ball or roller. Similarly, the source of iron as a contaminant in the stained silver plate is probably other steel components of the bearing itself. The presence of oxygen only reflects the lack of complete conversion of the silver oxide film to sulfide and/or chloride.

Corrosive attack of stored M50 steel races and rolling elements was several orders of magnitude less severe in appearance than that of the associated silver-plated cages. However, even the lightest corrosive attack of the functional surfaces of the M50 steel components was considered much more serious than the plated cages due to the potential catastrophic failure of these parts from progressive spalling initiated at such sites. Corrosive attack of the M50 steel components varied from widespread, extremely light stains, barely discernible to the eye (and invisible to standard macrocameras, SEM and XES), to very heavy, black or brown stains and pitting. The lightest stains generally conformed to the thick-thin preservative boundary morphology, and heavier stains to the race-rolling element contact morphology as shown in Figures 9 and 10.

FD 230896

Figure 9. Thick-Thin Preservative Boundary Morphology As Seen Through Plastic Skin-Pack (Main Shaft Bearing N)

4146C

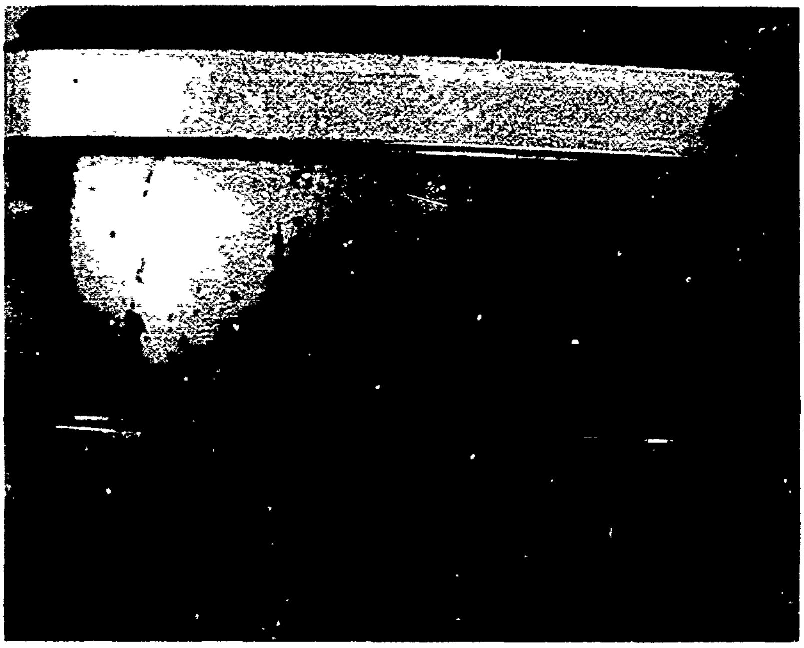

Mag 3 1/2X Corrosion of Inner Race

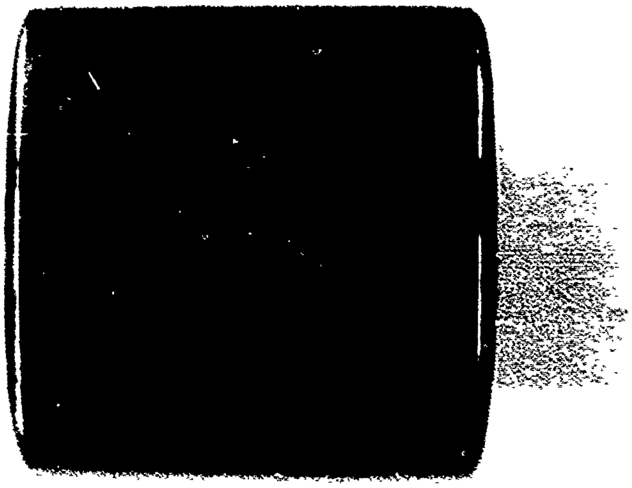

Mag 6X Corrosion of Roller

FD 230892

Figure 10. Dark Black Stains of M50 Steel Conforming to Rolling Element — Race Contact Morphology (Accessory Bearing F)

SEM and XES analyses of the lightest stains observed proved fruitless (Figures 11 and 12) due to the stronger background emissions of the base material through the stains (films less than 3000 angstroms composed of light elements) and noise. AES analysis of lightly stained areas of two separate mainshaft bearings (A, B) which had been protected in MIL-C-11796B, a cosmoline-type preservative revealed almost identical results. Both unstained as well as as stained areas usually exhibited spectra for oxygen, carbon, calcium, sulfur, and chlorine with phosphorous, nitrogen, nickel, sodium, zinc, aluminum, and silicon observed in some locations as well. This layer of contaminants was rapidly removed by ion sputtering leaving a bright, clean base metal surface in unstained locations and a slightly thicker layer of oxygen containing material with some carbon and calcium in stained areas as shown in Figure 13. Total thickness of the layers in the stained regions was estimated to be less than 1000 angstroms.

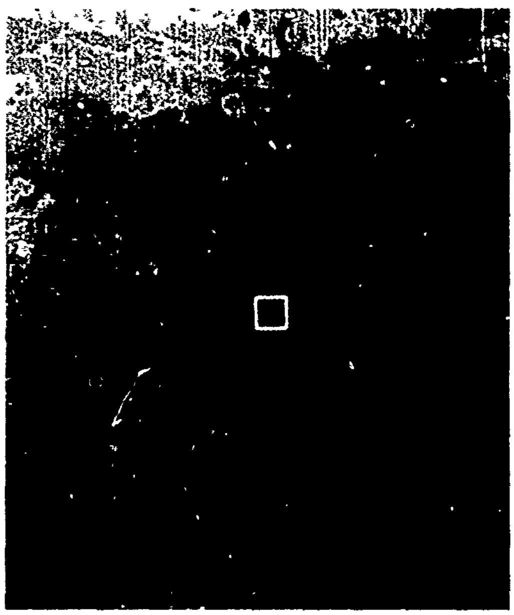

Mag 100X

Stained Area

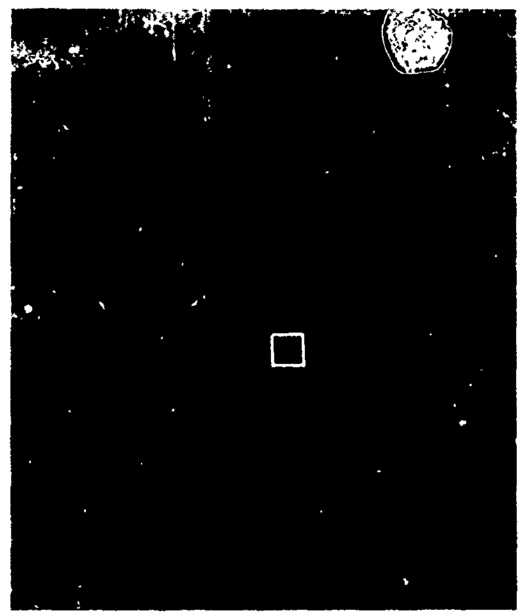

Mag 100X

Unstained Area

FD 230897

Figure 11. SEM Photomicrographs of Stained and Unstained Areas of M50 Steel Race (Main Shaft Bearing B). Indicated Areas are Examined Further in Figure 12

Of the contaminants encountered, chlorine, sulfur. and oxygen (present in corrosion products as chlorides, sulfides, and oxides) are considered the primary corrodents.

Chlorides are believed to be present in the storage environment as chlorinated hydrocarbons, solvated chloride ions (if water is present in solution with preservative), and chloride ions or compounds adsorbed to metal surfaces. Sources of this contamination include standard petroleum impurities and incorrect handling techniques shown in Figure 14.

Mag 5000X

Stained Area

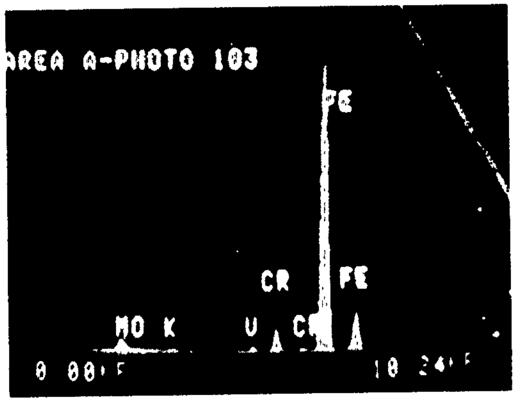

XES Spectra from Dark Region, Area A, of Stained M50 Steel Race

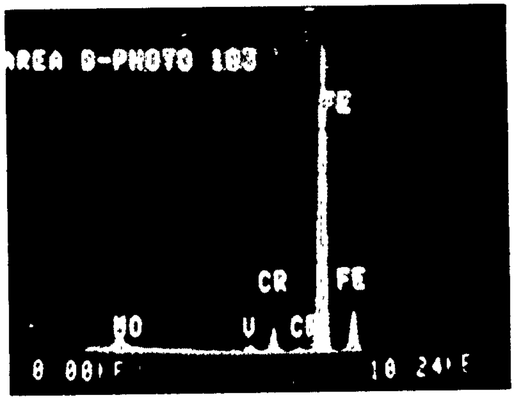

XES Spectra from Light Region, Area B, of Stained M50 Steel Race

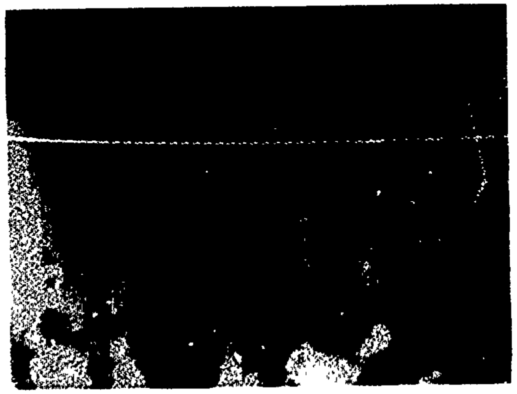

Mag 5000X

Unstained Area

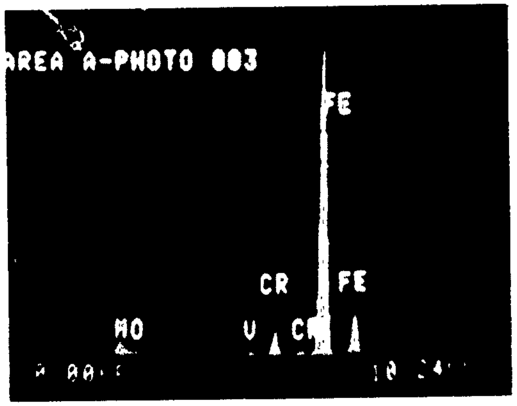

XES Spectra from Dark Region, Area A, of Unstained M50 Steel Race

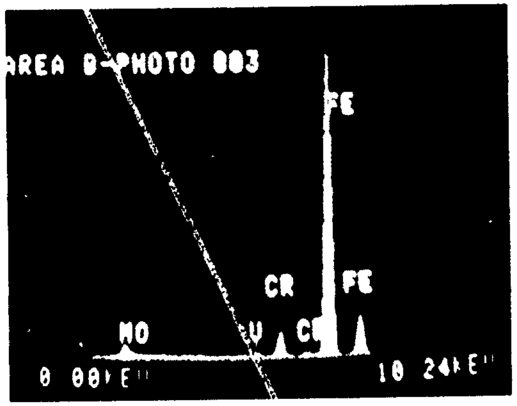

XES Spectra from Light Region, Area B, of Unstained M50 Steel Race

FD 230898

Figure 12. SEM Photomicrographs of Indicated Area in Figure 11 and Photographs of XES Spectra from Light and Dark Areas, Emphasizing Difficulty of Analyzing Lightest Stains

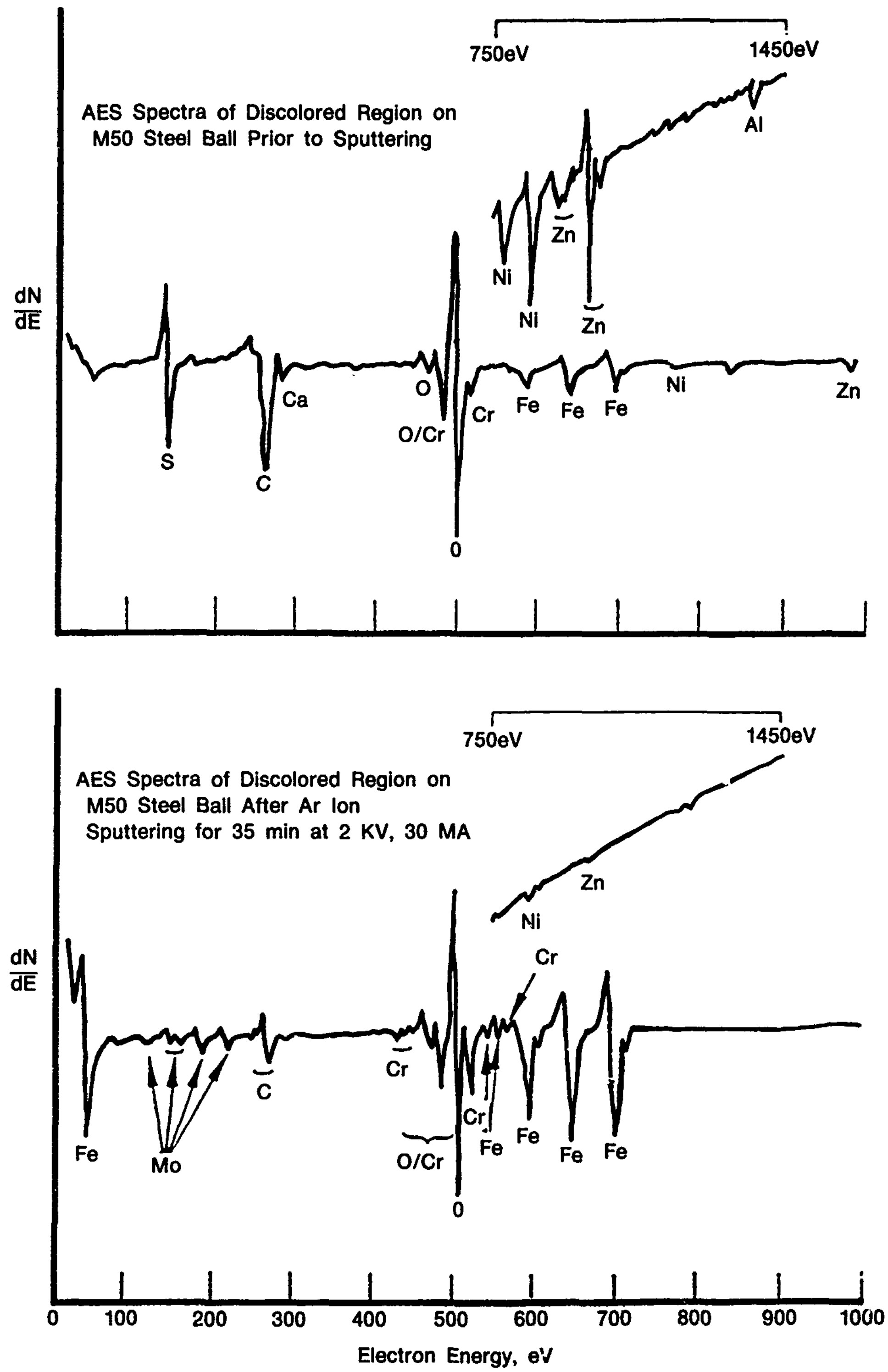

FD 230888

Figure 13. AES Spectra of Stained Region of M50 Steel Ball from Main Shaft Bearing C, Stored in MIL-C-11796B Preservative, Showing Variation of Chemical Composition With Depth

4146C

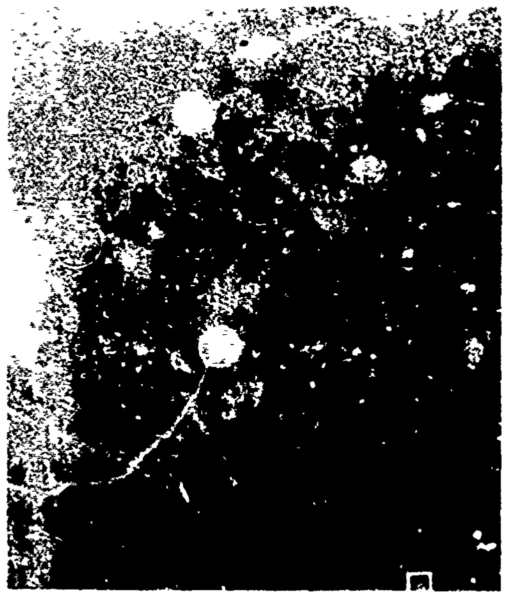

Mag 50×

Surface of Contaminated Ball
Indicated Area Enlarged at Right

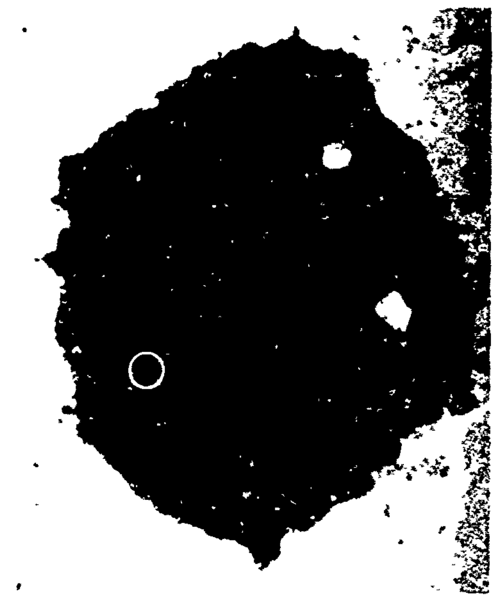

Mag 2000×

Enlarged Area Showing Dendrite
Network of Chloride Crystals

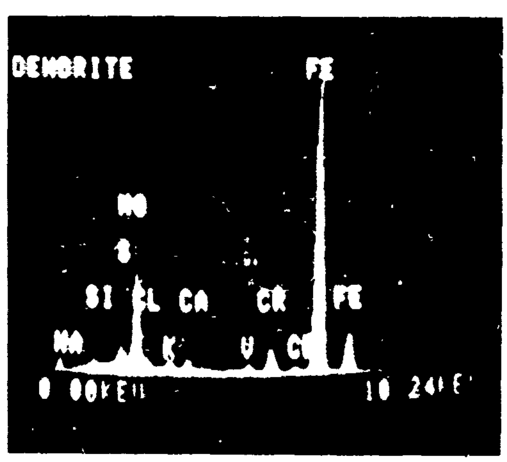

XES Spectra of Dendrite

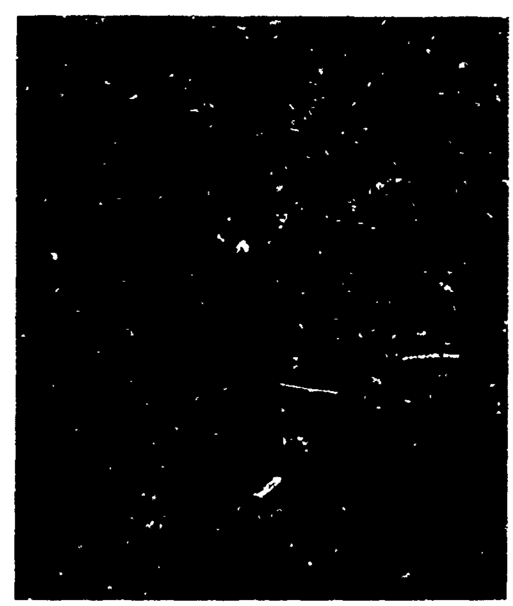

Chloride X-Ray Map of Above Area

FD 230899

Figure 14. SEM Photomicrographs, XES Spectra, and Chlorine X-ray Map of Adsorbed Dendrites Comprised of Sodium, Potassium, and Calcium Chloride on an M50 Steel Ball; the Result of Handling Ball Without Gloves or Suitable Protective Film on Hands

4146C

Reactive sulfur (as organic thiols, sulfides, disulfides, etc., and if water is present, as SO_3^{-2}, SO_2, S^o, H_2S, HS^-, and S^{-2}) is undoubtedly a preservative contaminant, the result of residual petroleum impurities during manufacture or reduction of sulfate/sulfonate corrosion inhibiting additives.

Oxygen is available to the bearing surface via water dissolved in the preservative and by penetration of air through bearing packaging and preservatives.

Carbon may be present as a normal alloy constituent or due to entrapment of the hydrocarbon preservative in the corrosion product. Similarly, the alkali metals, lithium, sodium, and potassium plus magnesium, calcium, and possibly aluminum are frequent saponification components in greases and preservatives and may also be entrapped in the corrosion product. Corrosion inhibiting additives often contain barium, phosphorous, nitrogen, zinc, and sulfur as well. Nickel and silicon are the only two elements for which a plausible explanation cannot readily be found other than impurities in the preservative. Nickel is an alloying element of AISI 4340 steel and could find its way into the preservative if the integrity of the silver plate were breached. Silicon as a substituent of silicones may be present as a vendor proprietary ingredient or from contamination with ordinary sand (SiO_2).

Corrosion corresponding to slightly darker stains of the M50 material (mainshaft bearing C) which was amenable to SEM, XES analyses, appeared to follow the grain boundary morphology (Figure 15). Localized stress concentration in the lattice structure along the grain boundary, i.e., grain boundary energy, rather than transgranular differences of chemistry, is believed to be a primary mechanism responsible for initiating autocatalytic pitting corrosion along grain boundaries in the storage environment.

The most severe corrosive attack of M50 components in storage was manifested by dark black stains usually conforming to rolling element-race contact morphologies (Figure 10). SEM photomicrographs of these stains revealed severe *mudcracking* and spalling of the *mudcracked* corrosion product. XES analysis of these *mudcracked* regions typically revealed enrichment of the alloying elements (Cr, Mo, and V) relative to iron except in locations of spalling in which fresh unaffected surface was exposed (Figure 16). This is probably due to the leaching out of the more soluble iron corrosion products or, similarly, precipitation of less soluble alloying element corrosion products due to the decreasing concentration gradient of the attacking media from the bottom of a local pit to the surface of the alloy.

The *mudcracking* effect may represent the final stages of autocatalytic pitting corrosion initiated along grain boundaries (compare 200× photos in Figures 15 and 16) and producing a trench-shaped crevice (crack) which ultimately spalls, exposing fresh surface to further attack. This type of corrosion of functional bearing surfaces, if undetected, can result in failure.

Contaminants present in the corrosion products of the most severely attacked areas were essentially the same as those described previously, implying involvement of the same mechanism but under more severe conditions or for a longer duration.

4146C

Mag 200X

Mag 500X

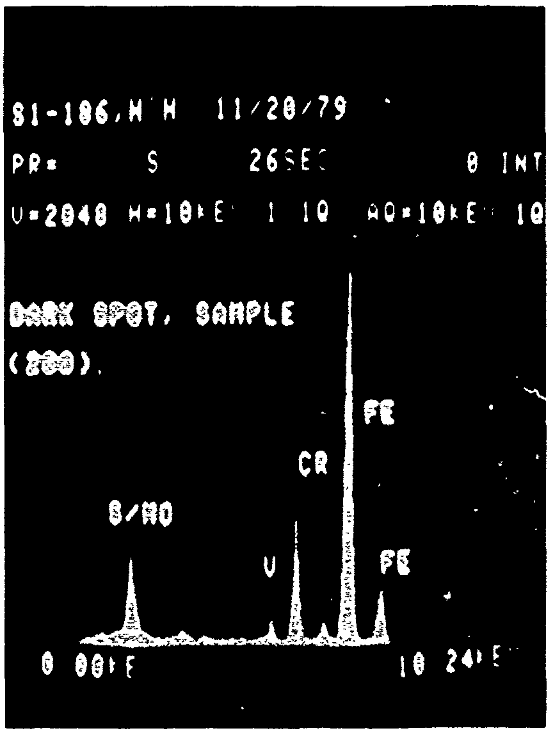

Mag 2000X

FD 230889

Figure 15. SEM Photomicrographs and XES Spectra of Lightly Stained M50 Bearing Material (Main Shaft Bearing C) Which Appears to Follow the Grain Boundary Morphology (Arrows)

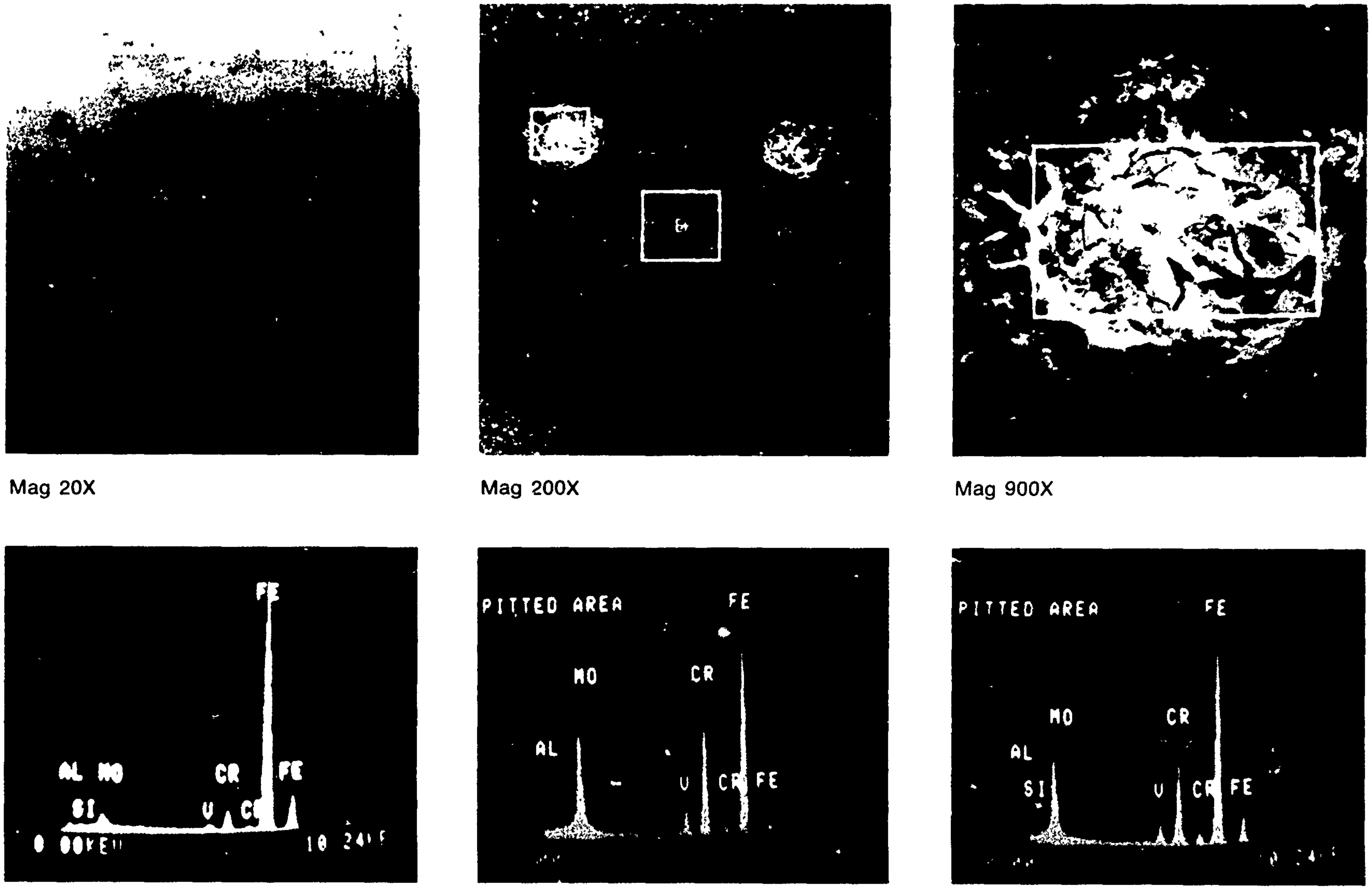

Mag 20X — Mag 200X — Mag 900X

XES M50 Base Metal Spectra — XES Spectra in "Mudcracked" Region, Area B — XES Spectra in Pit, Area A

FD 230900

Figure 16 SEM Photomicrographs and XES Spectra of Dark Black Stains on M50 Steel Roller Showing Apparent Enrichment of Alloying Elements (Cr, Mo, V) Relative to Iron in Location of Corrosive Attack

2) Service Bearings

Analyses of service-rejected bearings for corrosion were conducted on three main shaft bearings employing SEM, XES, microprobe, and MET techniques. Two of the bearings possessed similar material construction, i.e., M50 steel balls and races. Quantitative XES analysis of the third bearing, however, revealed the inner race base metal to have a composition similar to M50 steel, whereas the outer race and rollers exhibited spectra similar to that of Bower 315, a high temperature carburizing grade, alloy steel. In each case, the cage material was the standard silver-plated AISI 4340 steel. The three bearings are listed below:

Bearing	*Condition*	*Oil*	*Type*	*Outer Race and Roller Material*
J	Used	MIL-L-7808J	Mainshaft	M50
K	Used	MIL-L-7808J	Mainshaft	Bower 315
L	Used	MIL-L-7808J	Mainshaft	M50

Other than minor physical damage, such as indenting, scratches, and wear, the silver-plated cages of the service-rejected bearings exhibited virtually no evidence of detrimental effects from the service environment, including corrosive attack of the silver plate.

Corrosive attack of M50 and BOWER 315 steel rolling elements and races of service bearings was less evident than that of stored bearings (Figure 17). Staining of the alloy surface was not encountered. Rather, the morphology of the corrosive attack of these bearing components was confined to almost microscopic pitting which, though widespread, was difficult to see except at higher magnification (Figures 18 and 19).

On examination, the most common functional surface condition encountered with the rejected service bearings was indentation from contaminants entrained in the oil. Aluminum and silicon (probably as oxides) were the usual contaminants associated by SEM and XES analyses with indentations (Figure 20). The relatively higher proportion of aluminum encountered suggests contamination with residuals from some manufacturing process as opposed to common sand or dust contamination, since the silicon/aluminum ratio for most sands is greater than 1:1.

Corrosion-like morphologies were found in the regions of some indentations (Figure 20). In the absence of static exposure to a relatively corrosive environment (storage with MIL-C-11796B), it is postulated that corrosive attack is more readily initiated at locations of physical damage rather than at grain boundaries. Small particles embedded in functional surfaces provide relatively large areas of closely conforming surfaces which are very amenable to capillary adsorption of water in the system (and attendant reactive species). Thus, an area of physical damage is easily converted to a site for autocatalytic pitting attack as seen in Figures 21 and 22.

XES analysis revealed little evidence of contamination of the corrosion site by potentially reactive species. This is to be expected, since the corrosion damage was probably experienced during a period of extended idleness when water condensed from the air and/or oil in the bearing housing, and corrosion products (scale) along with contaminants were dislodged and entrained in the oil upon subsequent engine operation. In addition, bearings are generally inspected only after thorough cleaning. The rejected service bearings examined in this program had been packaged in MIL-L-8188 oil during shipment to prevent further corrosion, all of which served to mask the chemical species responsible for the corrosion.

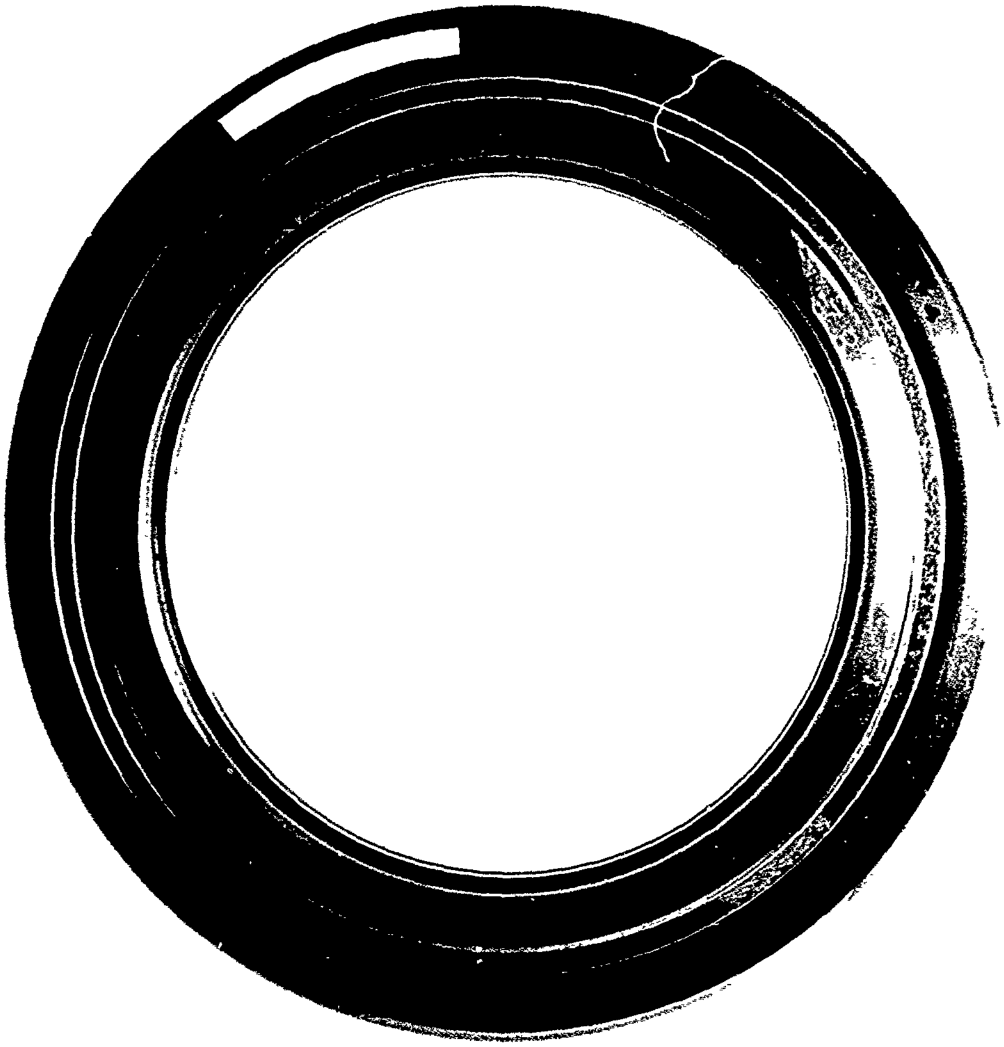

FE 352762

Figure 17. Typical Appearance of Service-Rejected Bearing Does Not Suggest Corrosive Attack (Mainshaft Bearing J, Service in MIL-L-7808J Oil)

The morphology of service-related corrosion sites was similar to that of the freshly exposed material of a recent spall in a region of storage-related corrosion. This suggests that after initiation, a similar mechanism of corrosion is at work in both the stored and service bearing, but the physical environment of the service bearing subsequently dislodges the corrosion product (scale).

3) Stored, Service Bearings

Bearings which exhibited characteristics of both service and storage environments are described in this section.

Mag 5X

Pitting Attack of Ball

Mag 3 3/4X

Pitting Attack of Outer Race

FD 230890

Figure 18. Pitting Attack of Functional Surfaces of Service-Rejected Bearing (Main Shaft Bearing J, Service in MIL-L-7808 Oil)

FE 352766

Figure 19. Pitting Attack of Ball in Figure 18 (Mainshaft Bearing J, Service in MIL-L-7808J Oil)

Mag 200X
Indented Region of M50 Outer Race

XES Spectra of Dark Spot
Note High Aluminum Content

Mag 200X
Indented Region of M50 Inner Race Showing
Corrosion - Like Pitting Morphology

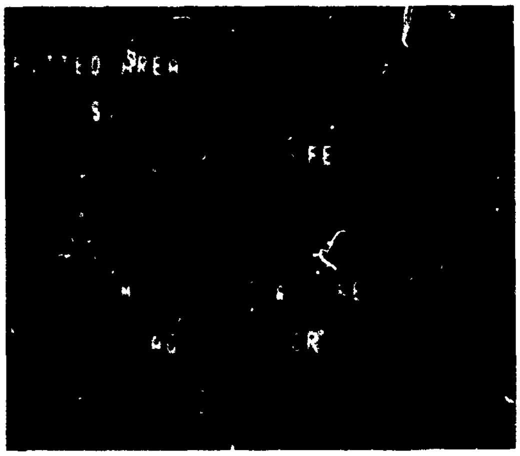

XES Spectra of Indicated Area
Note High Silicon Content

FD 236801

Figure 20. SEM Photomicrographs and XES Spectra of Indentations (Main Shaft Bearing J)

4146C

Mag 3000×
Embedded Particle in Functional Surface of Rolling Element

Mag 8000×
Embedded Particle in Functional Surface of Rolling Element

Mag 1500×
Site of Probable Autocatalytic Pitting Attack

XES Spectra of Region With Embedded Particle Above

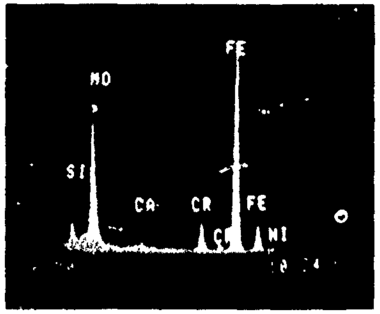

XES Spectra of Region With Embedded Particle Above. Higher Concentration of Alloying Elements May Be Due to Leaching Effect of Corrosive Attack

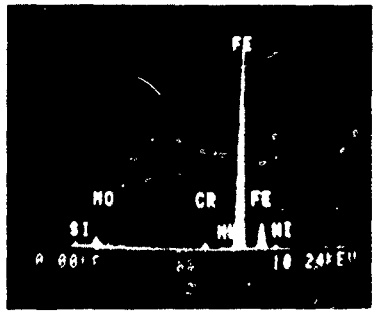

XES Spectra of Bower 315 Base Material for Comparison

FD 236802

Figure 21. SEM Photomicrographs and XES Spectra of Locations of Embedded Particles and Probable Autocatalytic Pitting Attack Initiated at Those Locations (Main Shaft Bearing K)

Mag 500X

Pitting Attack of Functional
Surface of Roller

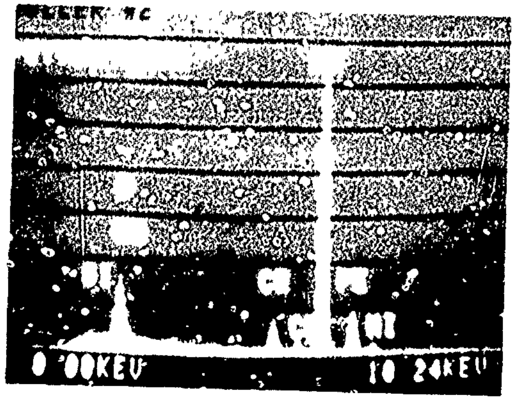

XES Spectra in Pitted Region Showing
Higher Concentration of Alloying
Elements Due to Leaching Effect

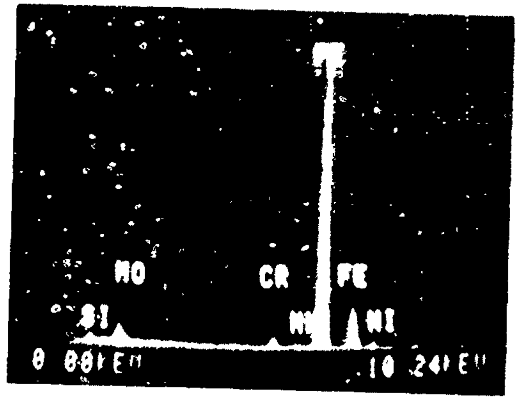

XES Spectra of Base
Material for Comparison

FD 236803

Figure 22. SEM Photomicrographs and XES Spectra of Area of Pitting Attack (Main Shaft Bearing K)

Originally considered as corrosion-rejected bearings from service, examination via SEM, XES, and MET analyses revealed evidence of corrosive attack that could not be explained on the basis of previous experience with service bearings and the hypotheses generated as a result of this experience. A review of the history of these bearings showed that all had seen a *storage* environment of one sort or another.

All of the *used* bearings examined were of similar material construction, i.e., M50 steel balls and races with silver-plated AISI 4340 steel cages.

For the most part, corrosion of the silver-plated AISI 4340 steel resembled that of bearings subjected to a storage environment. The cage of one accessory bearing exhibited a feature not previously encountered with silver plating, i.e., *mudcracking.* Examination of thin, dark stains of the cage (Figure 23), via SEM and XES analyses, revealed heavy *mudcracking* and pitting (spalling) similar to that seen on M50 steel components subjected to a severe storage environment (Figure 24). *Mudcracking* of the silver plate is not serious in terms of precipitating a failure of the cage, but spalls can cause indenting of functional surfaces (Figure 25), and may progress to flaking of the silver plate.

Corrosive attack of the silver plate leading to the *mudcracking* morphology may be due to autocatalytic pitting attack involving formation of an aqueous sulfur concentration cell during storage. Incorrect handling (skin moisture) and saturation of the preservative due to condensation are the most probable sources of water contamination.

SEM and XES analyses of M50 steel components revealed characteristics of both storage and service environments. They exhibited the *mudcracking* and spalling corrosion typical of storage, as well as, the indenting, scratches, wear, and embedding of silicon and aluminum (oxide) particles representative of parts exposed to service (Figures 26 and 27).

The history of mainshaft bearing D (Figure 28) is somewhat unique. The bearing, presumably protected with the short-term preservative oil MIL-C-15074C, was assembled into its housing and left in a horizontal position for approximately six months before the assembly was completed and the engine run. This was sufficient time for the oil to drain, concentrating a corrosive mixture of absorbed particles of dust, water, salt, etc., on the surface of a puddle in the outer race, leaving the remainder of the bearing exposed to the atmosphere (i.e., equivalent to storage without a preservative). Inspection of the bearing at teardown revealed extensive attack of the bearing including an elliptical zone of heavy pitting in the outer race. The pitting corresponded to the interface of the preservative puddle, air, and M50 steel.

Mudcracking (characteristic of a storage environment) was the predominant corrosion morphology in nonfunctional areas (Figure 29). Pitting (more typical of the service environment) was found on functional surfaces (Figure 30). These observations tend to verify the hypothesis that the corrosion mechanisms (not rates or modes of initiation) of stored and service bearings are similar (compare Figure 29 with Figure 16, and Figure 30 with Figures 20 and 22).

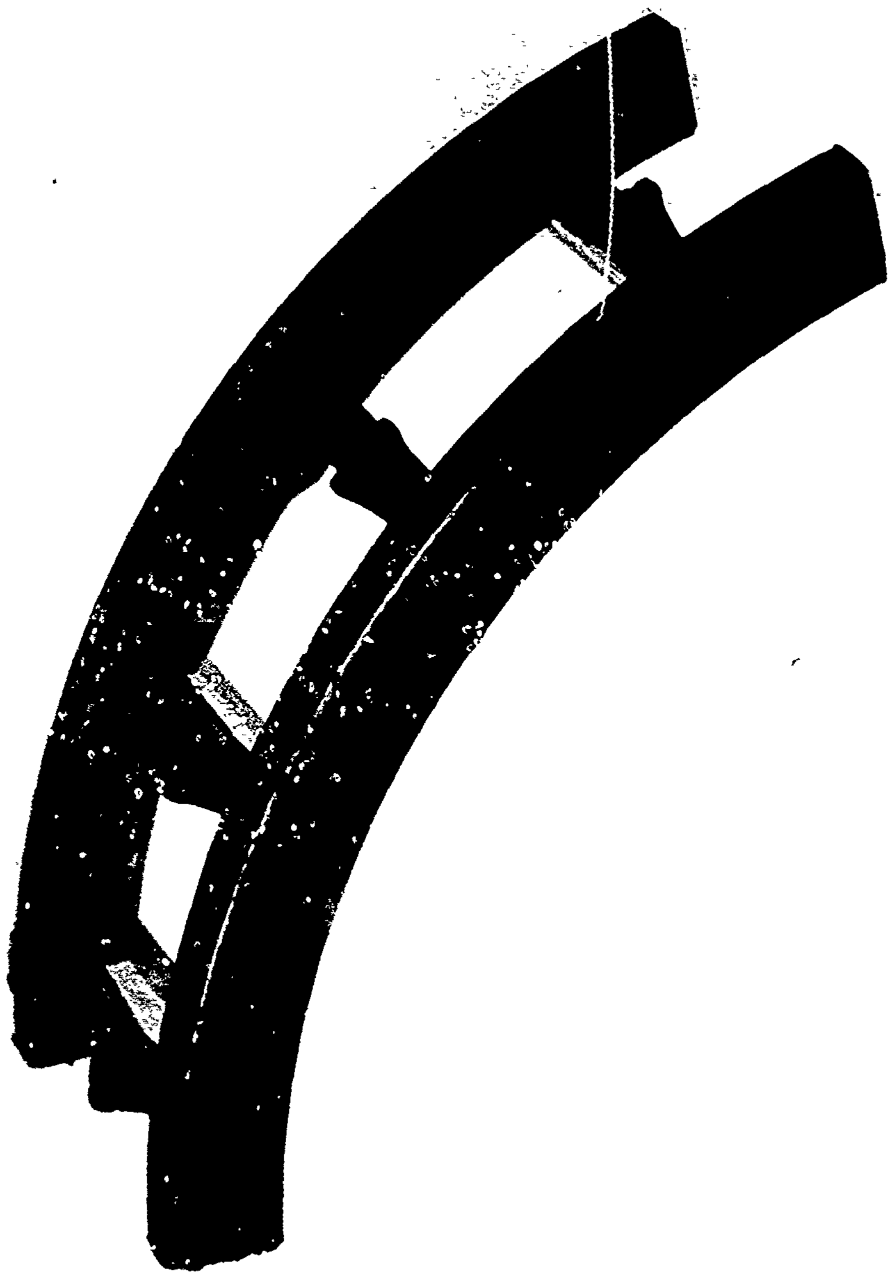

FE 352756

Figure 23. Section of Cage Examined Via SEM, XES and MET Analyses for Thin Dark Stains (Accessory Bearing H)

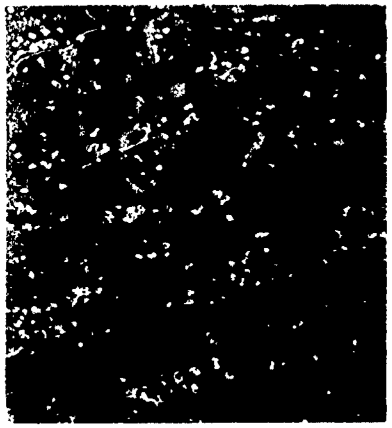

Mag 80×
Thin Dark Stain of Silver Plate

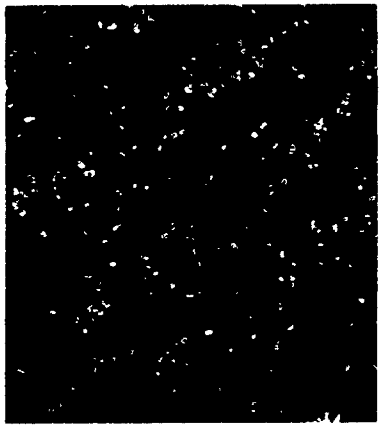

Mag 500×
Thin Dark Stain of Silver Plate Showing "Mudcracked" Morphology

Mag 500×
Spall in "Mudcracked" Region

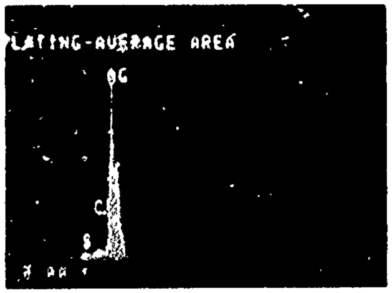

XES Spectra of Unstained Region

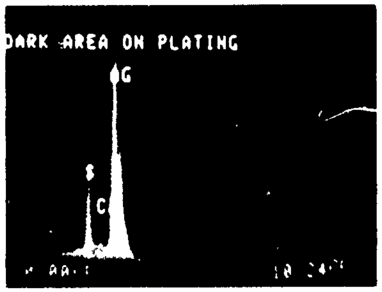

XES Spectra of Dark Stain Showing High Sulphur Content

Sulphur X-ray Map of Location Shown Above. Note Lower Intensity in Region of Spall

FD 236804

Figure 24. SEM Photomicrographs and XES Spectra of Thin, Dark Stains of Silver-Plated AISI 4340 Steel Showing "Mudcracked" Morphology and High Sulfur Content in Locations of Corrosive Attack (Accessory Bearing H)

Mag 1000X
"Mudcracked" Region Showing Location of Spalls of Silver/Silver Sulfide

Mag 3000X
Pit Formed as a Result of Spalling of Silver/Silver Sulfide

Example of Silver Particle Lodged in Extreme Right of Indentation or Incipient Spall of Functional Surface of Outer Race

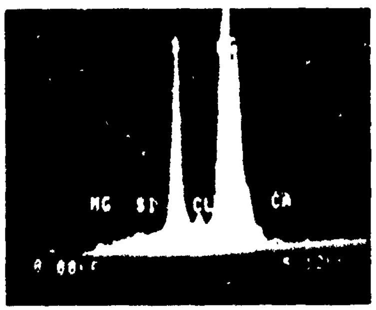

XES Spectra of "Mudcracked" Area Adjacent to Pit

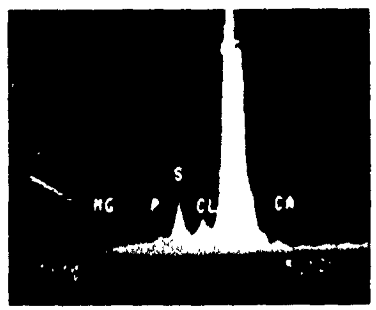

XES Spectra of Pit Bottom Note Lower Sulfur Intensity (Less Attack) and High Silver Intensity (Plate Still Intact)

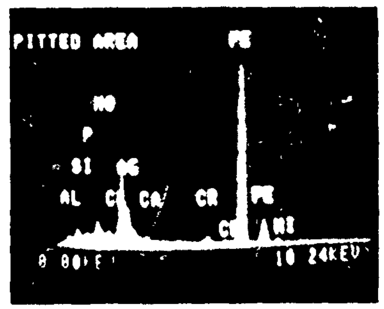

XES Spectra of Above Particle Note High Silver Intensity

FD 236805

Figure 25 SEM Photomicrographs and XES Spectra of "Mudcracked" Morphology of Silver-Plated AISI 4340 Steel Cage and Damaged Bower 315 Steel Outer Race (Main Shaft Bearing K)

Mag 200X

Roller Surface Showing Scratches, Indentations, and Mudcracking Corrosion

Mag 2000X

Embedded Particle in Roller Surface

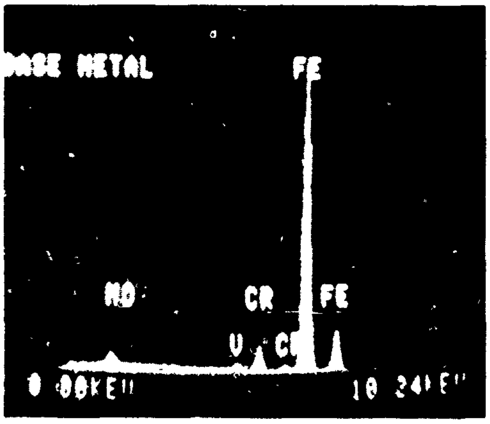

XES Spectra of M50 Base Material

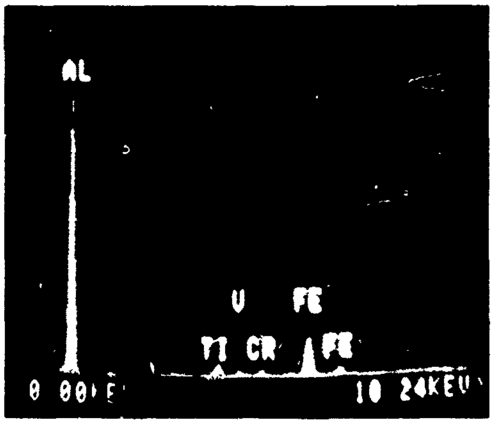

XES Spectra in Location of Embedded Particle Above

FD 236806

Figure 26. SEM Photomicrographs and XES Spectra of M50 Steel Roller Exposed to Service and Storage Environments (Accessory Bearing G)

4146C

Mag 800X
Mudcracked Region

Molybdenum X-ray Map

Chromium X-ray Map

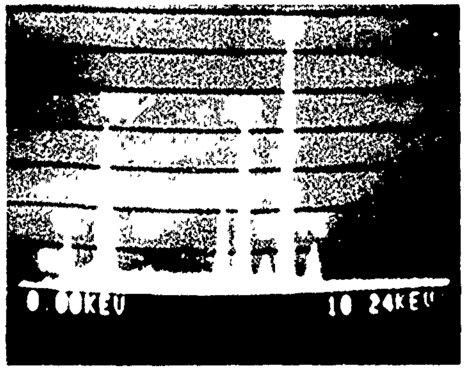

XES Spectra of Mudcracked Region
Compare Spectra of M50 Base Material
Figure 26

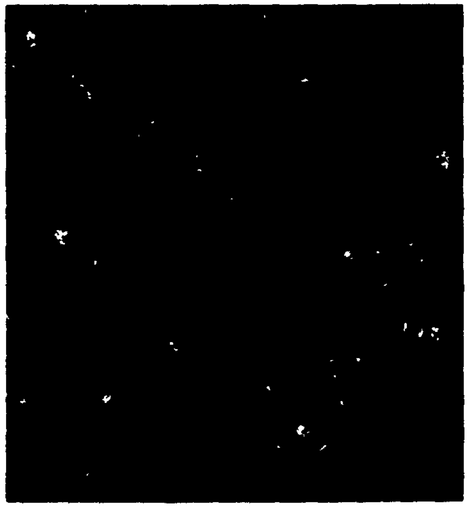

Aluminum X-ray Map Showing Large
Number of Embedded Particles

Vandadium X-ray Map

FD 236807

Figure 27. SEM Photomicrographs, XES Spectra, and X-ray Maps of "Mudcracked" Region of Figure 26 Showing Relative Enrichment of Alloying Elements Due to Leaching Away of Iron Corrosion Products

Mag 1 1/2X
Typical Appearance of Corrosion
of Non-Functional Surfaces

Mag 1 3/4X
Pitting Corrosion at Preservative-Atmosphere
Phase Boundary on Outer Race Surface

FD 230891

Figure 28. Corrosion of Main Shaft Bearing D Inadequately Preserved During Delay in Assembly

3. Analyses of Preservatives and Used Engine Oils

To determine the source of reactive species responsible for the corrosion of bearings, short-term preservative MIL-C-15074C, long-term preservatives MIL-C-11796B and MIL-C-16173D, and engine oils MIL-L-7808 and MIL-L-23699 were analyzed.

1) Storage Preservatives

Samples of storage preservative from three freshly opened mainshaft bearing *skin-packs* (MIL-C-11796B or MIL-C-16173D), as well as, samples of a long-term preservative (MIL-C-11796B) and a short-term preservative (MIL-C-15074C) were analyzed for sulfur, chloride and water content with the following results as listed in Table 1.

Mag 60X

Mag 200X

Corrosion of Non-Functional Surface

Mag 900X

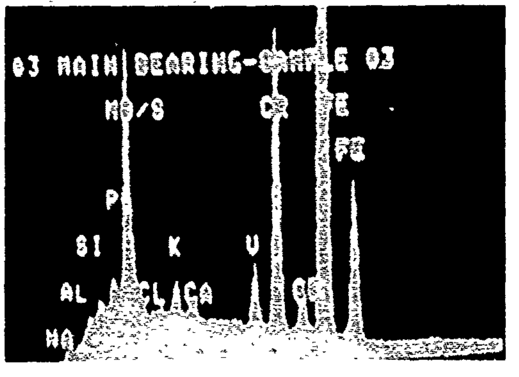

XES Spectra of Scale at Left

FD 236808

Figure 29. SEM Photomicrographs and XES Spectra of "Mudcracking" Corrosion of M50 Steel, Nonfunctional Surfaces (Main Shaft Bearing D)

Mag 10X

Crescent Shaped Pitting Attack
Seen in Figure 28

Mag 60X

Mag 400X

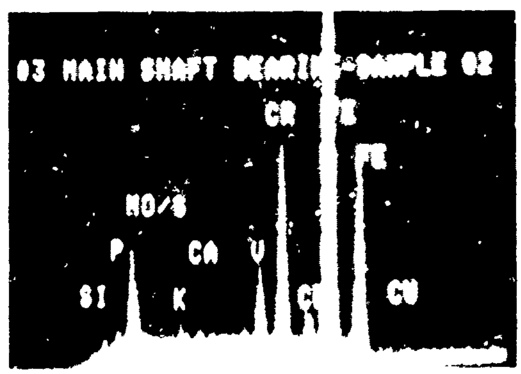

XES Spectra in Location at Left

FD 236809

Figure 30. SEM Photomicrographs and XES Spectra of Pitting Attack of M50 Steel Outer Race Along Phase Boundary (Main Shaft Bearing D)

4146C

TABLE 1. STORAGE PRESERVATIVES

Preservative	*Bearing*	*Sulfur*	*Chloride*	*Water*
MIL-C-11796B (or MIL-C-16173D)	M	0.56W%	≥0.0028W%	Not Run
MIL-C-11796B (or MIL-C-16173D)	N	0.20W%	≥0.0024W%	0.14V%
MIL-C-11796B (or MIL-C-16173D)	A	0.13W%	≥0.0023W%	0.12V%
MIL-C-11796B	N/A	0.30W%	≥0.0024W%	0.09V%
MIL-C-15074C	N/A	0.14W%	≥0.0013W%	0.06V%

W% = Weight percent

V% = Volume percent

Despite the lower mobility of ions and water in the viscous preservatives, these levels of contaminants are expected to cause corrosion of bearings based on tests conducted at P&WA/GPD and the Navy (Reference 5), where corrosion of M50 steel was observed in oils contaminated with only 0.0003 weight percent (W%) chloride and 0.0600 W% water.

2) Service Oils

Similar efforts were made with the service environment fluids (MIL-L-7808 and MIL-L-23699 oils). Requests to the Air Force and Navy have resulted in samples of used engine oils from a variety of sources (Table 2). Unfortunately, analyses of these oils for the reactive species sulfur, chloride, and water were frustrated because the levels of these contaminants were at or below the threshold of detectability of the available analytical instruments. Because of the lack of resolution, the data remains incomplete, except that the chloride concentration for all of the oils is probably less than 0.0005 W% (5 ppm).

Higher levels of water contamination were encountered, but no significant trend could be established. Results of oil analyses from water wash tests of a test engine indicate that condensation during cool down and changes of weather are more significant contributors to the water content of the oil than the water washing procedure (Table 3).

4. Galvanic Cell Tests

Galvanic corrosion could multiply the rate of attack above that of crevice or pitting corrosion alone. With the use of dissimilar metals (silver plate vs M50 and AISI 4340 steel) in bearing construction, the confirmed presence of several potentially reactive chemical species that readily dissociate in water solution and water contamination of preservatives and oils, all of the elements required for galvanic corrosion are present. In a bearing, a local galvanic cell could be formed by interposing between the steel components and the silver plate, condensation water in petroleum solution containing dissolved ions from the surrounding environment.

TABLE 2. HISTORY AND ANALYSIS OF USED ENGINE OILS

Base	*Total Engine Time (hours)*	*Oil Type*	*Time On Oil (hours)*	*Sulfur (W%)*	*Chloride (W%)*	*Water (V%)*
366TH TFW	—	7808	501	<0.002	<0.0005	0.01
Mt. Home AFB	—	7808	62	<0.002	<0.0005	0.02
	—	7808	311	<0.002	<0.0005	0.01
	—	7808	248	<0.002	<0.0005	0.01
Oceana NAS	1173	23699	—	<0.002	<0.0005	0.03
VA	1581	23699	190	<0.002	<0.0005	0.02
	902	23699	473	<0.002	<0.0005	0.03
	578	23699	578	<0.002	<0.0005	0.05
27th AGS	1734	7808	268	<0.002	<0.0005	0.025
Cannon AFB	951	7808	18	0.002	<0.0005	0.010
NM	964	7808	13	0.002	<0.0005	0.16
	1210	7808	263	<0.002	<0.0005	0.015
48th TFW	652	7808	652	0.003	Not Run	0.02
Lakenheath	493	7808	493	<0.002	Not Run	0.01
RAFB	489	7808	489	<0.002	Not Run	0.01
England	369	7808	117	<0.002	Not Run	0.01
20th TFW	—	7808	48	<0.002	Not Run	0.01
RAFB, Upper	—	7808	106	<0.002	Not Run	0.01
Heyford	—	7808	297	<0.002	Not Run	0.01
England	—	7808	498	<0.002	Not Run	0.01
48th TFW	2328	7808	562(TSO)	0.002	Not Run	0.12
Lakenheath	1052	7808	468(TSO)	<0.002	Not Run	0.10
RAFB	655	7808	—	<0.002	<0.0005	0.10
England	922	7808	649(TSO)	0.002	Not Run	0.03
PWA-GPD		7808	144	<0.001	Not Run	0.015
		7808	—	Not Run	Not Run	0.015 to 0.040

TABLE 3. OIL ANALYSIS RESULTS AFTER ENGINE WATER WASHDOWN

Engine Test Conditions	*Duration*	*Material Ingested*	*Rate of Ingestion*	*Volume-Percent Water in Oil*	
				Before	*After*
Idle	5 hr	Water	10 gal/min	0.015	0.03
Idle	10 min	Water + B&B 3100*	2.5 gal/min	0.04	0.02
Windmill	2 min	Water + B&B 3100	2.5 gal/min	0.02	0.02
Static	Overnight	—	—	0.02	0.04

*B&B 3100 — Concentrated liquid compound for cleaning gas paths in turbine engines (FSN 6850-181-7547).

4146C

To measure the galvanic potential of the silver-M50 and silver-AISI 4340 couples, samples of M50 and AISI 4340 steels were placed one at a time in a 3 W% sodium chloride solution coupled across a high impedence, high resolution voltmeter to a silver electrode also immersed in the salt solution. The potential generated for the M50 silver couple rose rapidly to approximately −0.23 vdc then more slowly, finally stabilizing around −0.550 ±0.015 vdc after 45 minutes. A similar performance of the AISI 4340 — silver couple was recorded with a final reading of −0.575 ±0.010 vdc.

Thus, the possibility for galvanic corrosion between the steel components and the silver-plating of bearings was confirmed.

5. Accelerated Corrosion Tests

Tests were conducted to evaluate the effects of various concentrations of sulfur and cloride ions in oil on M50 steel and silver-plated coupons.

Elemental sulfur along with several short chain organic mercaptan compounds dissolved in a neutral medium (water saturated mineral oil) were evaluated in simple qualitative tests for corrosive attack (staining) of silver plated coupons. Water-saturated mineral oil mixtures evaluated included: Sulfur, sulfur dissolved in carbon disulfide, carbon disulfide (control), sulfur dissolved in carbon tetrachloride, carbon tetrachloride (control), thioacetamide, sulfanilic acid, ethanethiol, 2-mercaptoethanol, benzenethiol, and thiophene. Of the mixtures tested, only those containing elemental sulfur and thioacetamide would stain silver plate within a 24-hour period at room temperature. 2-mercaptoethanol had to be heated to 180°F before it would attack the silver during a similar interval.

Mixtures which produced relatively rapid attack of the silver plate, however, inevitably presented miscibility problems with oils. Therefore, tests were first conducted to evaluate the ability of MIL-C-15074C, MIL-L-7808J, and MIL-L-23699C oils to counteract the corrosive effects of saturation with water, chloride ions, and reactive sulfur. The oils were saturated with these contaminants by first emulsifying water, thioacetamide, and sodium chloride (to an equivalent of 0.1000 W% water, 0.0100 W% chloride, and 0.0100 W% sulfur), allowing time for equilibrium and phase separation, then decanting of the saturated oil over M50 steel/silver plated coupon pairs. Specimens exposed to the contaminated oils, along with controls, were then placed in an oven at 140°F for 24 hours. Results indicated MIL-L-23699C oil was superior followed by MIL-L-7808J then MIL-C-15074C (Figures 31 through 33). The silver-plated coupons exhibited stains ranging from very light (MIL-L-23699) to very heavy (MIL-C-15074C). The M50 steel components were unaffected, indicating the need for longer duration tests.

M50 steel and silver plated pairs were also tested by immersion in dry mineral oil solutions containing tritylthiol (triphenymethyl mercaptan) at 0.0100 W%, 0.0020 W% and 0.005 W% sulfur concentrations and solutions containing trityl chloride (chlorotriphenylmethane, triphenylmethyl chloride) at the same levels of chloride concentration. Samples were again placed in an oven at 140°F for 24 hours. Results indicated that the silver plate was the most susceptible material to attack by both chloride ions and reactive sulfur down to the lowest concentrations tested, sulfur producing the heaviest stains. M50 steel was unaffected by the reactive sulfur and all but the highest concentrations of chloride ions (Figures 34 through 39).

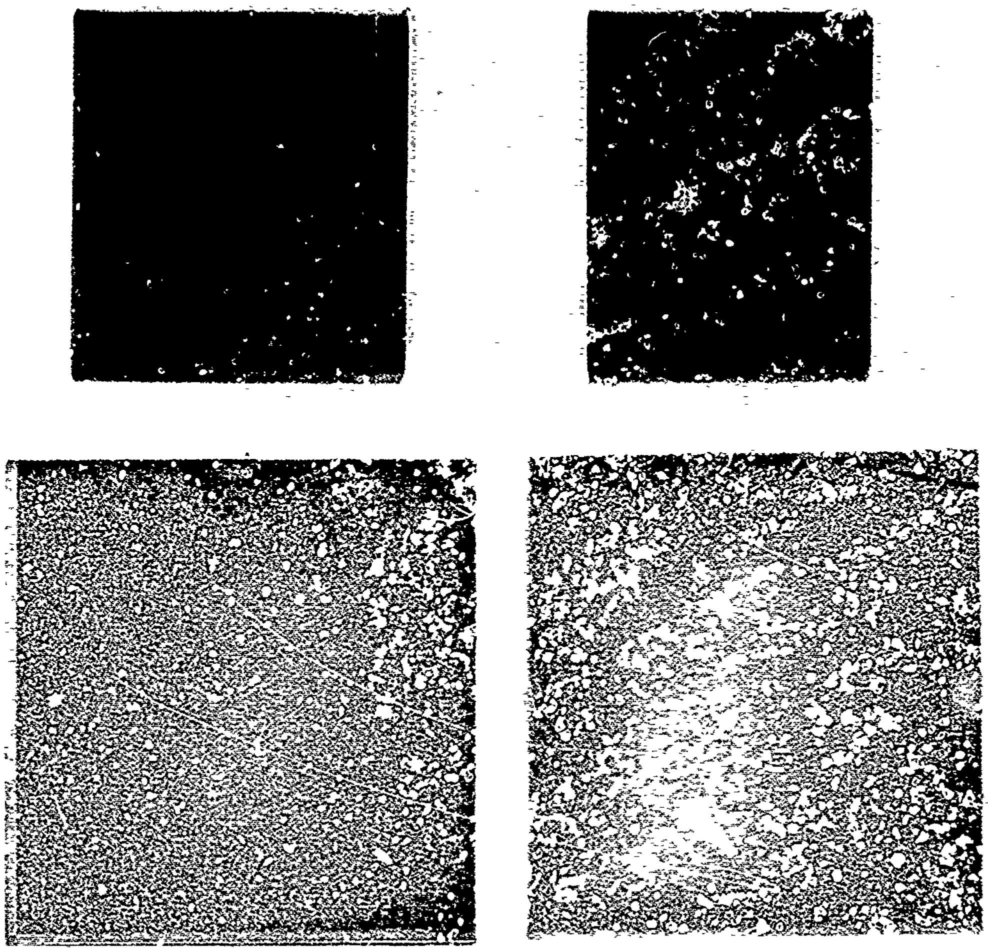

FE 352627

Figure 31. Specimens (M50 Steel at Top; Silver-Plated Coupon at Bottom) Exposed to MIL-L-23699 Oil (Contaminated at Left; Control at Right) at 140°F for 24 Hours

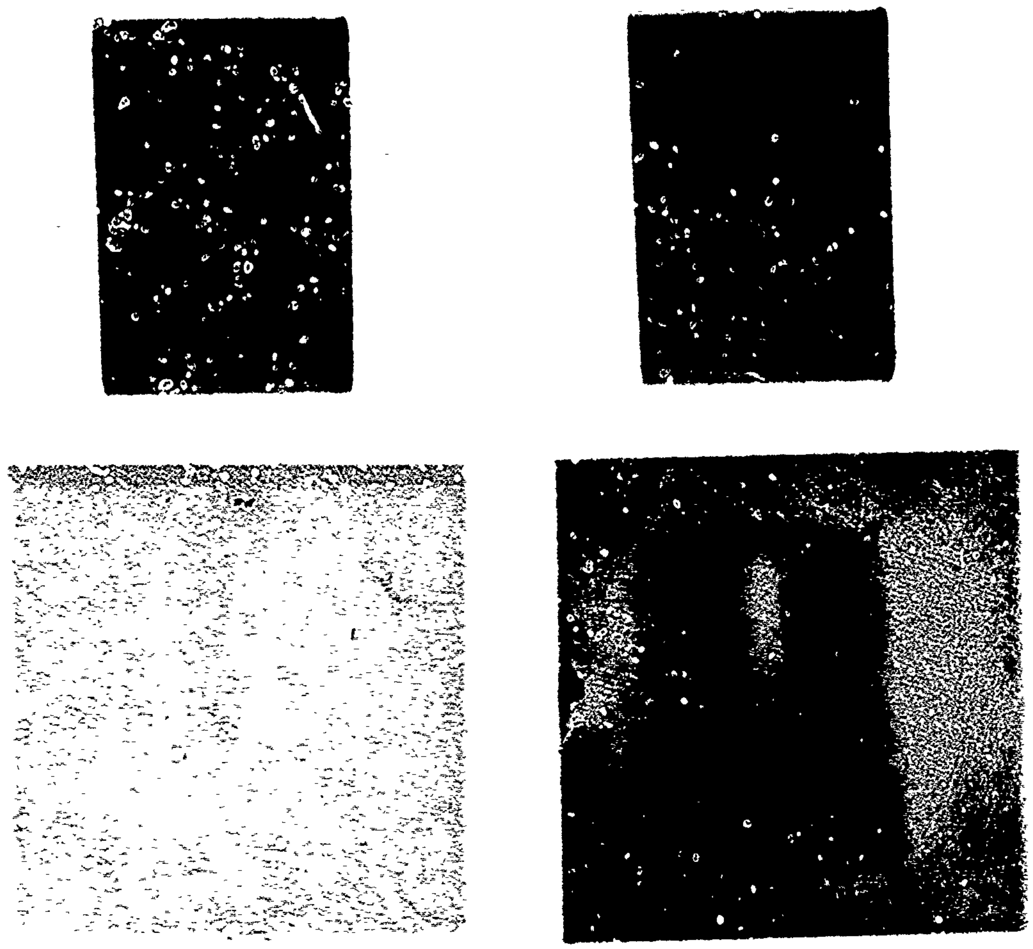

FE 352625

Figure 32. Specimens (M50 Steel at Top; Silver-Plated Coupon at Bottom) Exposed to MIL-L-7808J Oil (Control at Left; Contaminated at Right) at 140°F for 24 Hours

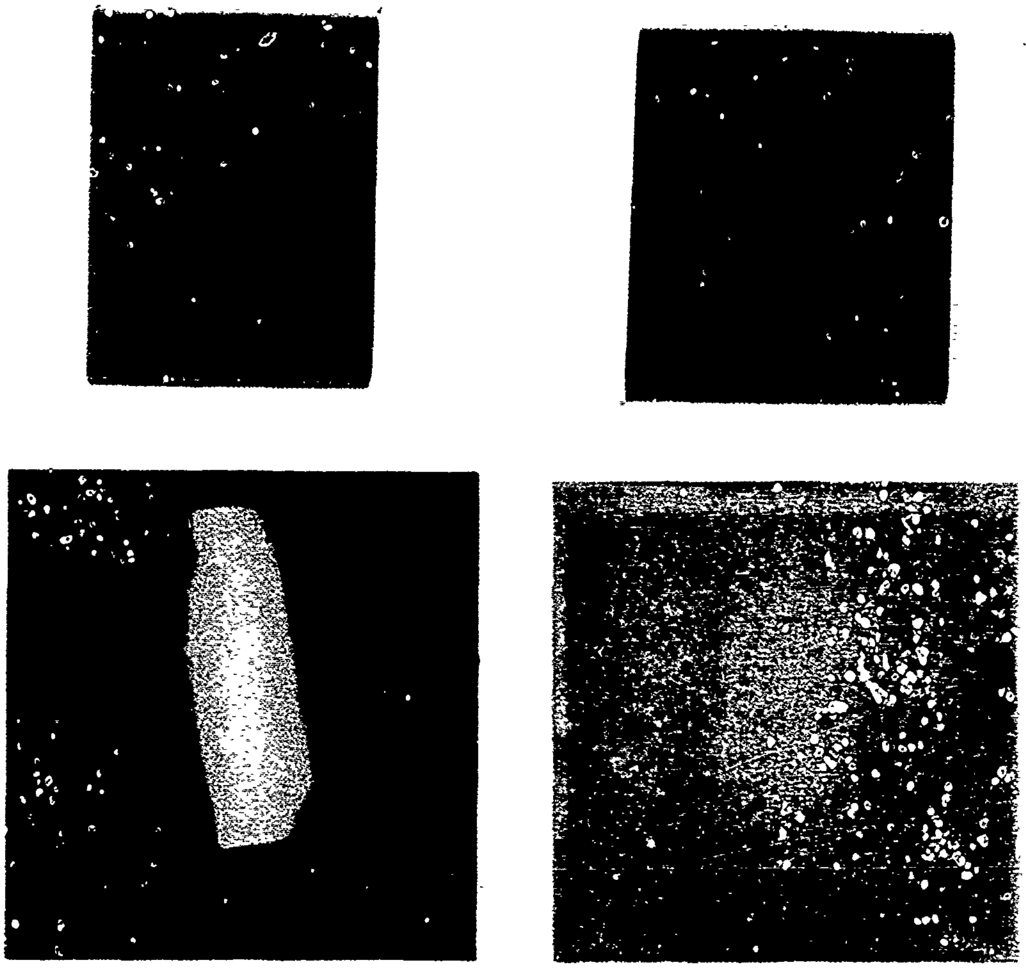

F. 352623

Figure 33. Specimens (M50 Steel at Top; Silver-Plated Coupons at Bottom) Exposed to MIL-C-15074C Oil (Contaminated at Left; Control at Right) at 140°F for 24 Hours

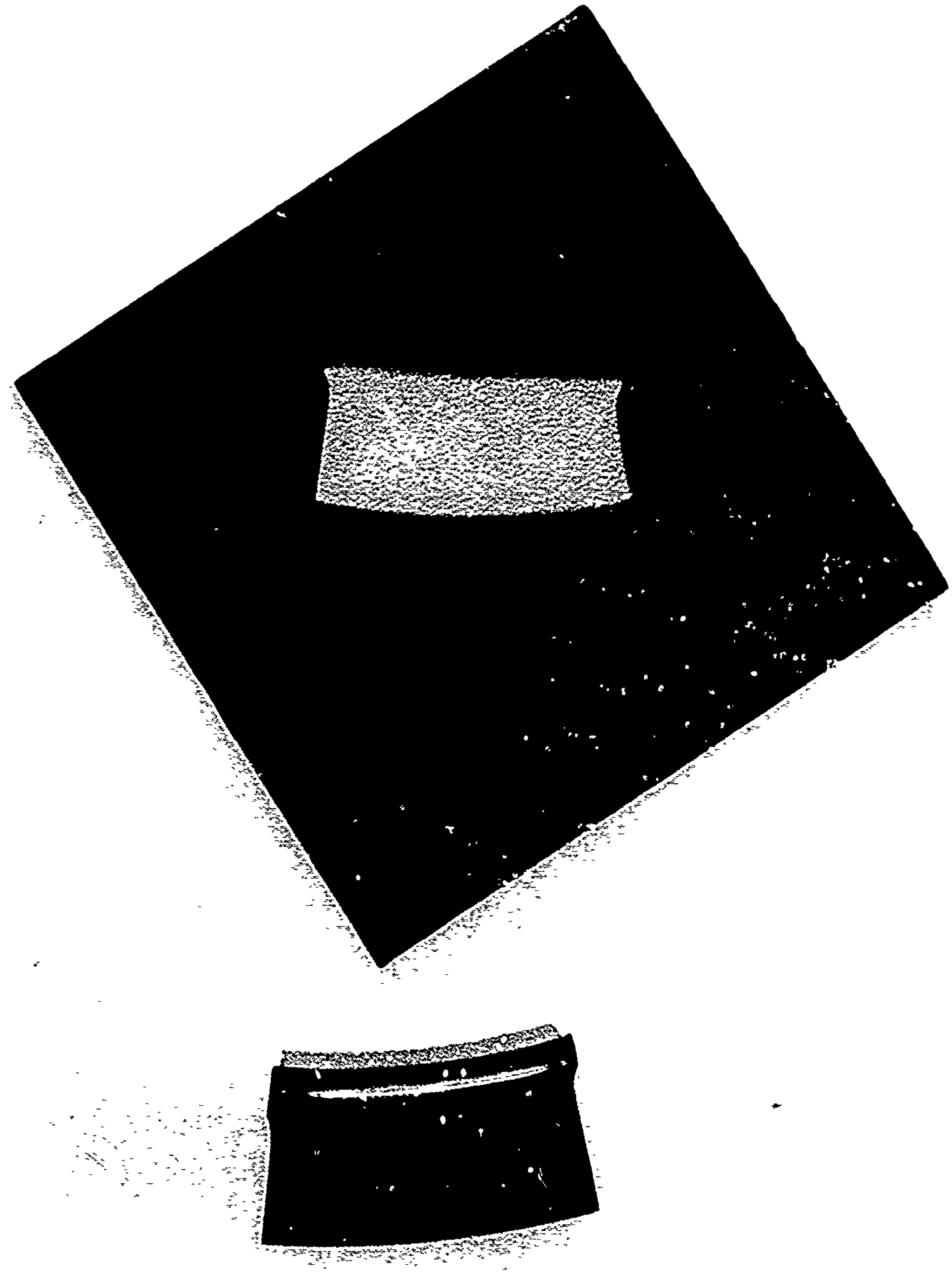

FE 352750

Figure 34. Specimens (M50 Steel at Bottom; Silver-Plated Coupon at Top) Exposed to 0.0005 Wt% Sulfur (as Trityl Thiol) in Mineral Oil at 140°F for 24 Hours

4146C

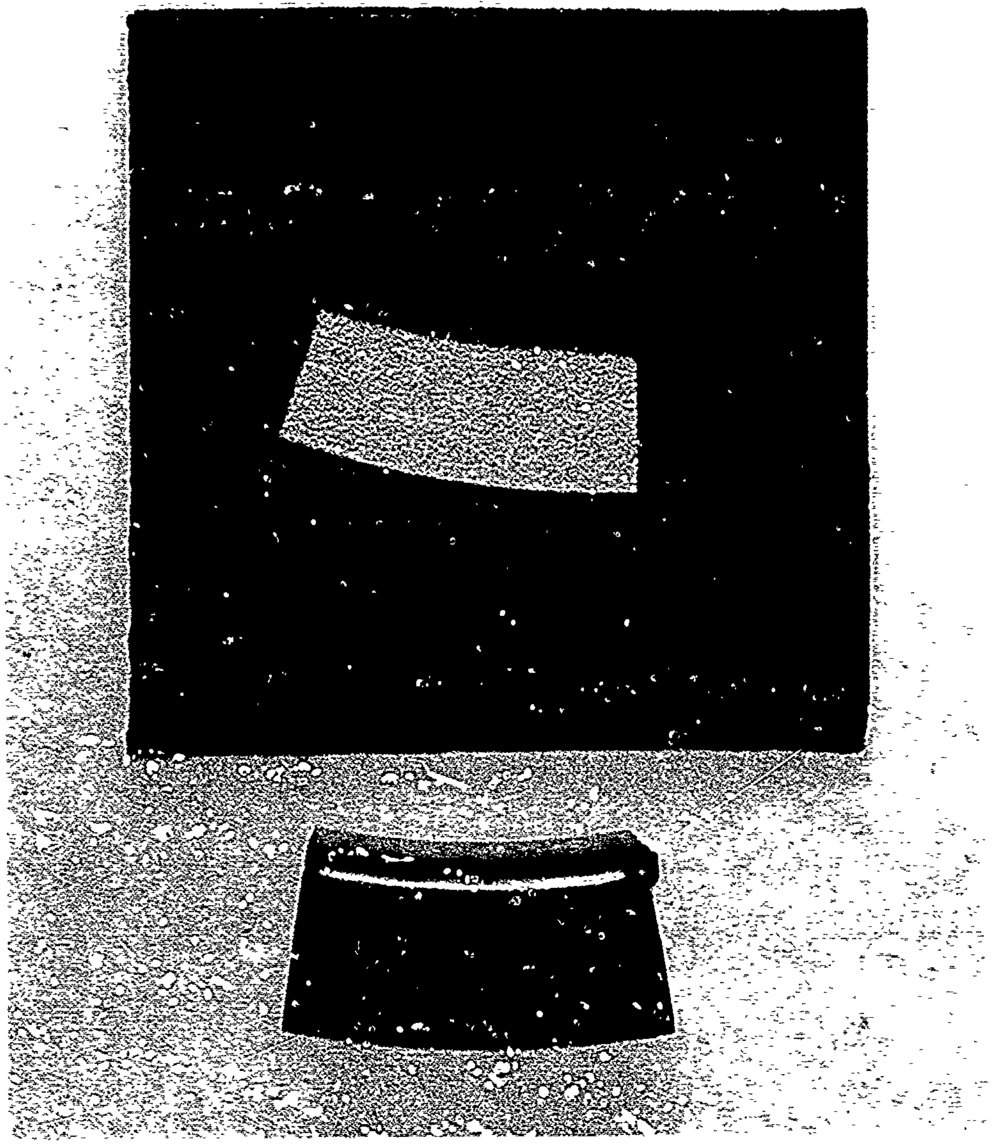

FE 352751

Figure 35. Specimens (M50 Steel at Bottom; Silver-Plated Coupon at Top) Exposed to 0.0020 Wt% Sulfur (as Trityl Thiol) in Mineral Oil at 140°F for 24 Hours

41461

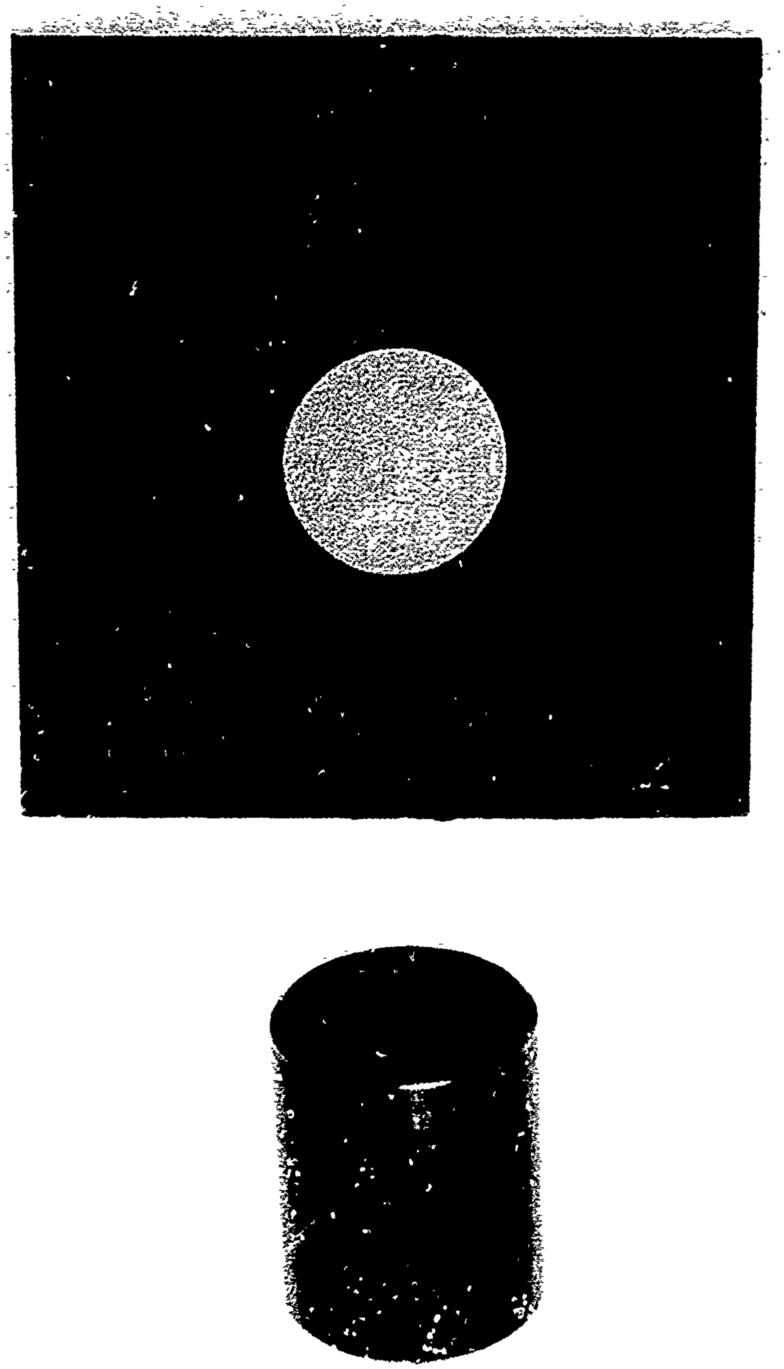

FE 352740

Figure 36. Specimens (M50 Steel at Bottom; Silver-Plated Coupon at Top) Exposed to 0.0100 Wt% Sulfur (as Trityl Thiol) in Mineral Oil at 140°F for 24 Hours

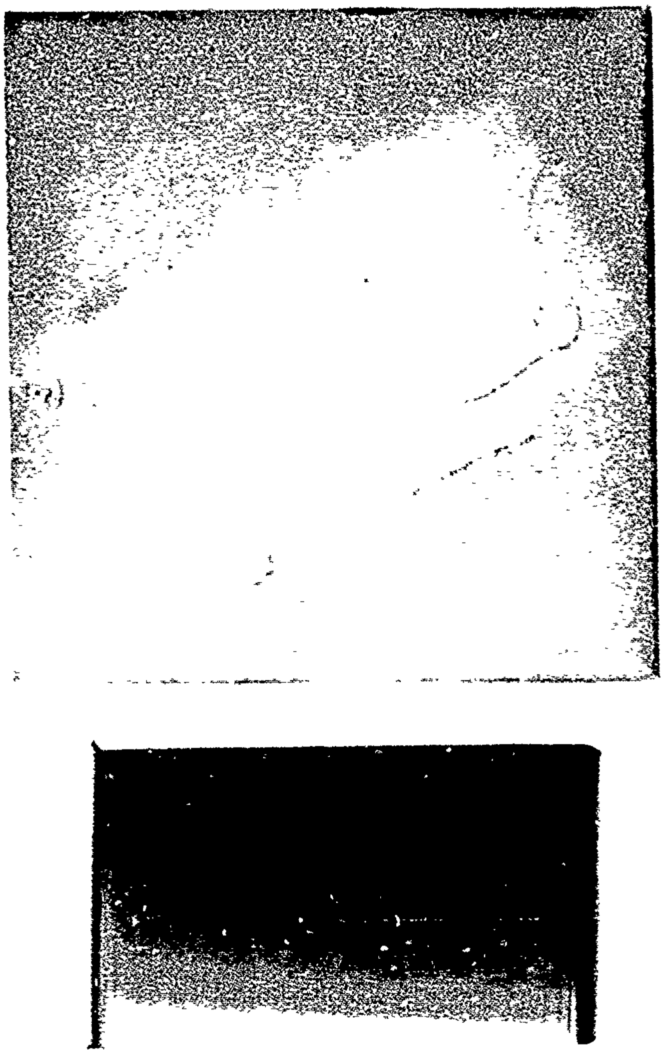

FE 352726

Figure 37. Specimens (M50 Steel at Bottom; Silver-Plated Coupon at Top) Exposed to 0.0005 Wt% Chloride (as Trityl Chloride) in Mineral Oil at 140°F for 24 Hours

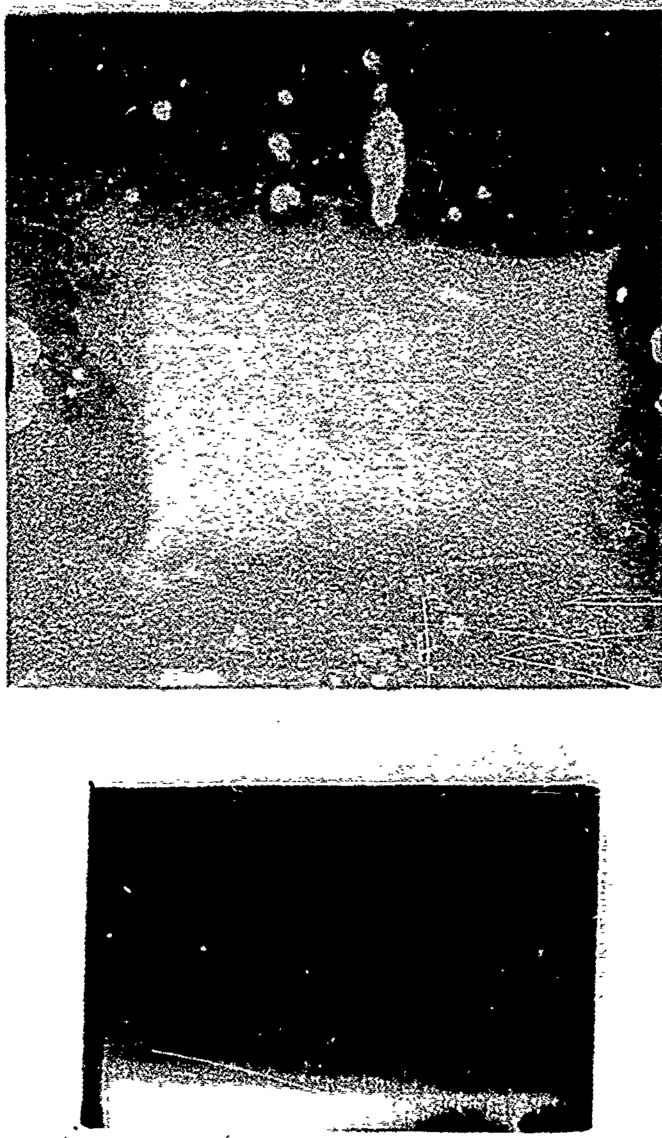

FE 352725

Figure 38. Specimens (M50 Steel at Bottom; Silver-Plated Coupon at Top) Exposed to 0.0020 Wt% Chloride (as Trityl Chloride) in Mineral Oil at 140°F for 24 Hours

4146C

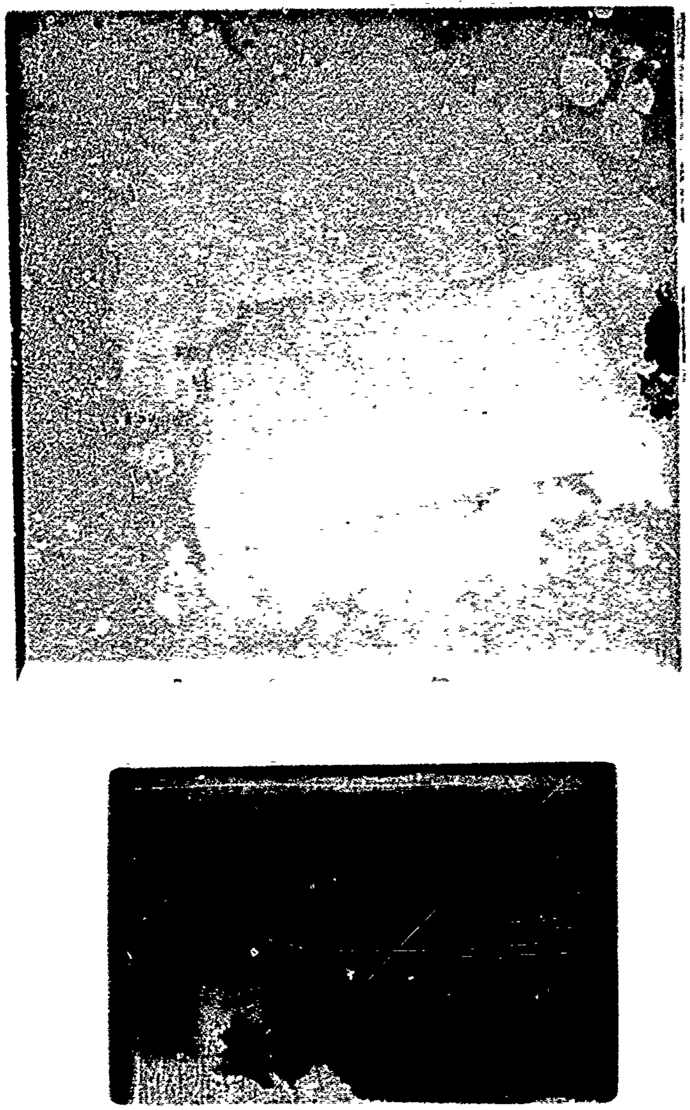

FE 352724

Figure 39. Specimens (M50 Steel at Bottom; Silver-Plated Coupon at Top) Exposed to 0.0100 Wt% Chloride (as Trityl Chloride) in Mineral Oil at 140°F for 24 Hours

4146C

6. Corrosion Investigation Conclusions

- The results of the studies indicate that water, chloride ions, reactive sulfur and oxygen are the principal contaminants responsible for corrosion of bearings.

- Temperature and temperature cycles also contribute to the corrosion problem as they affect reaction rates and the saturation level of contaminants in oils and preservatives.

- Random instances where improper handling procedures are employed are also contributing factors in that they impact the above conditions.

- The principal sources of the contaminants include:

Water	—	Condensation in the lubrication system and preservation processing operations Improper handling procedures
Chloride ions	—	Improper handling procedures Engine ingestion of humid, salt laden air Occur as a standard petroleum contaminant
Reactive sulfur	—	Occurs as a standard petroleum contaminant Possible result of a reduction of sulfur compound in bearing corrosion inhibitors
Oxygen	—	Air in lube system Also occurs dissolved in water and oil

- Corrosion mechanisms responsible for the attack of bearings in storage and service are similar in nature and include pitting and intergranular corrosion.

C. CANDIDATE SELECTION

1. Initial Screening

Increased bearing corrosion resistance can be achieved by using corrosion resistant alloys or by providing a protective coating or surface treatment to existing alloys. With either approach, bearing performance should at least equal the state of the art bearing alloy; VIM-VAR M50. In the initial screening and subsequent testing, candidates had to show superior corrosion resistance, as well as, equivalence in rolling contact fatigue, hot hardness and wear resistance compared to a VIM-VAR M50 baseline.

For the initial screening, the material reference resources and (in the absence of hard data) the metallurgical experience of Pratt & Whitney Aircraft, TRW Inc. and material supplier contacts were surveyed.

For preliminary consideration, a list of 28 candidates with potential for rolling element bearing application was compiled. The list included some materials which were lacking in certain state of the art turbine engine bearing properties. These materials were included to insure that consideration was given to materials which potentially might benefit from coatings, surface treatment or other material processing.

Even as the preliminary list was being generated, the candidates with the greatest and least potential for success were being identified. The first culling reduced the list of 28

candidates to 17 candidates. This ranking was based on obvious and inferred risks and deficiencies with respect to basic bearing material properties.

The list of 17 candidates is presented in Table 4. The list includes 8 alloys and 9 coatings. Seven of the eight alloys (MRC2001, RSR405, BG42, CRB7, WD65 and 14-4 Mo) are high chrome martensitic steels. Studies conducted in the past several years (Reference 6 and 7) have shown that high chrome stainless steels, potentially suitable for high temperature, high performance bearings, can be developed. These steels achieve corrosion resistance by forming a passive iron-chrome oxide film at the surface. They may be hardened by conventional heat treat techniques. Some of these alloys are currently used in rolling element bearings.

Powder metallurgy is an alternate processing technique with the potential for significant alloy modifications and microstructural improvements. Potential benefits include finer and more uniformly distributed carbides, better homogeneity of alloying elements, and improved material utilization due to near net shape forming.

Four of the alloy candidates considered were powder processed materials; MRC2001, RSR405, WD65 and CRB7 (CRB7 was also considered in wrought form). MRC2001 is an experimental alloy being developed for rolling contact bearing use and it had shown excellent corrosion resistance in preliminary tests at TRW. These tests ranked MRC2001, CRB7, WD65, and M50 in corrosion resistance and included tests identical to the corrosion screening tests performed in Task III of this program, as well as more severe salt spray tests. The properties of MRC2001, including hot hardness, were expected to exceed VIM-VAR M50. RSR405 is a high chrome, potential bearing alloy which was investigated in a related P&WA program, "Application of Rapidly Solidified Alloys" Contract F33615-76-C-5136. Rolling contact fatigue test results from this program showed life equal to M50. In an earlier program (Contract F33615-75-C-2009), P&WA demonstrated that powder processed CRB7 (AMS5900) had a rolling contact fatigue life (RCF) at least equal to, and in most cases better than, M50 in single ball tests. A concurrent rolling contact fatigue bar test performed by the USAF also showed CRB7 to be at least equal to M50.

All the powder processed materials incorporated a degree of risk in that all were unproven experimental bearing alloys and the process development and qualification procedures required for production use of powder metallurgy bearings may exceed the 3- to 5-year introduction goal.

BG42 (AMS5749) is another stainless steel that is potentially suitable for high performance bearing applications. PWA has experience with BG42 bearings in the exhaust nozzle air motor for an Air Force F100 engine. In this application, the BG42 bearings operate dry and at a very high temperature, about 700°F. This environment differs radically from that of a mainshaft bearing but it did demonstrate suitability of BG42 for production and for high temperature applications. Rolling contact element life tests comparing VIM-VAR BG42 and VIM-VAR M50, (Reference 6) showed fatigue life at least equal to VIM-VAR M50.

The commercial availability and excellent preliminary rolling contact fatigue results for both CRB7 and BG42 made those two high chrome alloys prime candidates for use in high performance corrosion resistant bearings. Both alloys have demonstrated hot hardness equal to M50, (Reference 8 and 9). In addition, these alloys are commercially available in wrought form as is the currently used VIM-VAR M50.

TABLE 4. LIST OF POTENTIAL CANDIDATES

		Chemical Composition											Hardness			Heat		
Candidate	*Process*	*Cr*	*C*	*V*	*Mo*	*Co*	*Ni*	*Mn*	*Si*	*W*	*Fe*	*Other*	*RT*	*400*	*800*	*Treat*	*Wear*	*Impact*
BG 42	Wrought	15	1.2	1.2	4			0.45	0.3		Bal		62	62	57	2050/950		
14-4 Mo	Wrought	14.5	1.07	0.15	4			1.0	1.0		Bal		60-63		54	2000/1000		IZOD 31.0
CRB7	Wrought	14	1.1	1	2			0.4	0.3		Bal	0.25Cb	61		57	2100/400		M/CVN 12
CRB7	Powder Metallurgy	14	1.1	1	2			0.4	0.3		Bal	0.25Cb	61		57	2100/400	Poor	M/CVN 12
WD65	Powder Metallurgy	14	1.1	2.8	4		5.3	0.2		2.4	Bal	0.15S	58-62	54-57	47	2100/1000	Poor	M/CVN 7-8.5
MRC2001	Powder Metallurgy	15	1.3	1.8	6.5			0.5			Bal	0.05Cb	60-62	54-57	50	2100/1000	Excellent	M/CVN 8
RSR405	Powder Metallurgy	19	1.3	1	2						Bal							
CBS 1000M	Wrought	1.07	0.11	0.37	4.5		3.0	0.5	0.5		Bal	0.03AL	61	59	53	2000/1000		
Armoloy	Plating																	
Nobilizing	Plating																	
Chrome	Sputter Coating																	
Nickel	Sputter Coating																	
Gold	Sputter Coating																	
Silver	Sputter Coating																	
Chrome Carbide	Sputter Coating																	
Titanium Carbide	Sputter Coating																	
Black Oxide	Salt Bath																	

AISI 440C is a common high carbon stainless steel which is widely used in bearing applications, but is not suitable for gas turbine use because of poor hot hardness characteristics. 14-4 Mo is a modified form of 440C. It has a molybdenum addition which improves the secondary hardening characteristics and hot hardness. The alloy is commercially available, but has not had extensive development testing for rolling contact bearing applications.

An alternate approach to achieve corrosion resistance is a protective coating or surface treatment applied to existing bearing materials. Coatings and surface treatments have the distinct advantages of being applicable to existing bearings and requiring a minimum amount of strategic elements. A successful coating or surface treatment must adhere to the substrate bearing material and endure millions of rolling contact stress cycles without impairing bearing performance. Conventional electroplates and electroless nickel have failed due to inadequate adhesion, allowing peeling and chipping to occur in the contact area (Reference 10). Three modern coating techniques were considered in this program, i.e., sputter coating, proprietary plating and black oxide coating processes. Chemical vapor deposition processes were not considered because the high substrate temperatures required would have adversely affected substrate hardness.

Ion implantation is a surface treatment that creates a surface alloy by injecting ions into a substrate. Depending on the ions and the substrate material the resulting surface alloy can have significantly improved corrosion resistance (Reference 5). The improved corrosion resistance of Cr, Cr + Mo and Cr + P ion implanted M50 specimens vs baseline M50 has been demonstrated by a joint Naval Air Propulsion Center/Naval Research Laboratory program. The improved corrosion resistance was achieved without expense to the substrate bulk properties. By joint USAF and P&WA agreement ion implantation was not considered as a candidate to avoid duplication of effort and to allow as broad a survey as possible of other potential candidates.

Two proprietary plating processes were considered. Armoloy and Noblizing have both shown potential for use in rolling contact bearing applications (Reference 10). Both of these processes deposit a thin (0.00005 to 0.00025 in.) coating of hard, dense chromium.

TRW Bearings Division has had good experience with Armoloy including ball bearings of both 52100 and M50 steel in a variety of applications including an experimental gas turbine engine. A partial listing of Armoloy-plated bearing applications is shown in Table 5.

TABLE 5. ARMOLOY-PLATED BEARING APPLICATIONS

Bearing	*Base Material*	*Application*	*Environment*
7203	52100	Ice Cube Machine	Water
R4	52100	Flow Meter	Sour (NaCl,S) Crude
7224/7228	52100	Stirring Motor	Polyethylene
R1907E101	M50	Exp Gas Turbine Engine	MIL-L-7808
9109UK108	M50	Exp Gas Turbine Engine	MIL-L-7808
2065	52100	Simulated Control Rod Mechanism (Nuclear)	De-Ionized Water

Sputtering is a physical vapor deposition technique. The coating chamber is evacuated to eliminate atmospheric gases, then back-filled with argon to low pressure, 1 to 30 $\times$ 10^{-3} torr. Figure 40 is a schematic representation of the RF diode sputtering process. An application of an RF potential of sufficient voltage to the target creates a plasma and accelerates positive argon ions to the target which is the coating material source. This ionic bombardment ejects (sputters) atoms from the target surface with sufficient energy to traverse the chamber and impact and bond to the substrate.

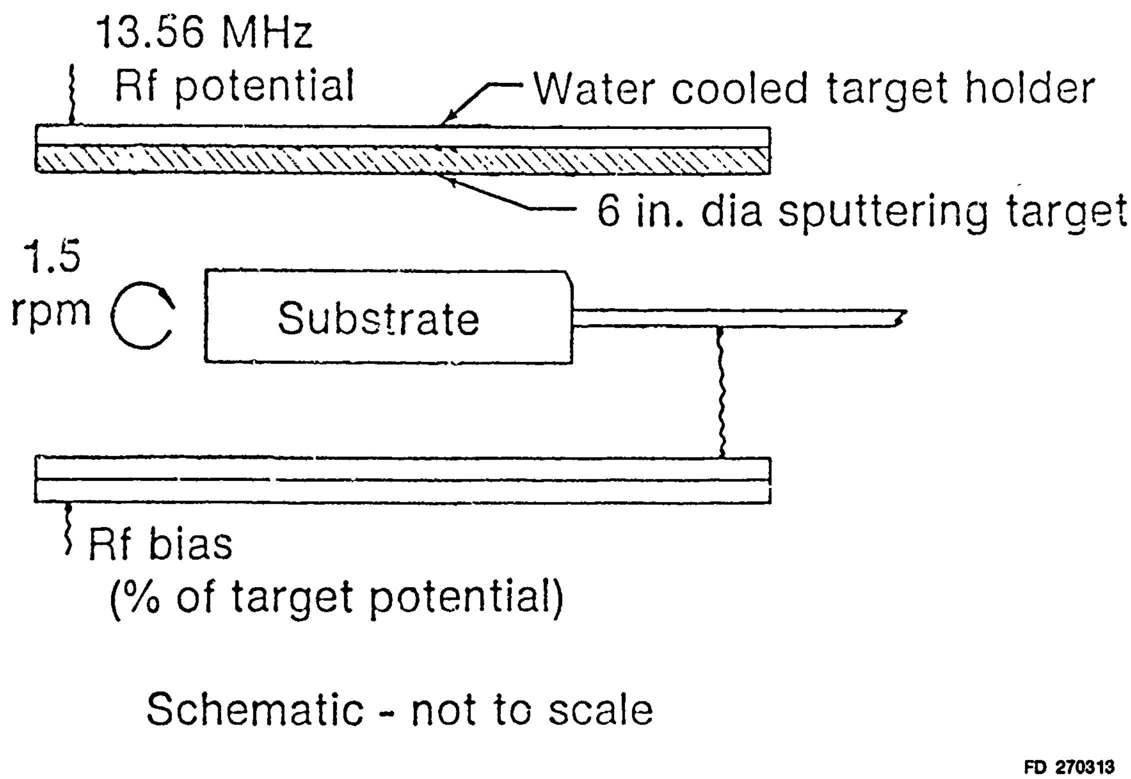

Figure 40. Diagrammatic Representation of the Radio Frequency (RF) Diode Sputtering Chamber

Adhesion is achieved by promoting interdiffusion. This may be accomplished by controlling substrate temperatures, which for bearing applications must be below the tempering temperature, and sputter etching of the substrate to remove impurities.

Almost all compounds and elements can be deposited by sputtering. P&WA has extensive experience with protective and wear resistant coatings including TiC on 440C and 52100 balls (not rolling element bearing applications, however). Selected initial candidate coating materials are from two classes of materials: (1) hard, wear resistant materials (chrome, chrome carbide, titanium carbide) and (2) the relatively soft, lubricating materials (gold, silver). Corrosion protection is achieved by enveloping the substrate M50 with a protective coating.

An oxide coating was also considered initially. In one study (Reference 11), bearings treated with a commercial black oxide coating and operated in a water environment showed significantly improved corrosion and wear resistance compared to noncoated bearings.

The natural oxide coating on steels confers a degree of passivity to the base material. This protection has been improved upon by several commercial processes which develop a thicker, stronger oxide film. These films do not provide much protection by themselves, but protective oils are retained by the porous coating.

Future turbine engines will require improved fracture toughness to accommodate anticipated higher rotor speeds. CBS1000M is a high temperature, secondary hardening,

carburizing steel with reported improved fracture toughness over M50. However, it has only 1% by weight of chrome compared to 4% for M50. It was included for consideration as an alloy which would provide an added benefit over M50 with the application of a corrosion resistant coating or surface treatment.

2. Initial Candidate Selection

State of the art turbine engine bearings are made from AISI M50 steel. The material was selected for turbine engine use due to its good rolling contact fatigue life, (RCF) life and high hot hardness.

In addition to superior corrosion resistance, any candidate selected for material property testing was required to be at least potentially equivalent in rolling contact fatigue, hot hardness and wear resistance.

All the material property data collected from literature searches and material supplier contacts was compiled for the 17 initial candidates. This initial ranking did not penalize an otherwise worthy candidate because of a lack of data. In order to allow a wider variety of candidates to be considered for basic material property evaluation, the secondary categories of frugal use of strategic elements, cost, other mechanical properties and potential for 3- to 5-year use were not weighed. It was decided that these criteria would be used to discriminate between otherwise equal candidates once back-to-back property data were available.

Given the lack of rolling contact fatigue data on coated candidates, it was assumed that fatigue life for a coated candidate would be the same as that of the substrate. For each category of RCF, corrosion resistance, wear and hot hardness a candidate was judged to be either better then (+), equal to (o) or less than (−) M50. A negative in any category was cause for elimination. Table 6 summarizes the results.

The remaining candidates were subdivided into four categories:

(a) State of the art corrosion resistant alloys
(b) Advanced powder processed corrosion resistant alloys
(c) Sputtered coatings (over M50 or CBS1000M)
(d) Proprietary chrome plating processes (over M50 or CBS1000M).

It was decided that risk to the program would be minimized and potential benefit maximized, if at least one candidate from each category were represented in the final list of five candidates.

Consideration was given in each category as to which candidate would provide the maximum information by tying into existing data. There appeared to be little difference between the chemically similar alloys CRB7 and BG42. Wrought CRB7 was chosen over BG42 because unexplained and disappointing wear data existed on powder processed CRB7 (Reference 7). It was felt that wear data on wrought CRB7 would provide additional data which might help in determining whether the process or the material was the cause of the wear.

TABLE 6. PRELIMINARY TASK 2 CANDIDATE SELECTION

Candidate	*Process*	*RCF*	*Corrosion Resistance*	*Wear Res.*	*Hot Hard*
BG 42	Wrought	0	+	0	0
CBS 1000M	Wrought	0	+ (with coating)	0	0
CRB7	Powder Metallurgy	0	+	– (Ref 7)	0
CRB7	Wrought	0	+	0	0
MRC2001	Powder Metallurgy	0	+	0	0
RSR405	Powder Metallurgy	0	+	0	0
WD 65	Powder Metallurgy	– (Ref 8)	+	0	0
14-4 Mo	Wrought	– (Ref 12)	+	0	0
Armoloy	Plating	0	+	0	0
Black Oxide	Salt Bath	0	+	– (Ref 11)	0
Chrome	Sputter Coating	0	+	0	0
Chrome Carbide	Sputter Coating	0	+	0	0
Gold	Sputter Coating	0	+	0	0
Nickel	Sputter Coating	0	+	0	0
Nobilizing	Plating	0	+	0	0
Silver	Sputter Coating	0	+	0	0
Titanium Carbide	Sputter Coating	0	+	0	0

Armoloy and Nobilizing were viewed as essentially equal in every respect. Armoloy was chosen because of TRW Bearing Division's previous experience with the process.

The corrosion resistance of all the sputtered coating candidates was judged equal. However, it was felt that the elemental metallic coatings could achieve adequate adhesion at lower substrate temperatures compared to either TiC or CrC. Sputtered elemental chrome was eliminated from consideration because a chrome coating, Armoloy, was already represented. Sputtered nickel was chosen over gold because of the availability and initial costs of target materials. Silver was eliminated because of the potential for galvanic attack at local defects. Nickel, being closer to steel in the galvanic series, should minimize this potential problem.

M50 was chosen over CBS1000M as the substrate material because back-to-back comparison with the M50 baseline would provide a means of isolating coating effects on property data.

RSR405 and MRC2001 are both experimental powder processed high chrome stainless steels. Existing data indicated both had RCF life at least equal to M50 and with 19% and 15% chrome respectively both were expected to exhibit excellent corrosion resistance. MRC2001 was selected as the fourth candidate. It was in a more advanced state of development compared to RSR405 and existing preliminary wear and corrosion test results were very promising.

To arrive at a fifth candidate, all categories were reviewed again. Two candidates surfaced as leading contenders: BG42 and RSR405. BG42 was initially selected over RSR405 because it was a readily available, lower risk, 15% chrome alloy with demonstrated corrosion resistance, whereas RSR405 was an experimental alloy with good potential but which required additional development. However, in subsequent discussions with the Air Force, it was decided that the Improved Corrosion Resistance Turbine Engine Bearings Program would be better served with RSR405, given its higher chrome content (19%), its unique rapid solidification rate powder processing and its encouraging RCF data.

Early in the course of the Program RCF testing, the RSR405 candidate experienced several premature spalls. RCF testing on this candidate was suspended and later examination revealed surface and subsurface aluminum oxide inclusions. There was also some evidence that the interdiffusion layer that existed between extrusion can material and the consolidated powder material after it has been extruded was not completely machined off during RCF specimen preparation.

The source of the aluminum oxide inclusions was traced to a crucible in which the alloy was melted during powder fabrication. In the interim period between the original candidate selection and the mechanical property testing, additional test results had become available from both an on-going P&WA Bearing Material Improvement Program and a Defense Advanced Research Project Agency (DARPA) sponsored program. In the DARPA program, "Application of Rapidly Solidified Alloys" (F33615-76-C-5136), RSR565, an experimental tool steel, had demonstrated superior RCF life compared to both M50 and RSR405. Also, preliminary data from the internal P&WA program, indicated that RSR565 had superior hardness retention characteristics compared to RSR405. RSR565, while not stainless by definition, was also expected to exhibit improved corrosion resistance compared to M50 because of its higher chrome and alloy content. RSR565 was readily available in form and quantity for Phase I evaluation, therefore, the Air Force program office was requested to, and did, approve the substitution of RSR565 for the RSR405 candidate.

As part of an ongoing P&WA material development program, an experimental high chrome RSR material, RSR113, was also evaluated for rolling contact fatigue life and corrosion resistance and the results are included as a part of this report.

3. Test Specimen Fabrication

1) Armoloy-Coated M50

Armoloy is a proprietary electro chemical hard chrome plating process. The coating thickness is self-limiting. The coating thickness range is 0.00005 to 0.00025 which reportedly is controllable to 0.0001.

The coating thickness of the specimens used in this program ranged from 0.00008 to 0.00009 in. in the as-received condition. An SEM photomicrograph of a cross sectioned Armoloy-coated specimen is presented in Figure 41.

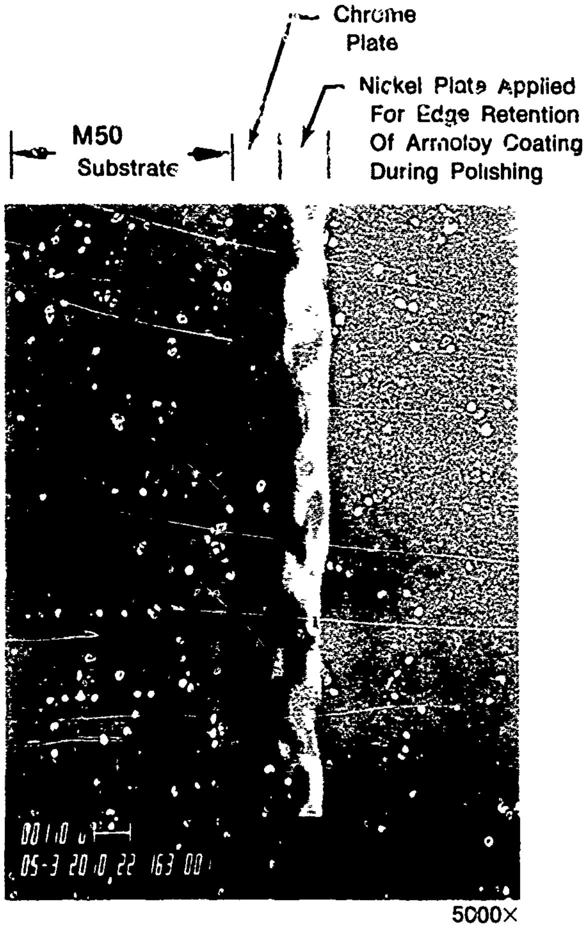

FD 270302

Figure 41. SEM Photomicrograph of a Cross-Sectioned "As-Received" Armoloy-Coated M50 Test Specimen

The Armoloy coating as received had a coarser average surface finish (9.2 micro inch) than either the VIM-VAR M50 substrate (4.6 micro inch avg) or the other candidates test specimens (4.6-5.4 micro inch avg) used in this program. To determine qualitatively what effect this coarsened surface finish would have on RCF life, the Armoloy test bars were split into two test lots. One lot was left in the as-received condition and the second lot was hand-polished on a coarse natural cellulosic fiber wheel using an iron oxide polishing compound to an average surface finish of 5 4 micro inch.

SEM photomicrographs of the surfaces of an M50 test bar prior to coating, an as-received Armoloy coating and a polished Armoloy coating are presented in Figures 42, 43, and 44 respectively.

Mag 1000×

FD 270307

Figure 42. SEM Photomicrograph of the Surface of a Typical VIM-VAR M50 Baseline Test Specimen and Coating Substrate Specimen

Mag 1000×

FD 270306

Figure 43. SEM Photomicrograph of the Surface of a Typical "As-Received" Armoloy-Coated M50 Test Specimen

4146C

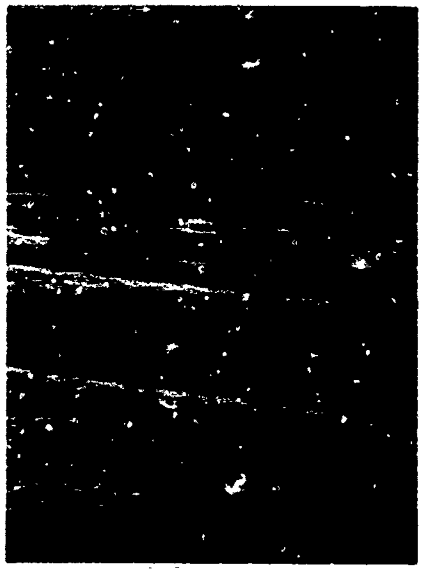

Mag 1000×

FD 270305

Figure 44. SEM Photomicrograph of the Surface of a Typical Polished Armoloy-coated M50 Test Specimen

The Armoloy coating was applied by the Armoloy Co. of Dekalb, Illinois. Within a half-hour after processing, all Armoloy test bars were subjected to a stress relief cycle of 425°F for 4 hours. A post processing bake is not a standard requirement in the proprietary Armoloy process. It has been TRW experience, however, that AISI 52100 bearings suffered a reduction in RCF life after armoloy processing unless they were post process baked.

2) Nickel Sputter-Coated M50

The nickel sputter coating was applied by the Pratt & Whitney Government Products Division, Materials Development Laboratory.

A cryopumped RF diode sputtering system which employs a one kilowatt RF power supply was used to sputter coat nickel over a VIM-VAR M50 substrate. Substrate temperatures typically did not exceed 400°F. The substrates were coated while rotating at one rpm one inch below a water cooled, sputtering target. The target, a flat disk 15.24 cm in diameter and 0.95 cm thick (6.00 in. diameter by 0.375 in. thick) was machined from commercial quality Ni-200 plate stock. Standard XES analysis run on a sample of this material revealed no trace elements present in excess of 0.1 weight percent concentration.

The RF sputtering system is shown in Figure 45 and the coating chamber was previously illustrated in Figure 40.

The substrates were cleaned just prior to fixturing in the coater, or stored in a clean stainless-steel container under an argon gas atmosphere until use to prevent contamination of the freshly cleaned surface. The cleaning procedure which produced the most satisfactory results was as follows:

(a) Three five-minute ultra-sonic baths in clean freon.
(b) A five-minute ultra-sonic bath in soap/water solution.

4146C

(c) Clean tap water rinse.
(d) A two-minute ultra-sonic bath in clean ethyl alcohol.
(e) Rinse in reagent grade ethyl alcohol.
(f) Forced warm air dry.

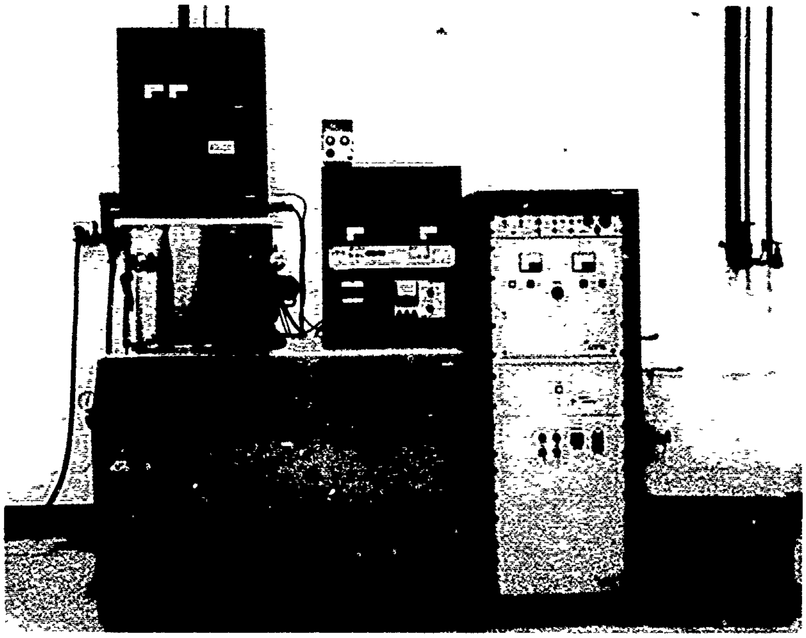

FD 270314

Figure 45. Planar Target Radio Frequency (RF) Diode Sputtering System

Four experimental coating cycles were run in the RF diode coater to obtain process parameters which would yield coatings with the desired characteristics. Once these parameters were finalized, coating of the actual bearing material began. All thirty of the bearing stock test specimens were coated using the following procedures:

(a) The loaded chamber was pumped down to the low 10^{-6} torr range.

(b) The chamber was back-filled with argon gas to approximately 6×10^{-3} torr.

(c) A plasma was established by applying 3Kv RF to the target.

(d) A bias voltage of 100v RF was applied to the substrate for the first ten minutes of deposition to assure a good coating bond.

(e) After ten minutes the bias voltage was removed from the substrate. The deposition process was continued to complete a full two-hour coating period.

The thickness of the sputtered deposit was determined from a scanning electron microscope photomicrographs of polished cross sections of coated trial specimens. Measurements taken from these photos showed that a two-hour deposition cycle would yield a coating approximately 0.000045 (11,300 angstroms) thick as illustrated in Figure 46.

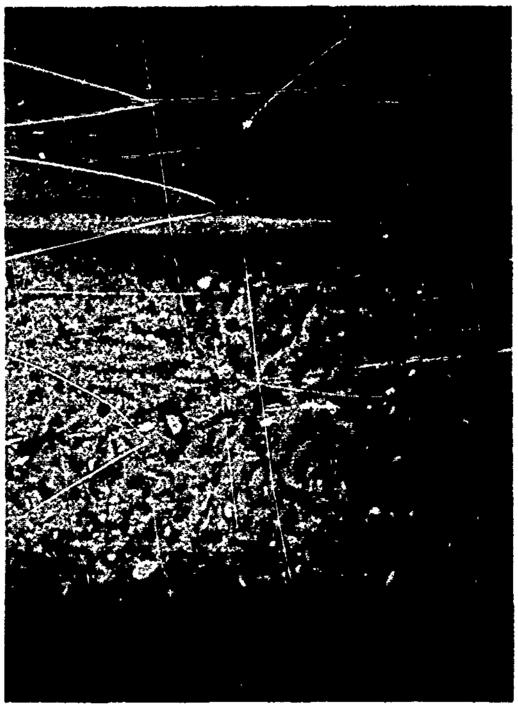

Figure 46. SEM Photomicrograph of a Cross Section of Sputtered Nickel on M50 Bearing Stock

The nickel coating appeared shiny and virtually defect-free to the unaided eye. Scratches, nicks and other defects which were present on the original bearing surfaces were mirrored by the thin nickel coating. Figure 47 illustrates the typical *as-coated* surface finish of test specimens used in this study.

Coating adhesion was determined using a SEBASTIAN 1 adherence tester on a witness tab which was coated along with the first M50 test specimen. The coating on this tab did not debond within the 10,000 psi limit of this tester, but the epoxy used to bond the witness tab to the tester loading mechanism failed at 9820 psi halting the test sequence.

The hardness of the bulk M50 bearing material was measured before and after coating experiments using a ZWICK microhardness tester with a diamond pyramid indenter under a 5Kg load. The *as-received* bulk hardness was found to be 739HV (RC 61.8) and the hardness after nickel coating was 800 HV (RC 64). This indicates that the hardness of the bulk material was virtually unaffected by the RF diode sputtering process.

Mag 1000×

FD 270299

Figure 47. SEM Photomicrograph of the Surface of a Typical Nickel Sputter-Coated M50 Test Specimen

3) VIM-VAR M50 Baseline

VIM-VAR M50 (Fe-4.25Cr-4.25Mo-1.0V-0.8C-0.25Mn) is a lean molybdenum type, through hardened high speed steel. It possesses high strength and high hot hardness and is considered the state of the art high performance turbine engine bearing material. However the material has low corrosion resistance. All the VIM-VAR material used in this program was the same heat lot (Altech Metals heat lot 46734). The baseline M50 test bars and coating candidate substrate bars were processed identically. The M50 heat treatment schedule is presented in Table 7.

TABLE 7. HEAT TREATMENT OF M50

	Temperature °F
Preheat	1550
Austenitize	2025
Quench	1100
Martemper	350
Air Cool	
Wash	
Temper	1000
Temper	1000
Temper	1000

4) MRC2001 Candidate

MRC2001 (Fe-15.2Cr-6.74Mo-1.81V-1.51C-0.32Mn-0.1Si) is a martensitic, high carbon, corrosion resistant and oxidation resistant alloy steel. The powder for this program was fabricated from vacuum melted prealloyed material which was atomized in a nitrogen gas atmosphere. The powder for the test specimens was encapsulated and hot outgassed at approximately 10^{-4} torr. It was then extruded at 1950°F and a 14 to 1 reduction ratio. The MRC2001 heat treatment schedule is presented in Table 8.

TABLE 8. HEAT TREATMENT OF MRC2001

	Temperature °F
Preheat	1500
Austenitize	2150
Martemper	350
Wash	
Air Cool	
Deep Freeze	−110
Liquid Nitrogen	−320
Temper	1000
Deep Freeze	−110
Liquid Nitrogen	−320
Temper	1000
Temper	1000

5) *Wrought CRB7 Candidate*

CRB7 (Fe-14.0Cr-2.07Mo-1.06V-1.11C-0.43Mn-0.29Si) is a patented, corrosion resistant secondary hardening tool steel with reported high temper resistance, hot hardness and wear resistance (Reference 8). The alloy was developed by the Carpenter Steel Division of the Carpenter Technology Corporation for improved hot workability compared to 14-4 Mo and WD65.

Wrought 0.520 inch diameter round stock was purchased from Carpenter Steel Co. (heat Lot 83434).

The CRB7 heat treatment schedule is presented in Table 9.

TABLE 9. HEAT TREATMENT OF CRB7

	Temperature °F
Preheat	1550
Austenitize	2100
Martemper	350
Air Cool	
Wash	
Deep Freeze	−110
Liquid Nitrogen	−320
Temper	1000
Deep Freeze	−110
Liquid Nitrogen	−320
Temper	1000
Temper	1000

6) *RSR565 Candidate*

RSR565 (Fe-9Cr-2Mo-1V-4Co-1C-0.2Mn-0.2Si) is a powder metallurgy, corrosion resistant secondary hardening tool steel developed on A/F contract F33615-76-C-5136. The alloy was designed to give adequate corrosion resistance to a lubricated bearing via the 9% Cr addition while minimizing the number of grain boundary chromium rich carbides so prevalent in 14% Cr bearing steels. The 4% Co addition was designed to raise the martensitic start (MS) temperature so complete transformation of austenite to martensite would occur without cold treatment. The alloy had superior rolling contact fatigue properties when compared to M50 tool steel in preliminary APL conducted tests. The test material for this program was made at

P&WA by direct extrusion of prealloyed RSR140 mesh powder at 1700°F and a 20:1 reduction ratio. The RSR565 heat treatment schedule is presented in Table 10.

TABLE 10. HEAT TREATMENT OF RSR565

	Temperature °F
Austenitize	2100
Air Cool	
Liquid Nitrogen	−320
Temper	1000
Air Cool	
Liquid Nitrogen	−320
Temper	1000
Air Cool	
Liquid Nitrogen	−320

7) RSR405

RSR405 (Fe-19Cr-2Mo-1V-1.25C-0.2Mn-0.2Si) is a powder metallurgy, ultra high chromium tool steel developed on USAF contract F33615-76-C-5136. The alloy was designed so that it would have more corrosion resistance than any other commercially available tool steel due to its very high chromium content. It was hoped that rapid solidification, powder metallurgy processing would help minimize an expected massive chromium rich carbide network at the prior austenite grain boundaries. The alloy had similar rolling contact fatigue properties when compared to M50 tool steel in APL conducted tests. The test material for this program was made at P&WA by direct extrusion of prealloyed RSR140 mesh powder at 1700°F and a 20:1 reduction ratio. The RSR405 heat treatment schedule is presented in Table 11.

TABLE 11. HEAT TREATMENT OF RSR405

	Temperature °F
Austenitize	2100
Air Cool	
Liquid Nitrogen	−320
Temper	400
Air Cool	
Liquid Nitrogen	−320
Temper	400
Air Cool	

8) RSR113

RSR113 (Fe-14Cr-4Mo-1V-2Co-1C-1Cb-0.2Mn-0.2Si) is a powder metallurgy modified version of the CRB7 tool steel developed by Carpenter Technology. The alloy was designed so it would contain more beneficial wear resistant MC and M_2C type carbides than are present in the CRB7 tool steel. This was achieved by increasing the molybdenum and columbium content of the alloy while adding cobalt to partially offset the reduction in MS temperature. This alloy has superior corrosion resistance due to its high chromium content. The alloy was not tested in rolling contact fatigue and wear prior to incorporation in this program. The test material for this program was made at P&WA by direct extrusion of prealloyed RSR −140 + 325 mesh powder at 1750°F and a 12:1 reduction ratio. The RSR113 heat treatment schedule is presented in Table 12.

TABLE 12. HEAT TREATMENT OF RSR113

	Temperature °F
Austenitize	2130
Air Cool	
Liquid Nitrogen	−320
Temper	925
Air Cool	
Liquid Nitrogen	−320
Temper	925
Air Cool	
Temper	925
Air Cool	

All the alloy candidate test bars and the baseline M50 test bars were centerless ground at TRW to final size (0.5 inch diameter) and finish (4-6 micro inch) using a 20 inch, 100 grit, A100M5 wheel rotating at 1300 rpm.

The metallurgical parameters of CRB7, MRC2001, RSR565, RSR113 and the VIM-VAR M50 baseline material are summarized in Table 13.

TABLE 13. METALLURGICAL PARAMETERS OF ALLOY CANDIDATES, RSR113 AND VIM-VAR M50 BASELINE

Candidates Material	*C*	*Cr*	*V*	*Mo*	*Chemistries Mn*	*Co*	*Si*	*Nb*	*O_2*		*Rockwell Hardness Rc*	*% Retained Austinite*	*ASTM Grain Size*
CRB7	1.11	14.0	1.06	2.07	0.43	—	0.29	—	—	Cb 0.31	62.5 62.9	3%	9.1
MRC2001	1.51	15.2	1.81	6.74	0.32	—	0.1	—	28ppm	—	62.6 63.1	3%	12+
RSR565	1	9	1	2	—	4	—	—	—	—	62.6 63.0	4%	5-8
RSR113	1	13.8	1.09	3.95	0.31	1.95	0.3	1.02	—	—	62.5 63.2	27* 9**	13-14
VIM-VAR M50 Base Mat'l	0.80	4.25	1.0	4.25	0.25	—	—	—			62.1 62.3	3%	8.9

*Transverse
**Axial

SEM photomicrographs of the M50 baseline, alloy candidates and RSR113 microstructure are shown in Figure 48.

4. Phase I Test Results

1) Rolling Contact Fatigue Testing

The rolling contact fatigue (RCF) characteristics of the above materials were investigated through performance testing on RCF-1 rolling contact fatigue testing machines (Figure 49), produced by Polymet Corporation, Cincinnati, Ohio. This type of RCF test is widely used throughout industry to reliably rank candidate materials.

VIM-VAR M50

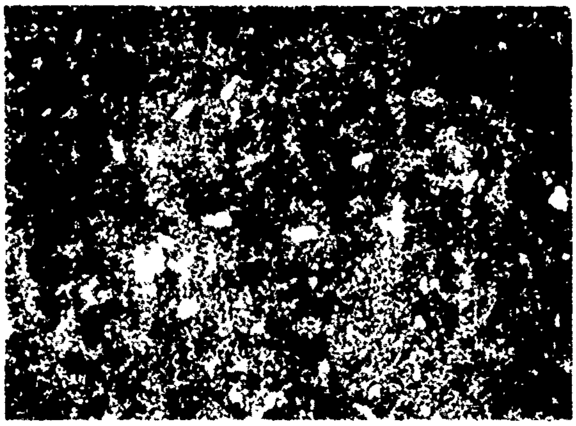

Alloy Carbide Size and Distribution in a Tempered Martensitic Matrix Is Typical of Wrought Ingot Metallurgy. Magnification : 400X

MRC2001

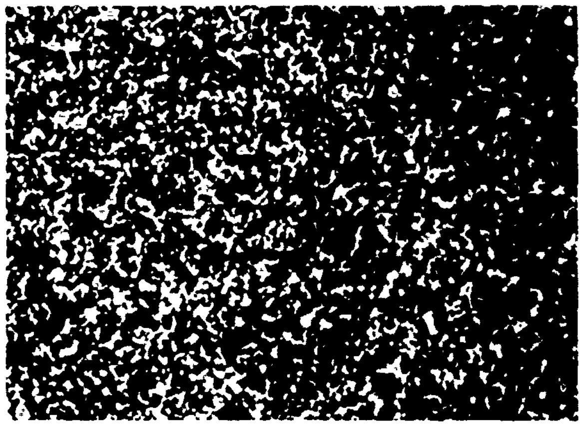

Evenly Dispersed Alloy Carbides of the MC and M_6C_{23}Type in a Matrix of Tempered Martensite. Magnification: 1000X

CRB 7

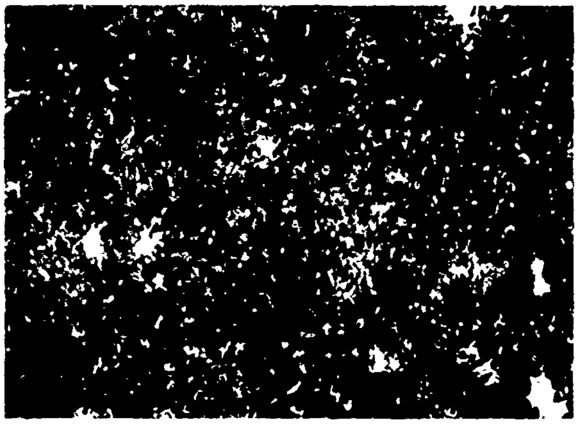

Alloy Carbides of Varying Size, Typical of High Chromium-Carbon Martensitic Stainless Steel Produced by Ingot Metallurgy. Magnification: 400X

RSR565

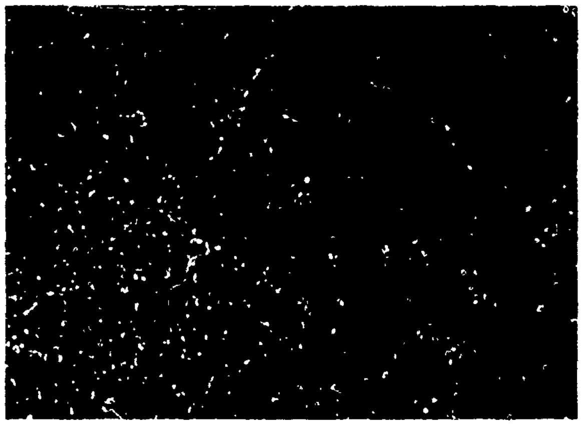

Evenly Dispersed Alloy Carbides in a Tempered Martensitic Matrix. Magnification: 400X

RSR113

Evenly Dispersed Alloy Carbides in a Tempered Martensitic Matrix. Magnification: 400X

FD 270312

Figure 48. Microstructure Photographs

4146C

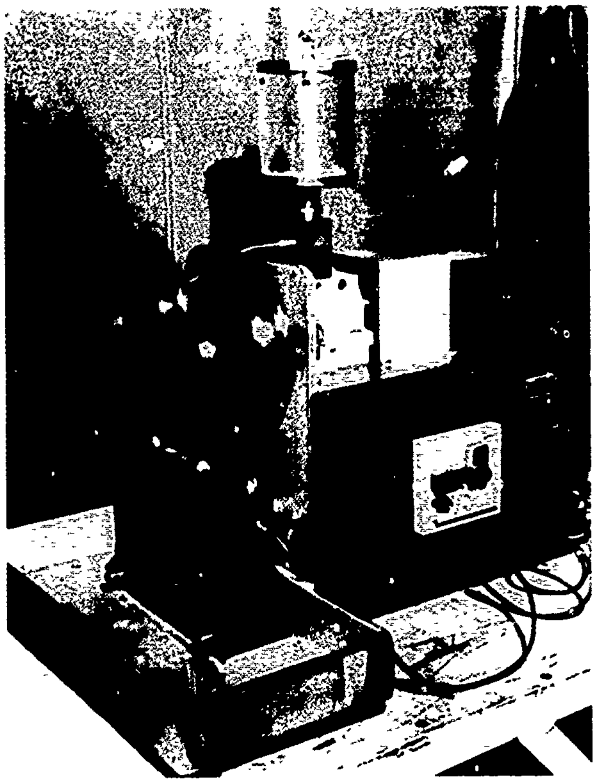

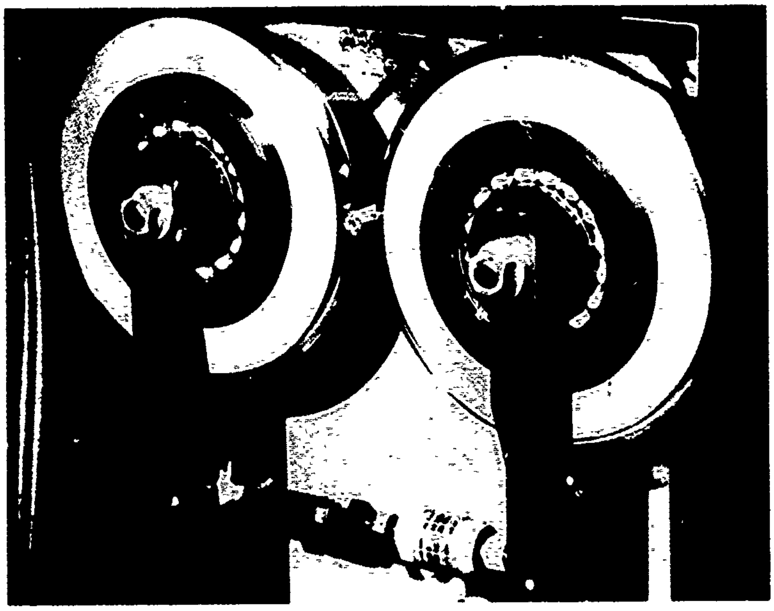

FD 216723

Figure 49. The Top Photo Depicts an Overall View of the Rolling Contact Fatigue Rig; the Bottom Photo is a Closeup View of Specimen and Test Rolls

4146C

The RCF-1 Tester, utilizes test specimens (0.50 in. diameter rods, 3 in. long) mounted in a precision chuck, rotating at 7000 rpm. The rotating test rod is diametrically loaded in rolling contact by two large contacting rollers (or loading disks) pendulum supported, and mechanically loaded against the test rod. The test load is continuously monitored by a strain analyzer. A fatigue spall is detected by an adjustable velocity vibration pickup with an automatic shutdown feature which senses the vibration increase associated with spalling. Lubrication was provided with gravity flow, once through lubricant system using MIL-L-23699 fluid. Total test specimen revolutions are automatically counted.

The loading disks (composed of CVM M50 steel, Rc 61-64, 7.5 in. dia by 0.5 in. thick, and with a 0.25 in. contact radius) exert a maximum Hertz stress test load on the test rod of 733,650 psi.

A minimum of twenty (20) rolling contact fatigue tests were produced for each candidate and reference M50 material.

Figures 50 through 57 are individual Weibull plots of the RCF test results. A data summary sheet and composite Weibull are presented in Table 14 and Figure 58, respectively. Of particular note is the outstanding performance of the VIM-VAR M50 reference material. Compared to other RCF studies conducted on 0.5 inch diameter rod specimens, the M50 demonstrated both a steep Weibull slope and a high L10 life. Confidence numbers were generated for the L10 and L50 lives using L. G. Johnson's technique (Reference 12). A 95 percent or greater confidence number (a 2 σ confidence level) is indicative of a high degree of confidence.

None of the candidates were shown to a high degree of confidence to be inferior to the M50 L10 RCF life although all but MRC2001 had a lower measured L10 life. All candidates had a higher measured L50 life and three candidates (MRC2001, Armoloy-coated M50 and CRB7) had to a high degree of confidence superior L50 lives compared to M50. However, the maximum spread in either the L10 and L50 life relative to M50 was 38%. The M50 used in this program was from one heat lot. Given the variability of RCF life between different heat lots and between different hardness values in one heat lot, a 38% difference in RCF life is not considered significant.

Three nickel sputter-coated bars and five Armoloy-coated M50 bars were subjected to Scanning Electron Microscopy (SEM) and Energy Dispersive X-ray (EDXR) analysis following the fatigue endurance testing of those bars. The purpose of these evaluations was three-fold:

(a) Determine physical characteristics of roller tracks;
(b) Evaluate integrity of surface treatment in tracks;
(c) Determine uniformity of surface treatments.

The results of the SEM and EDXR analyses are as follows:

(a) Sputtered nickel does not stand up under the contact pressures of this tests. See Figures 59 through 62.

(b) The chrome plating applied by Armoloy Corporation tends to have a pebbly surface. See Figures 63, 64 and 43.

(c) The pebbly surface of (b), above, can be removed by polishing. Compare Figures 62, 64 and 43 with Figures 65, 66 and 44. However, EDXR

examinations of polished chrome surfaces show some iron. See Figures 67 through 70.

(d) The chrome plating, polished or unpolished, did not flake or crack under rolling contact.

Figures 71 through 76 are SEM photographs of typical fatigue spalls from RC test bars of M50 and five candidate materials. (Nickel sputter-coated M50 is omitted here because the nickel coating has disintegrated from the contact zone before fatigue failure). The photos demonstrate that the same type of failure mechanism was at work in all materials. Failure initiated at a point, then progressed in a somewhat fan-shaped pattern in the direction of rolling. In Figures 71 and 76, flaking started near the bottom of the photos and progressed toward the top. In Figure 72, failure initiated at the top of the photo. In Figures 73, 74, and 75, spalling progressed from left to right. All show further cracks developing from the spalls. In each case the time lapse from the start of flaking until rig rotation stopped was a matter of seconds.

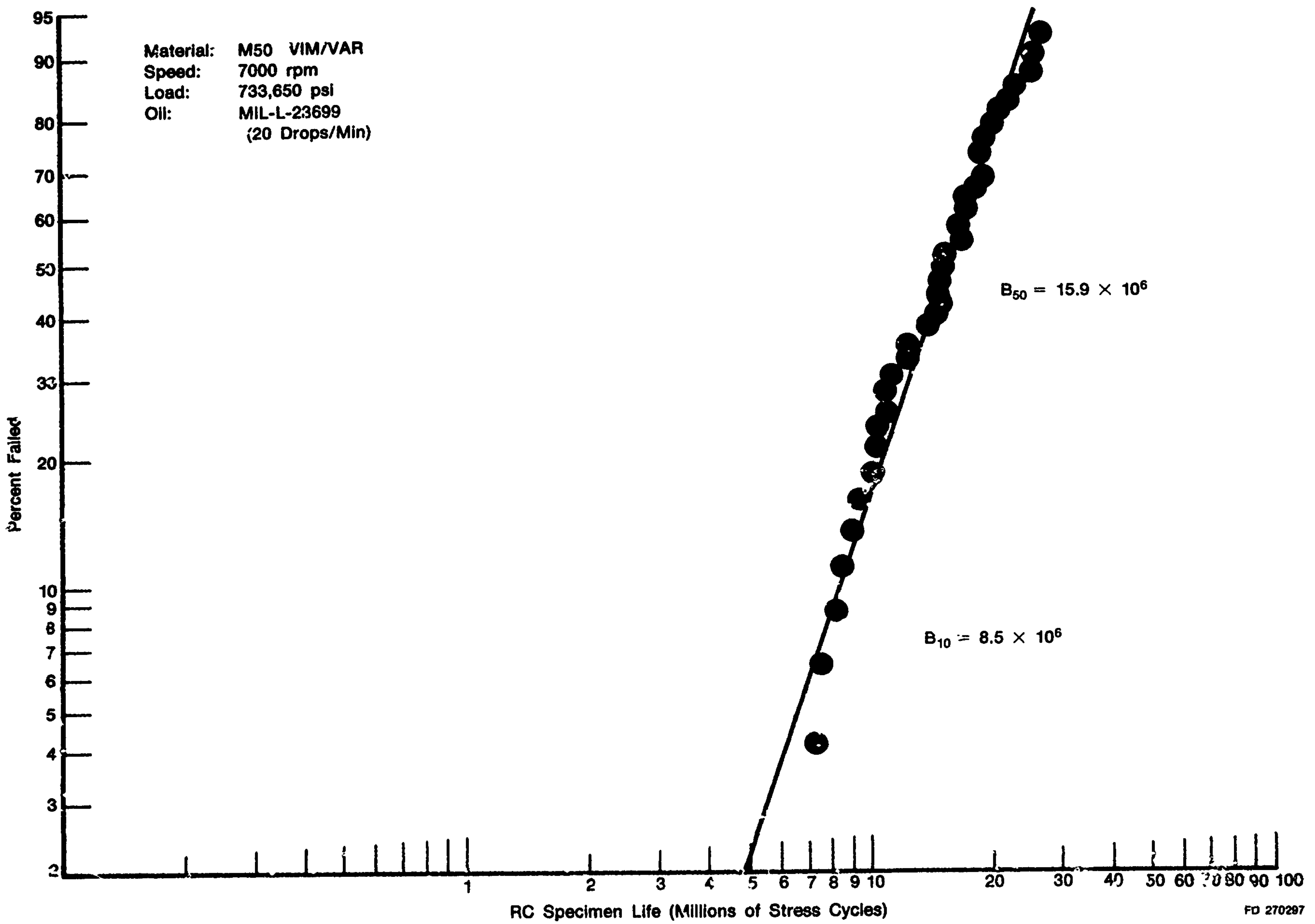

Figure 50. Weibull Plot of Baseline M50 Rolling Contact Fatigue Test Results

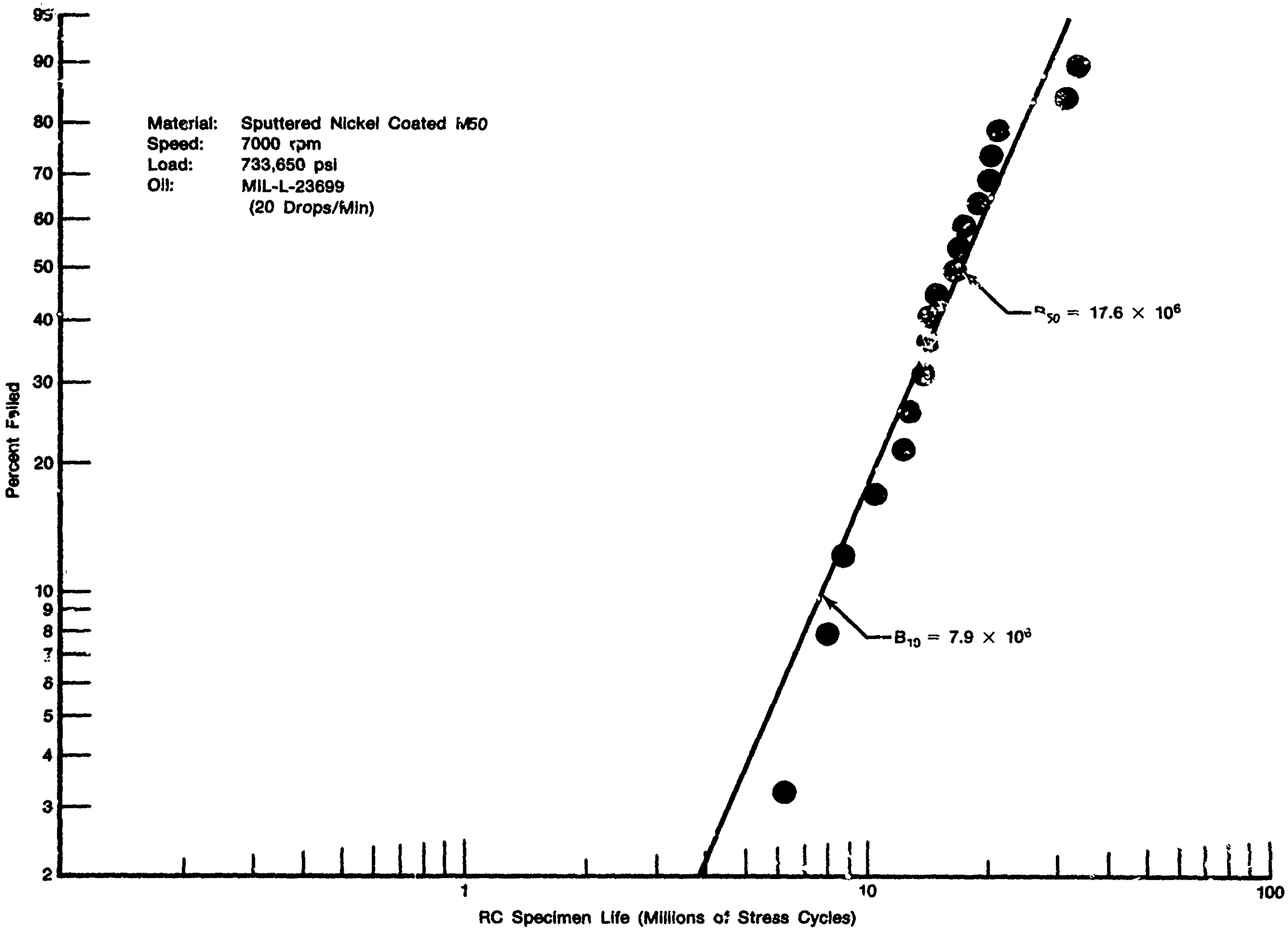

FD 27029

Figure 51. Weibull Plot of Nickel Sputter Coated M50 Rolling Contact Fatigue Test Results

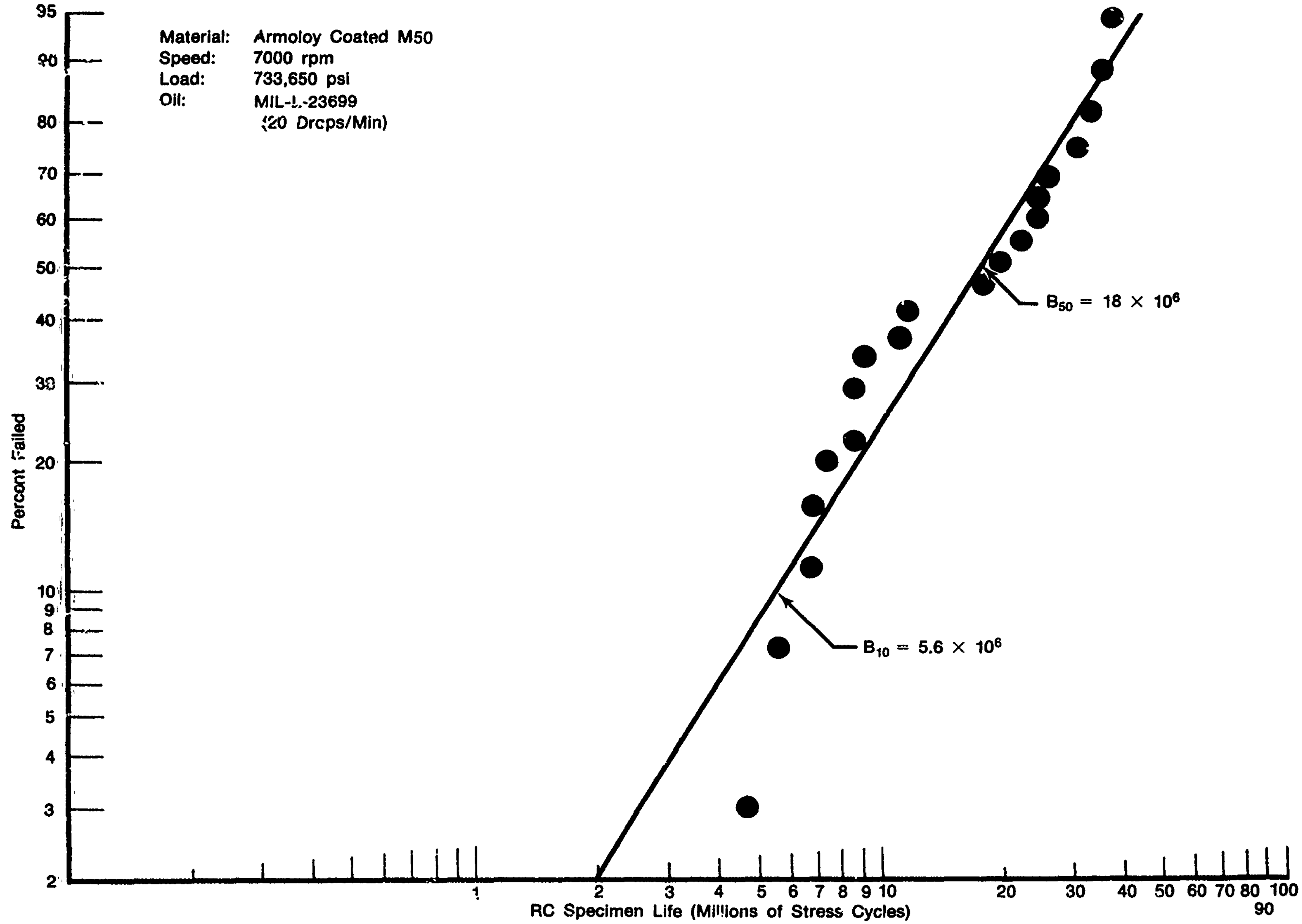

Figure 52. Weibull Plot of "As-Received" Armoloy-Coated M50 Rolling Contact Fatigue Test Results

FD 270291

4146C

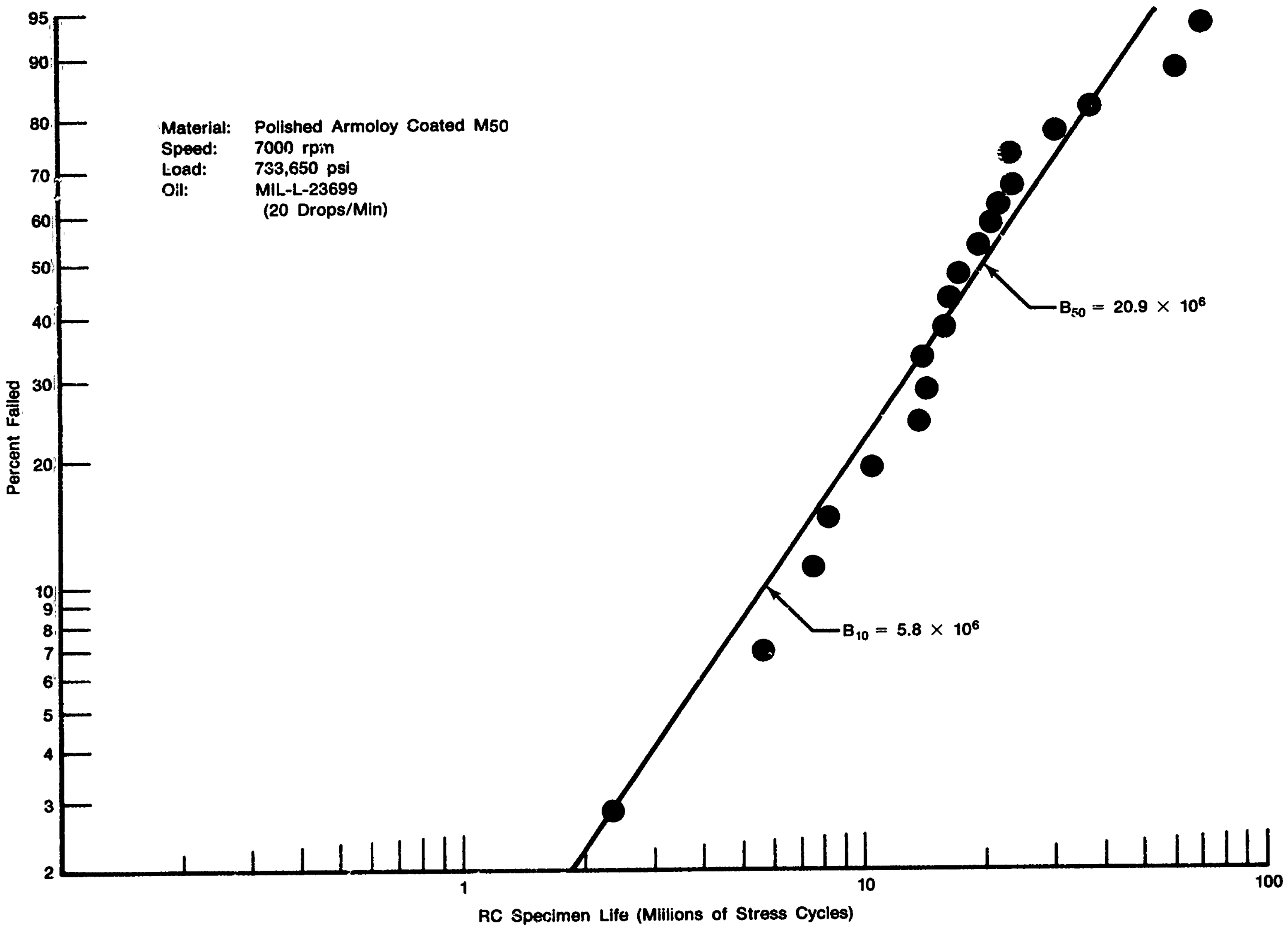

Figure 53. Weibull Plot of Polished Armoloy-Coated M50 Rolling Contact Fatigue Test Results

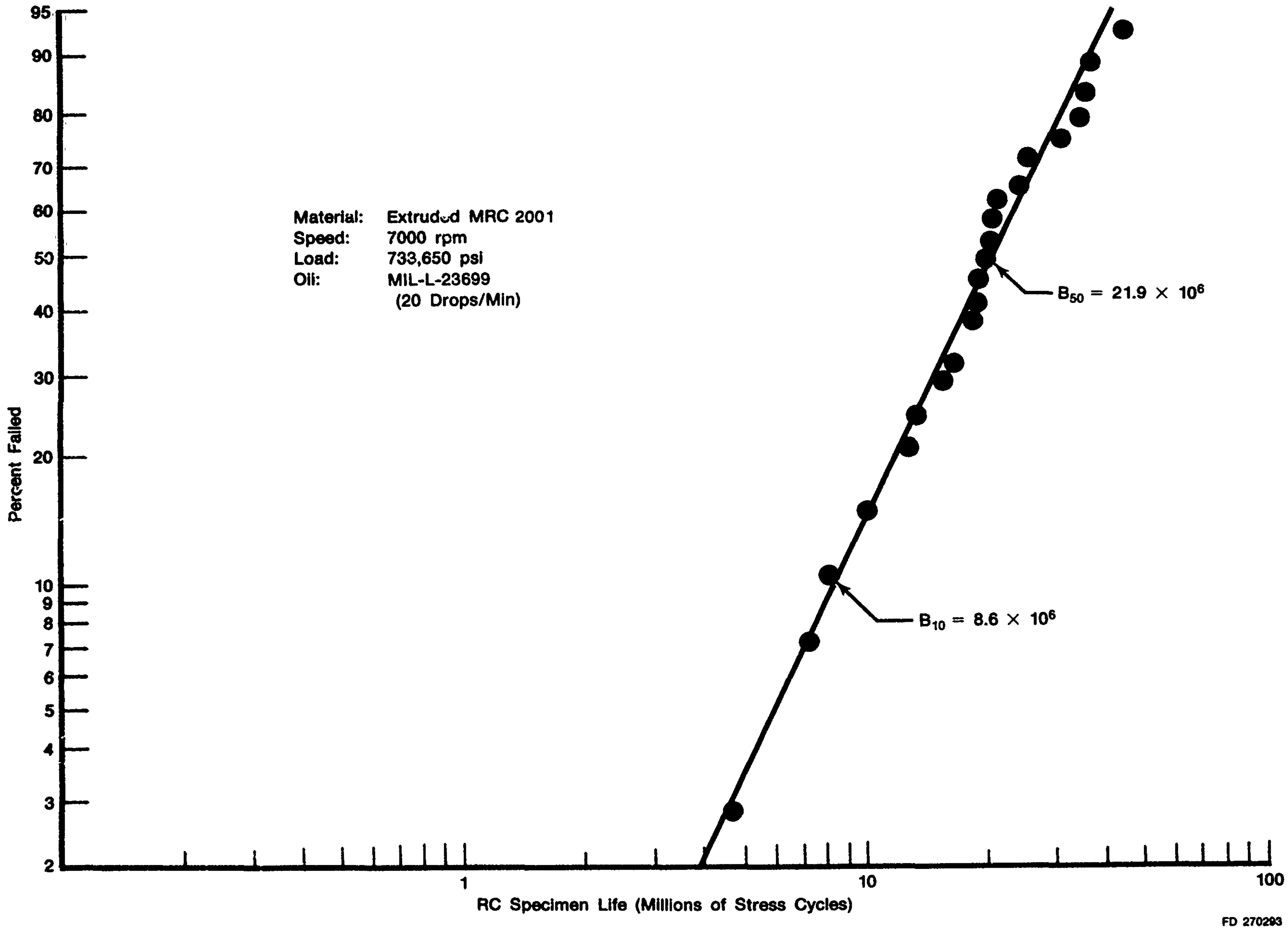

Figure 54. Weibull Plot of MRC2001 Rolling Contact Fatigue Test Results

4146C

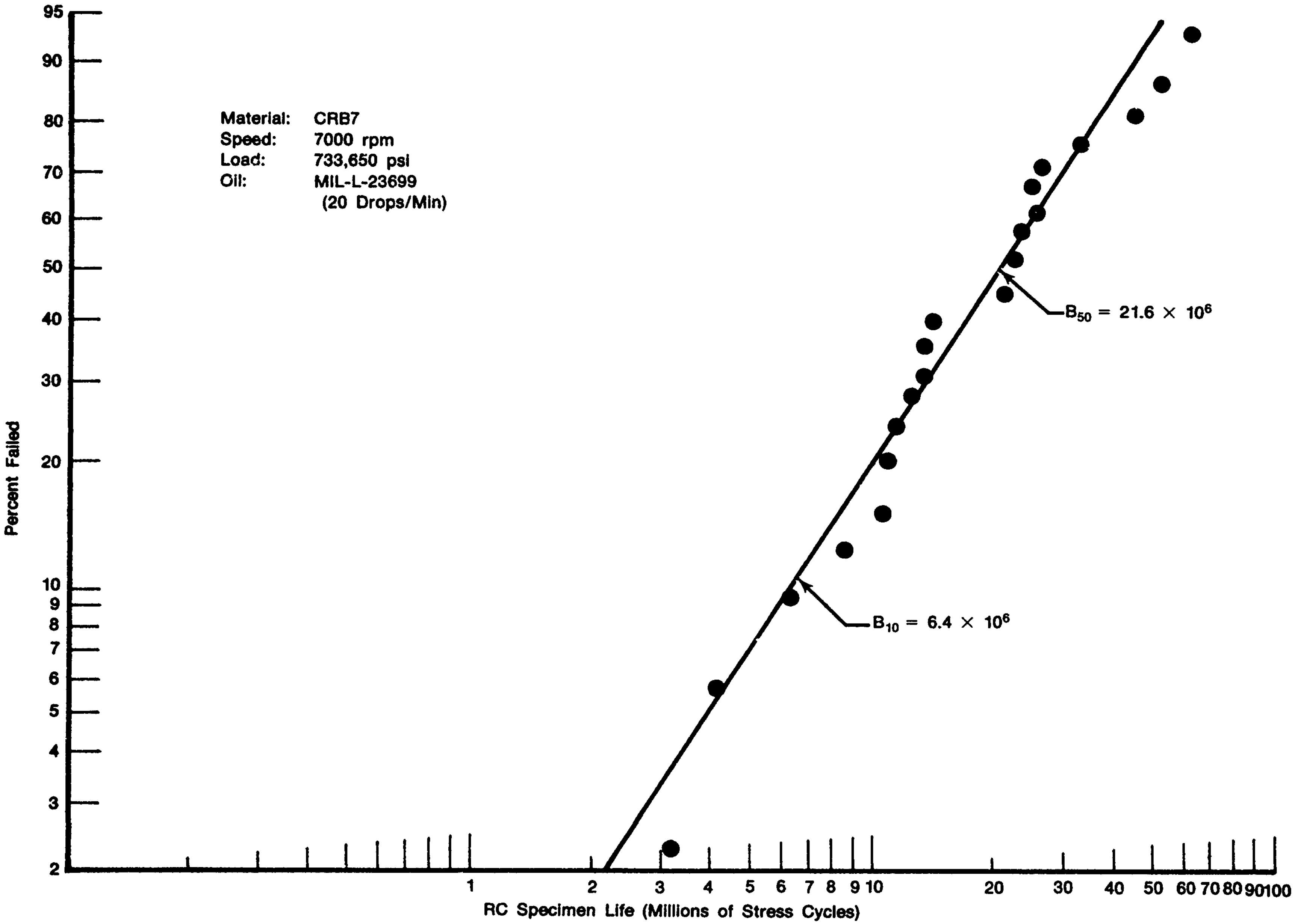

Figure 55. Weibull Plot of CRB7 Rolling Contact Fatigue Test Results

4146C

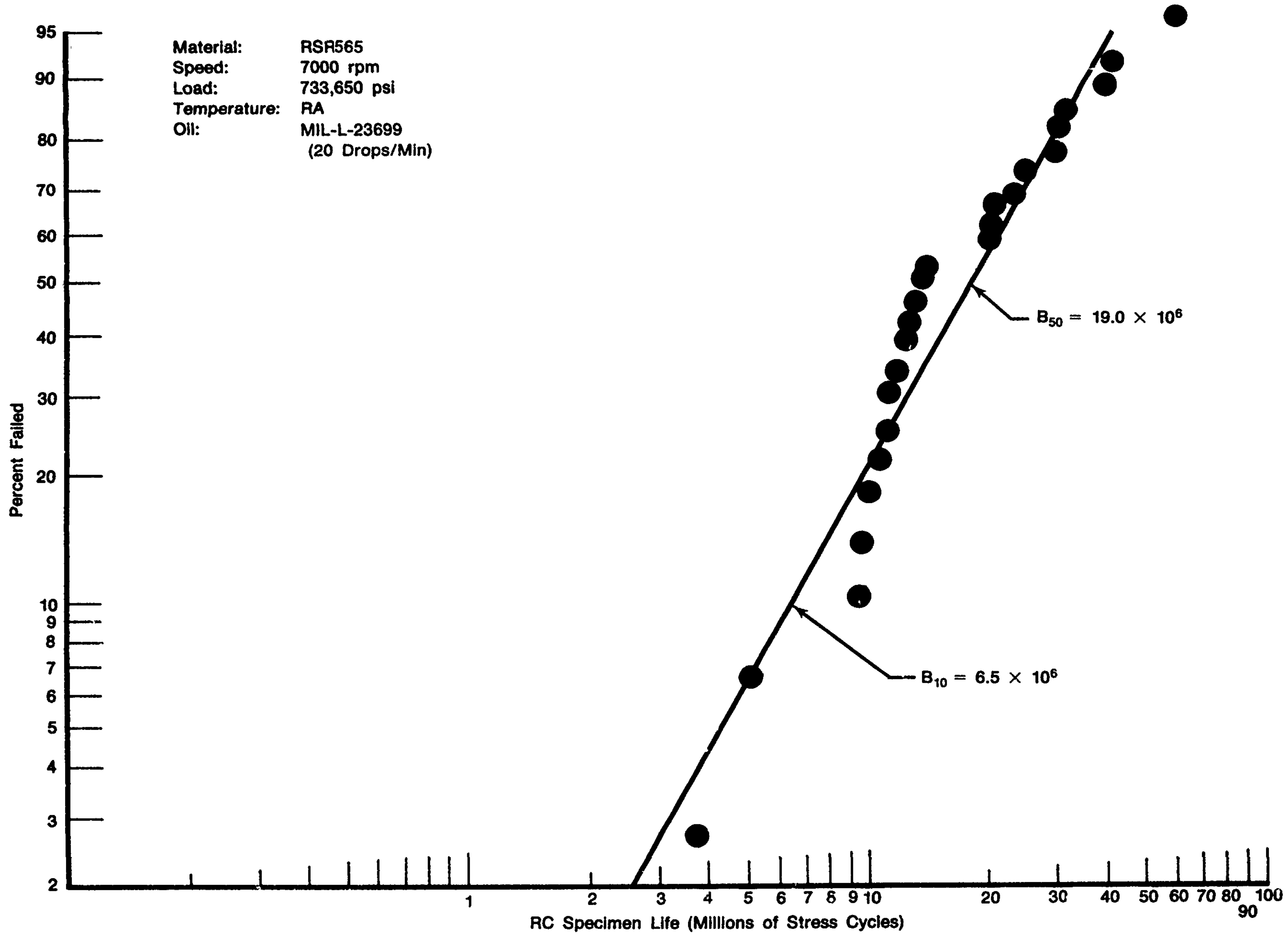

Figure 56. Weibull Plot of RSR565 Rolling Contact Fatigue Test Results

4146C

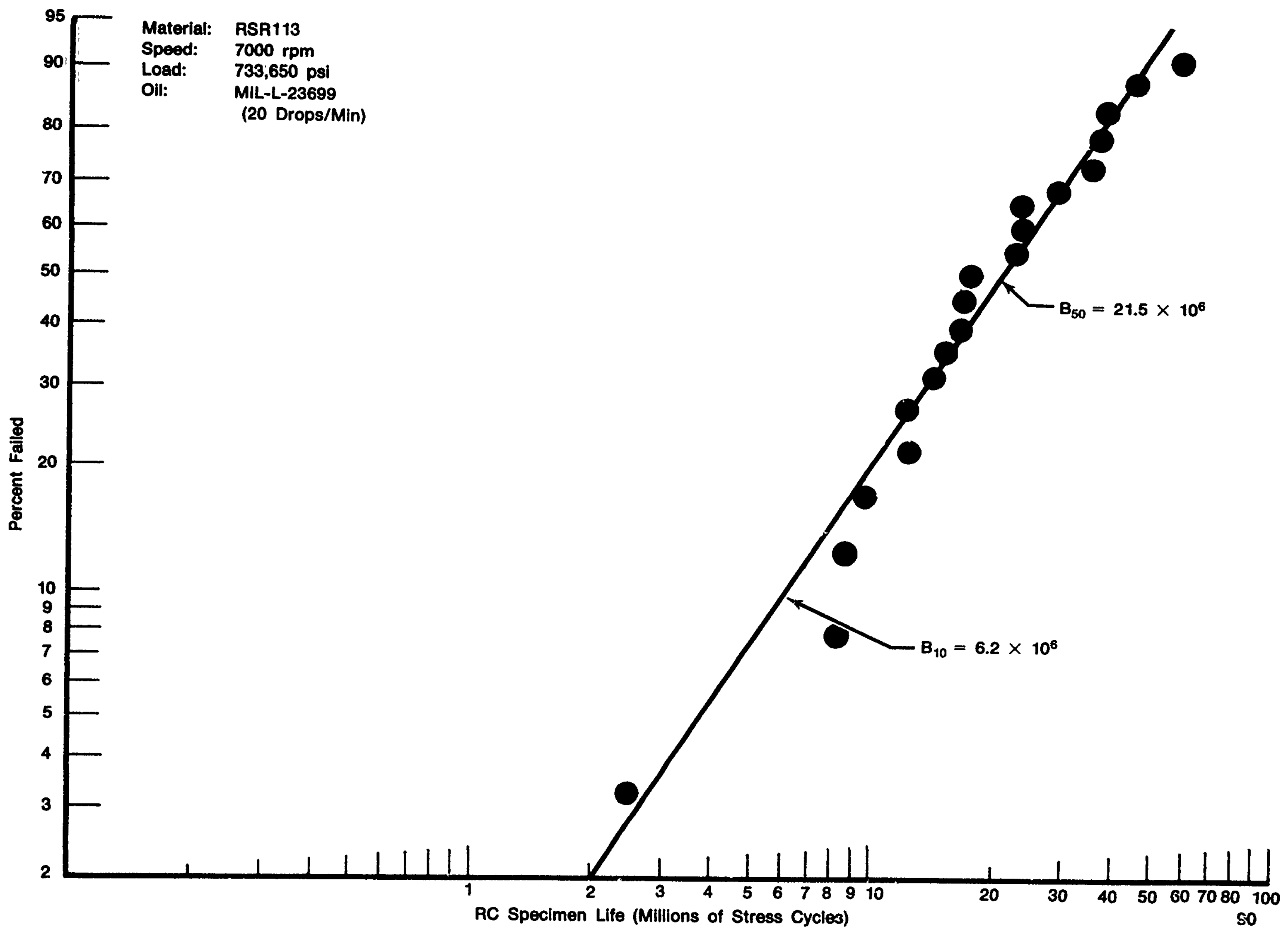

Figure 57. Weibull Plot of RSR113 Rolling Contact Fatigue Test Results

FD 270294

4146C

TABLE 14. ROLLING CONTACT FATIGUE TEST RESULTS

Candidate Material	*Life Stress Cycles — 10^6* L_{10}	L_{50}	*Weibull Slope*	*Life Ratio to M50* L_{10}	L_{50}	*Confidence Relative to M50* L_{10}	L_{50}
Armoloy-Coated M50 — Polished	5.8	20.9	1.47	0.68	1.31	90% Inferior	96% Superior
Armoloy-Coated M50 — Unpolished	5.6	18.0	1.60	0.66	1.13	90% Inferior	85% Superior
Nickel Sputter-Coated M50	8.0	17.6	2.37	0.94	1.11	No Significant Difference	85% Superior
MRC2001 Extruded	8.6	21.9	2.01	1.01	1.38	No Significant Difference	98% Superior
RSR113	6.2	21.5	1.52	0.73	1.35	90% Inferior	98% Superior
RSR565	6.5	19.0	1.82	0.78	1.24	80% Inferior	94% Superior
CRB7	6.4	21.6	1.56	0.75	1.36	80% Inferior	98% Superior
Reference M50	8.5	15.9	2.98	1	1		

4146C

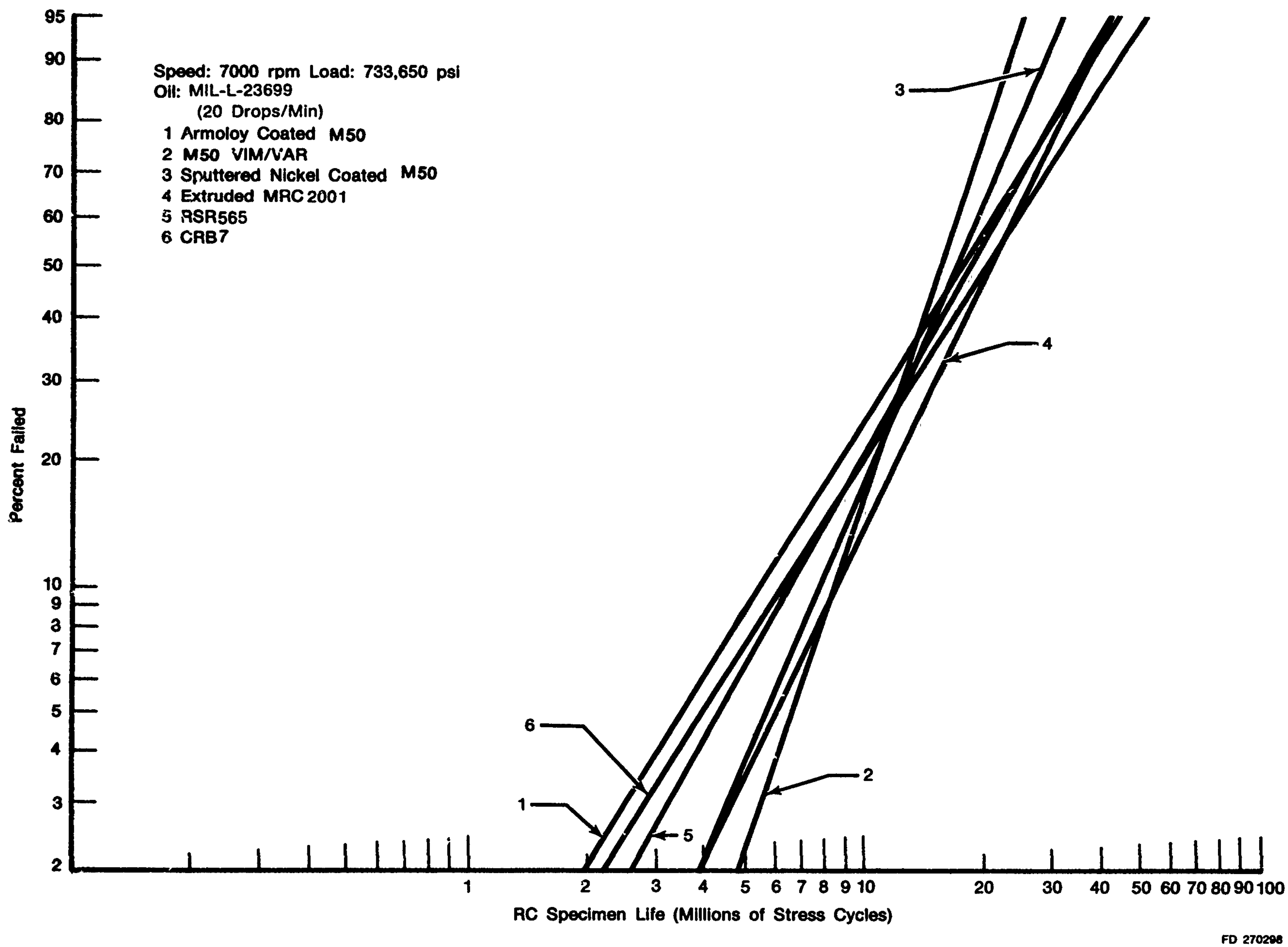

Figure 58. Composite Weibull Plot of Candidate and VIM-VAR M50 Rolling Contact Fatigue Test Results

4146C

Figure 59. EDXR Analysis of Nickel Sputter-Coated Bar Outside of Roller Track (Note Nickel Lines)

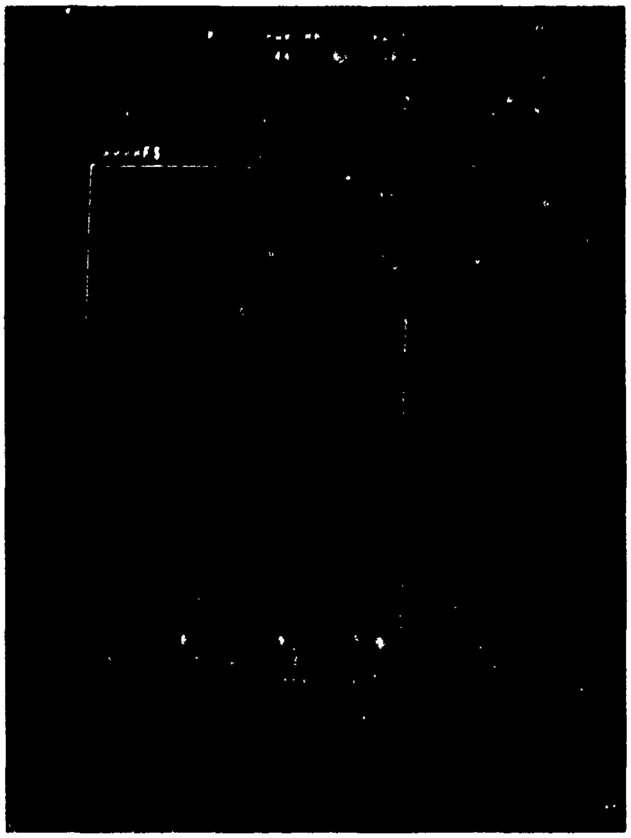

Figure 60. EDXR Analysis of Nickel Sputter-Coated Bar Roller Track (Nickel Has Been Lost)

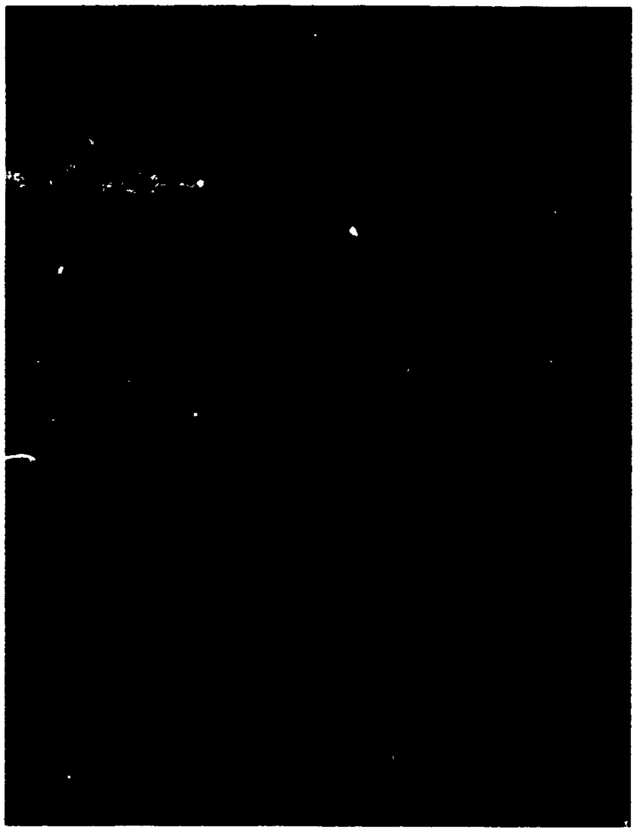

Figure 61. SEM Photo of Roller Track on Nickel Sputter-Coated Bar HN-2 (Note Flaking) Magnification: 50×

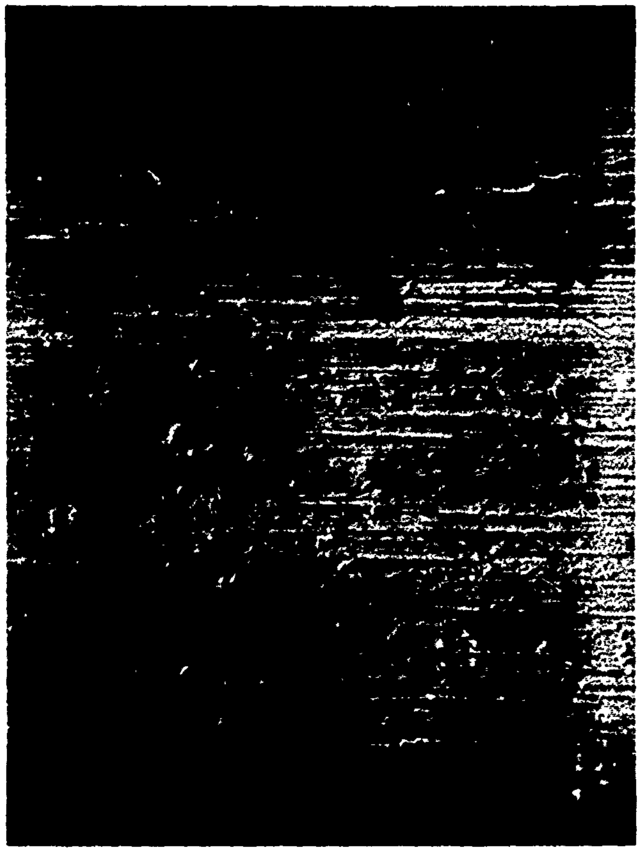

Figure 62. SEM Photo of Roller Track on Nickel Sputter-Coated Bar HN-2. Magnification: 200×

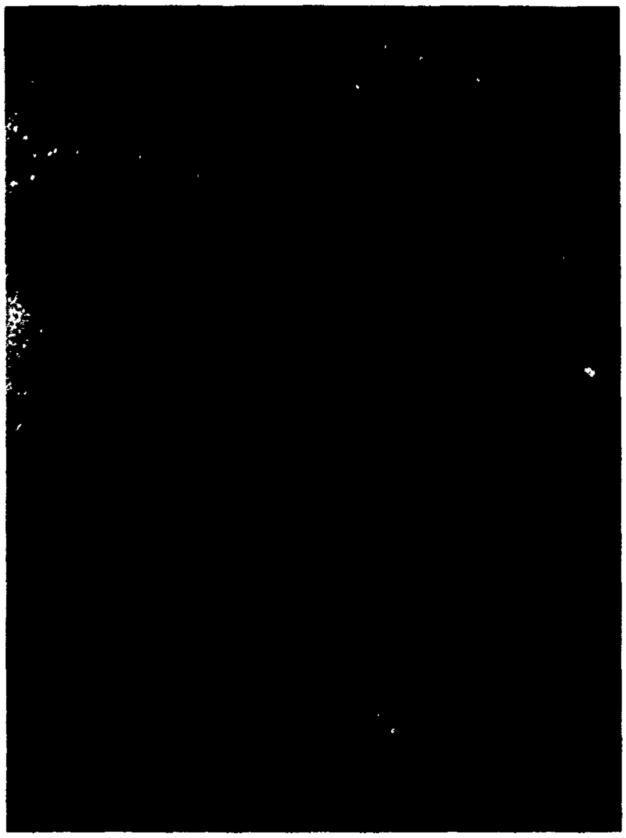

Figure 63. SEM Photo of Roller Track No. 3 on Chrome-Plated Bar HA-5 (Note Pebbled Surface Outside of Roller Path) Magnification: 50×

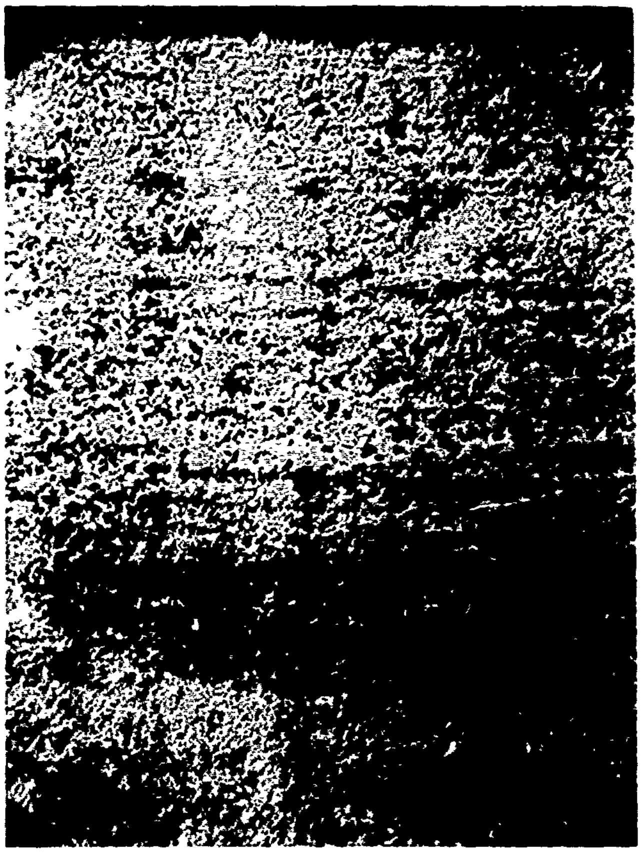

Figure 64. SEM Photo of Roller Track No. 3 on Chrome-Plated Bar HA-5 (Note Smeared Surface) Magnification: 200×

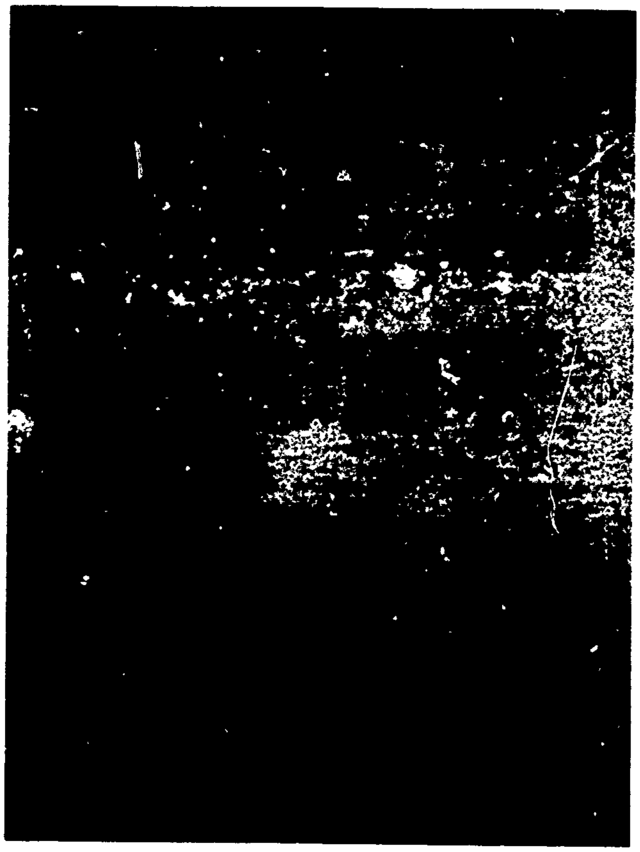

Figure 65. SEM Photo of Roller Track No. 6 on Chrome-Plated, Subsequently Polished, Bar HA-3. Magnification: 50×

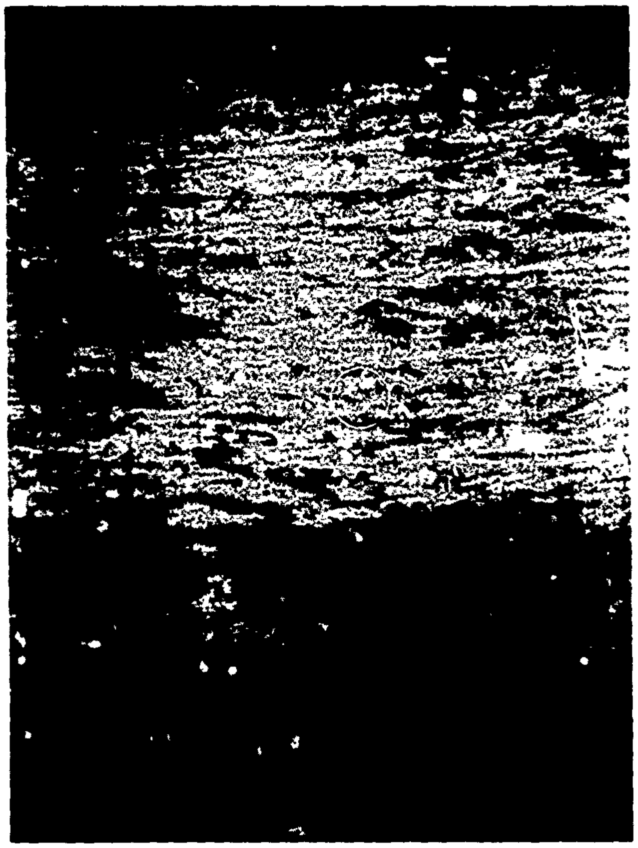

Figure 66. SEM Photo of Roller Track No. 6 on Chrome-Plated, Subsequently Polished, Bar HA-3. Magnification: 200×

4146C

Figure 67. EDXR Analysis of Chrome-Plated, Subsequently Polished, Bar HA-3 Outside of Track (Note Iron Lines)

.146C

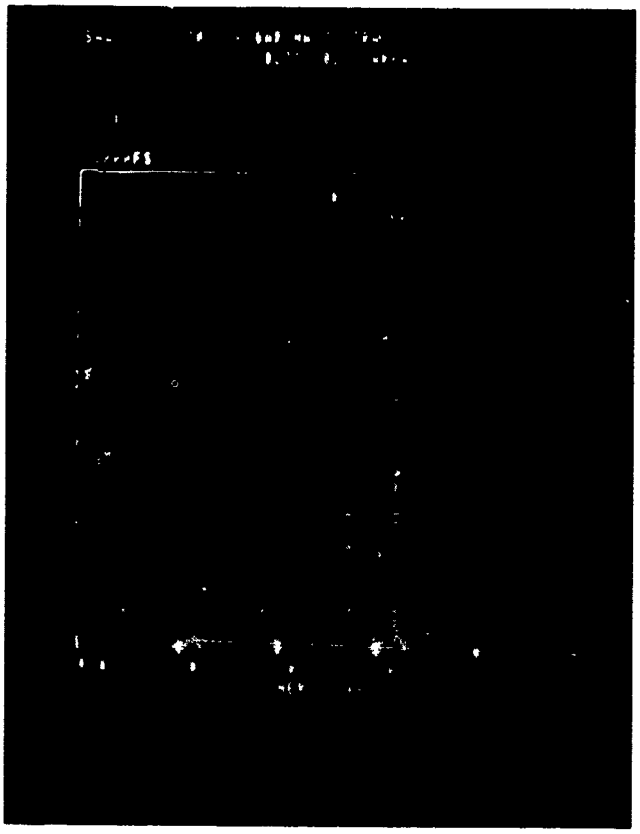

Figure 68. EDXR Analysis of Chrome-Plated, Subsequently Polished, Bar HA-3 in Track 1 (Note That Iron Is Present but Chrome Is Thicker than in Figure 67)

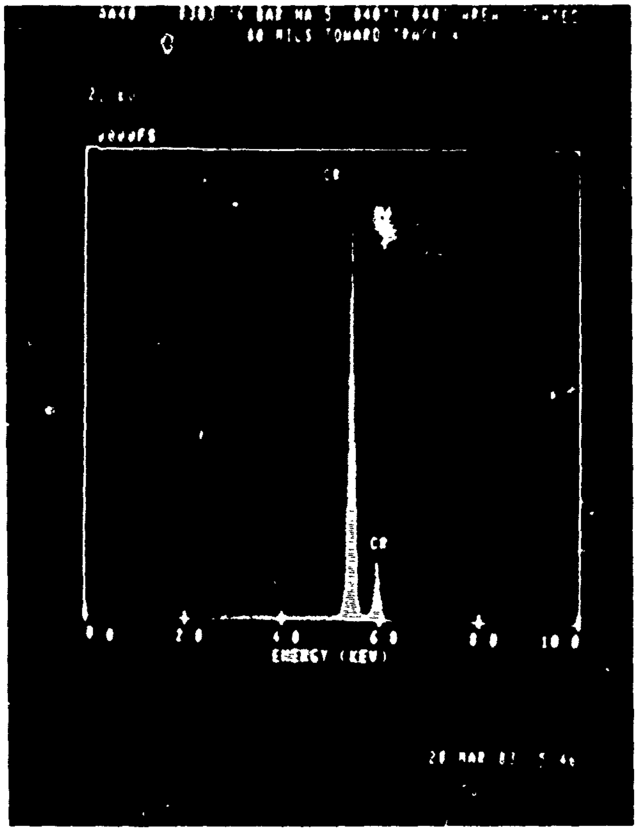

Figure 69. EDXR Analysis of Chrome-Plated Bar HA-5 Outside of Track

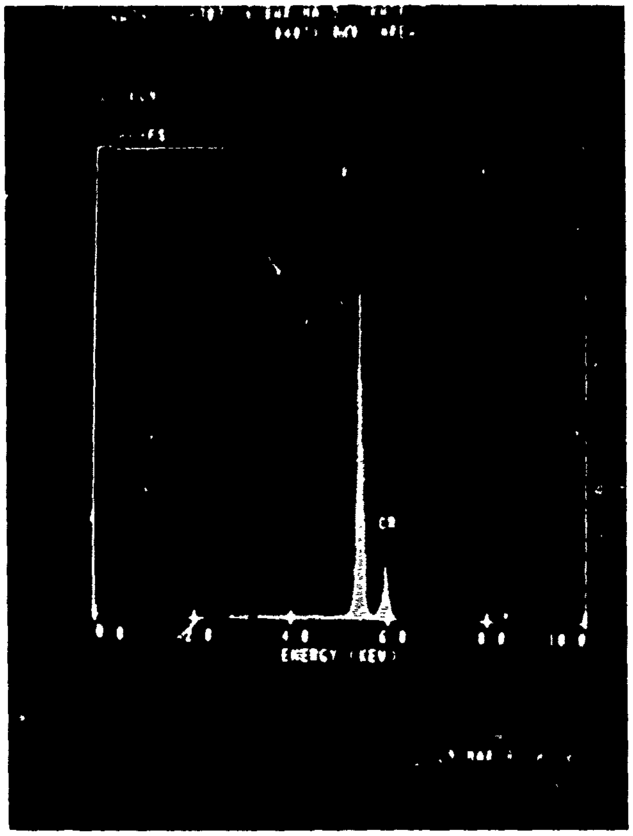

Figure 70. EDXR Analysis of Chrome-Plated Bar HA-5 in Track 3

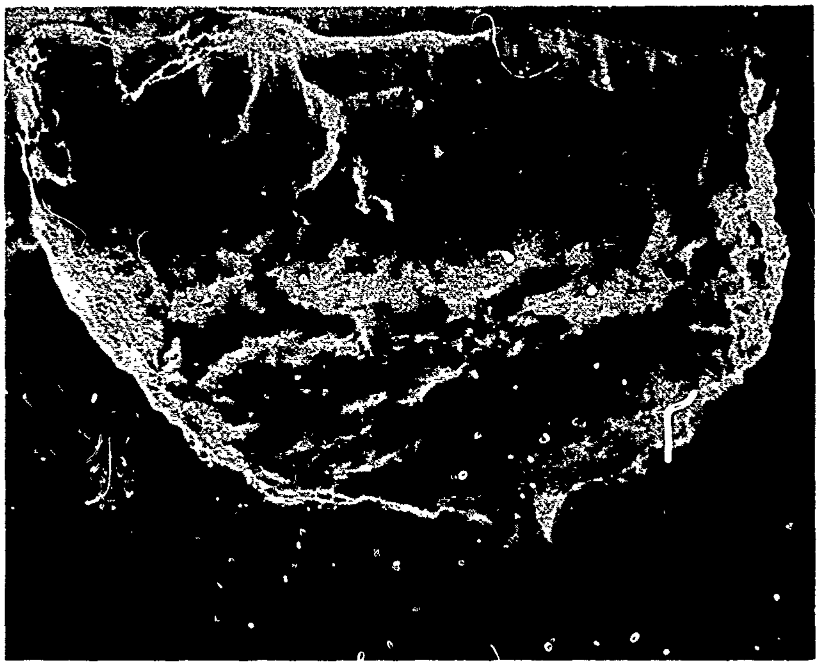

Figure 71. SEM View of Typical Spall M50 Reference Test Bar (H-4). Magnification: 110×

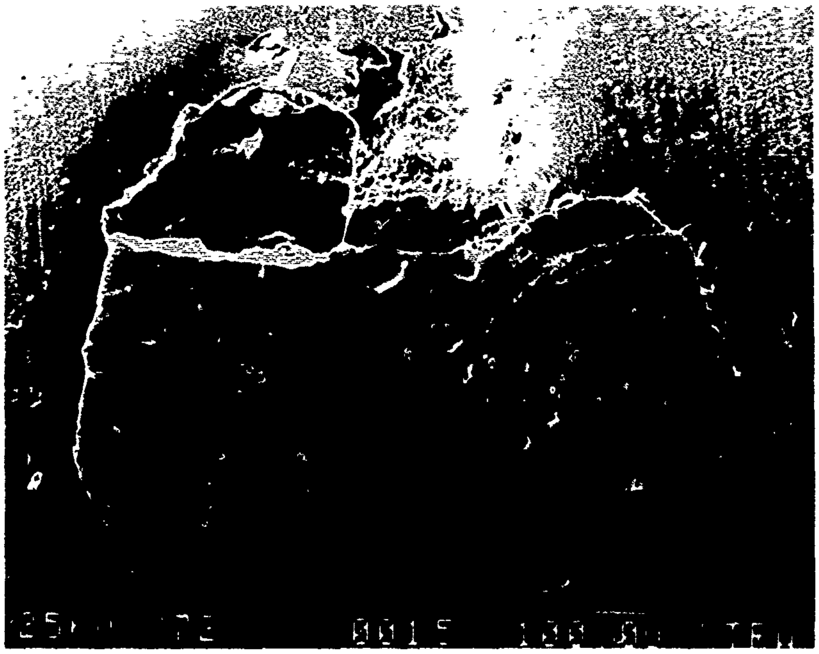

Figure 72. SEM View of Spall in Chrome-Plated Test Bar (HA-1). Magnification: 72×

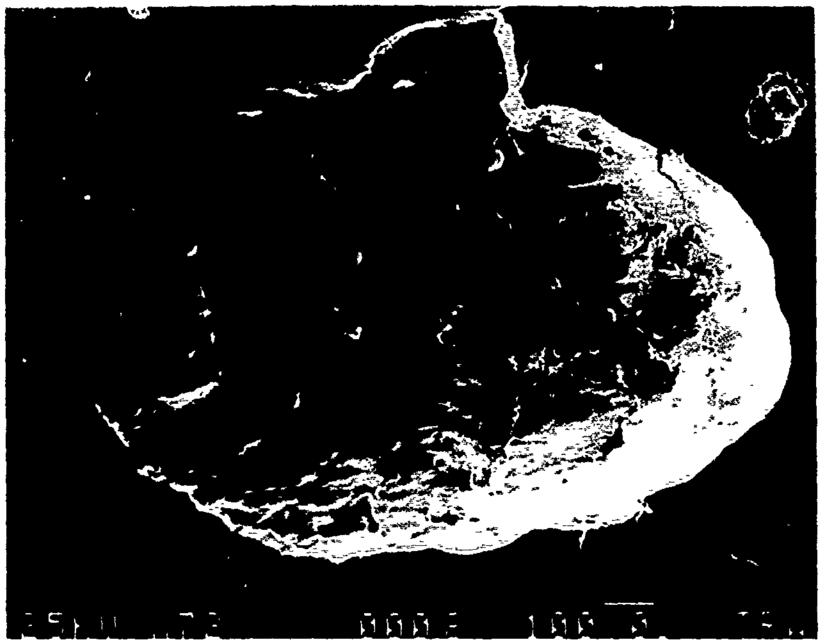

Figure 73. SEM View of Spall in CRB7 Test Bar (HC-2). Magnification: 72×

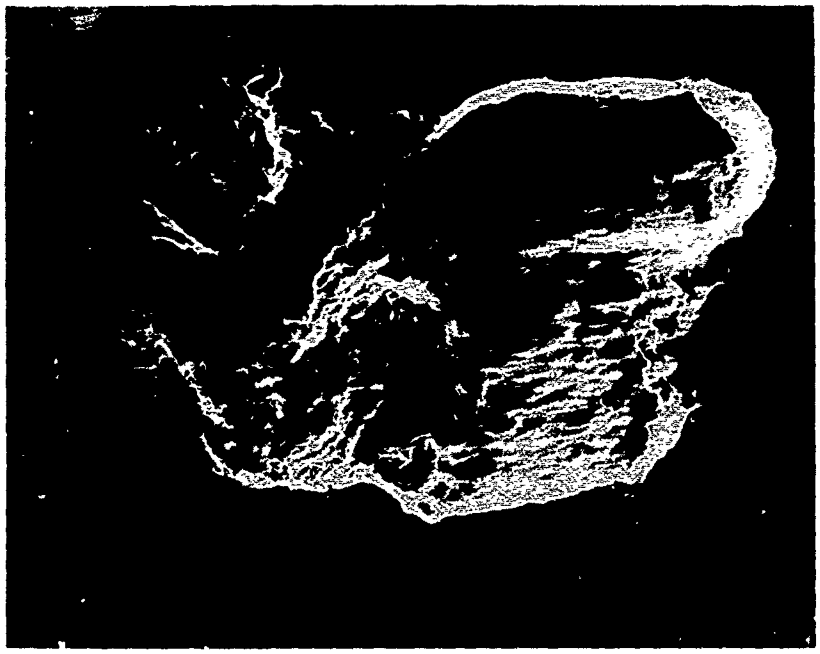

Figure 74. SEM View of Spall in RSR565 Test Bar (HR-1). Magnification: 72×

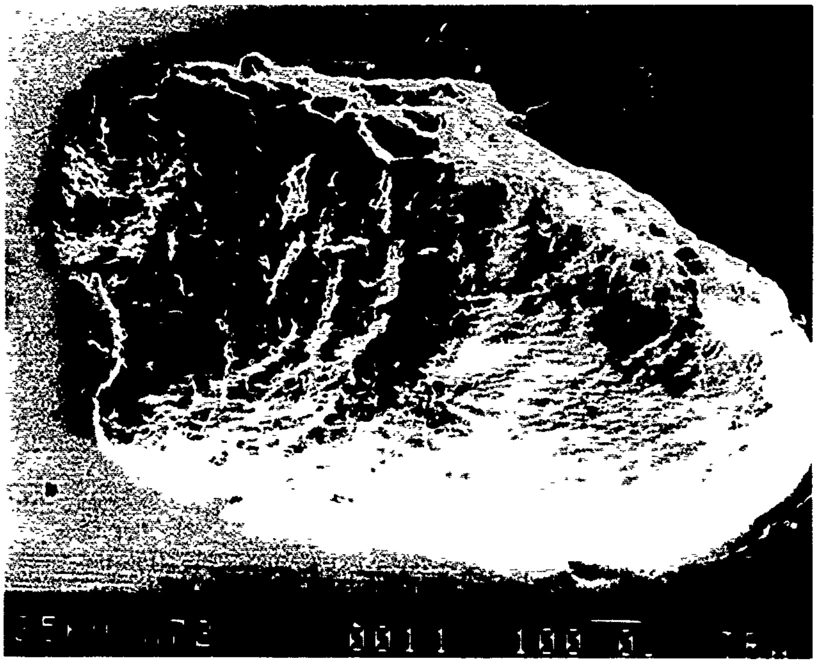

Figure 75. SEM View of Spall in RSR113 Test Bar (HB-2). Magnification: 72×

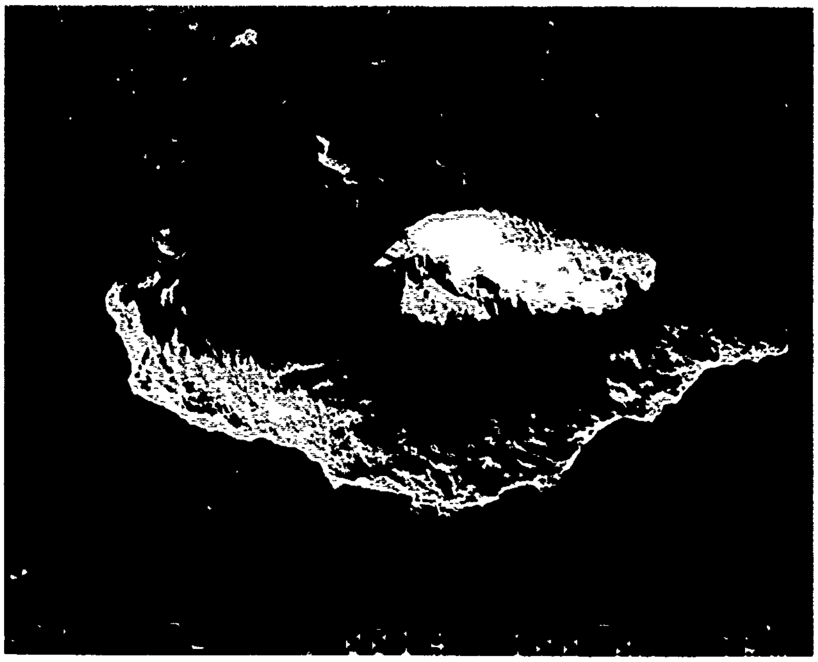

Figure 76. SEM View of Spall in MRC2001 Test Bar (HE-2). Magnification: 72×

4146C

2) Corrosion Resistance Testing

Material specimens approximately 0.500 inch diameter by 0.0500 inch long were cleaned in two successive washings in separate baths of toluene, ethanol, hexane and acetone, in that order. The specimens were allowed to drain between solvent baths. After the final bath the specimens were air dried at 65°C for ten minutes.

Specimens were installed in fixtures, Figure 77, so that they could be tested in pairs. The cylindrical surface of one specimen was pressed against the flat surface of another. Each pair consisted of like materials. Four pairs were installed in each of six fixtures so that 24 pairs of specimens were tested at a time. Typically, there were three pairs of samples of one material tested simultaneously; these three pairs were spread among the six fixtures so that there was no more than one pair of a particular material in a single fixture.

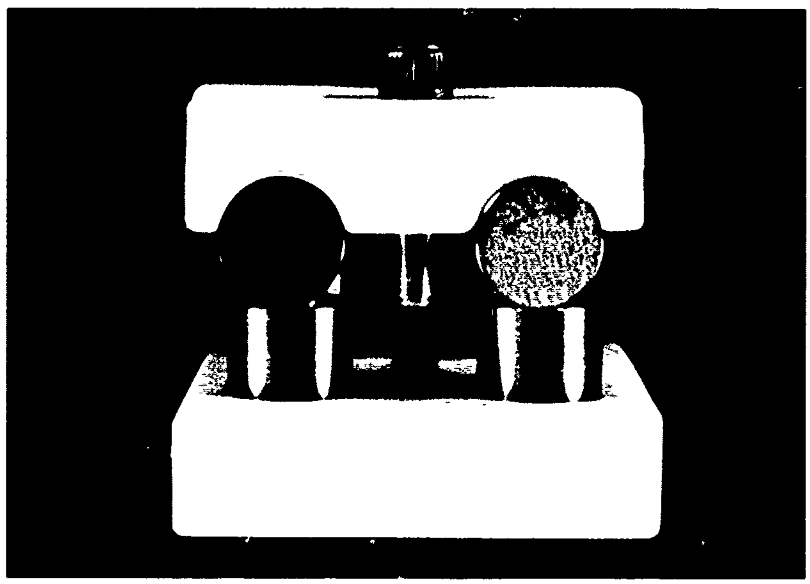

Figure 77. Corrosion Test Fixture With Four Pairs of Specimens

Using ASTM D665, synthetic seawater three parts per million (ppm) by weight of chlorides were added to MIL-L-7808H oil. The water content of the lubricant was then adjusted to 600 ppm by weight total by the addition of distilled water. The fixtured test specimens were immersed in the doped lubricant at room temperature and were allowed to soak for one hour, during which the doped lubricant was agitated periodically. The specimens were then removed from the lubricant and allowed to drain for thirty minutes at ambient temperature.

Corrosion test cells were prepared which consisted of a one-liter glass bottle fitted with a rubber stopper. A 100 ± 1 ml portion of distilled water was added to each cell. The fixtured test specimens were then hung in the test cells Figure 78 using a corrosion resistant suspension. The cells were loosely closed with a rubber stopper and placed in an oven set at 65°C ± 1°C for 8 hours. The cell was then placed in a refrigerator set at 3°C ± 2°C for 16 hours. This procedure was repeated an additional 13 times. After 14 days of thermal cycling, the specimens were prepared for inspection by cleaning with hexane and acetone and a second set of 24 specimen pairs were subjected to the same test.

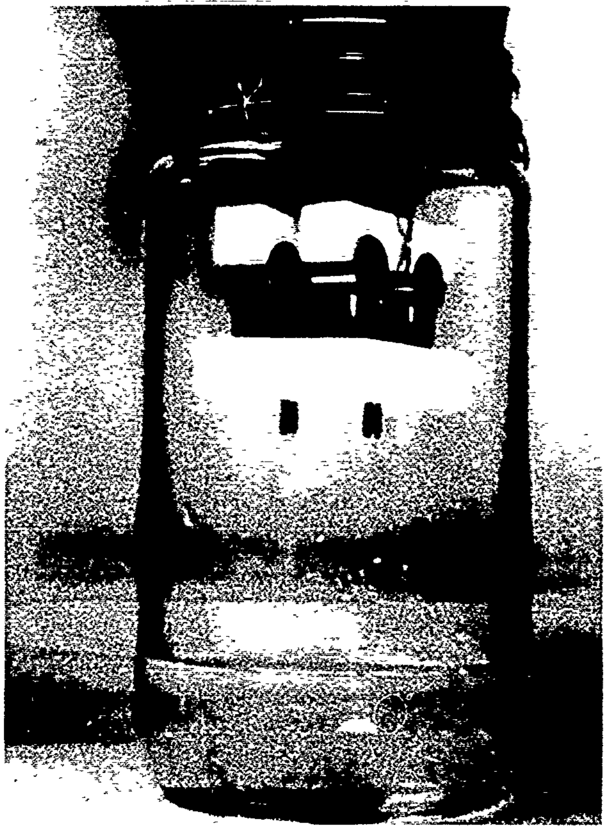

Figure 78. A Corrosion Test Setup

Results may be summarized as follows:

(a) M50 steel reference specimens experienced the most severe corrosion;

(b) All other materials and coatings were significantly better than the reference M50 in resisting corrosion at the contact between specimens;

(c) All coatings appeared to have occasional flaws and corrosion at these flaws was quite marked;

(d) Changes in specimen weight during the course of corrosion testing were small;

(e) Many specimens experienced significant corrosion at the contact between the plastic holder and the specimen. This was particularly the case with vertical members of a pair;

(f) Several vertical specimens experienced corrosion on the upper flat surface, but at a distance from the contact with the horizontal specimen; specimens which were so affected were two M50 reference, one nickel-coated, one chrome-plated, two RSR565, two-hipped 2001, and two-extruded 2001. In each case, the corrosion was miniscule compared to the corrosion in the contact area.

Figures 79 through 81 show corrosion in the contact meniscus area on specimen serial numbers 5 and 6. These were reference M50 steel specimens.

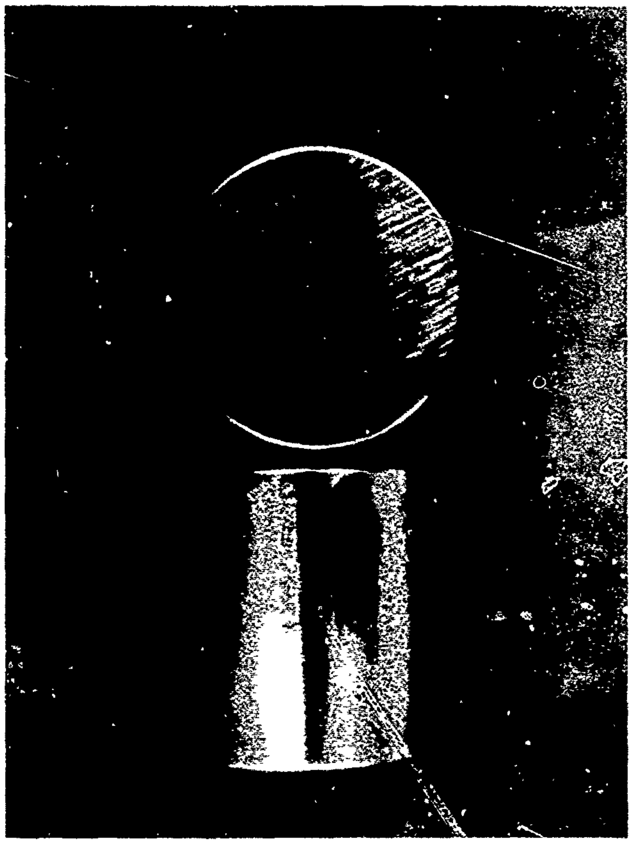

Figure 79. M50 Reference Specimens 5 and 6

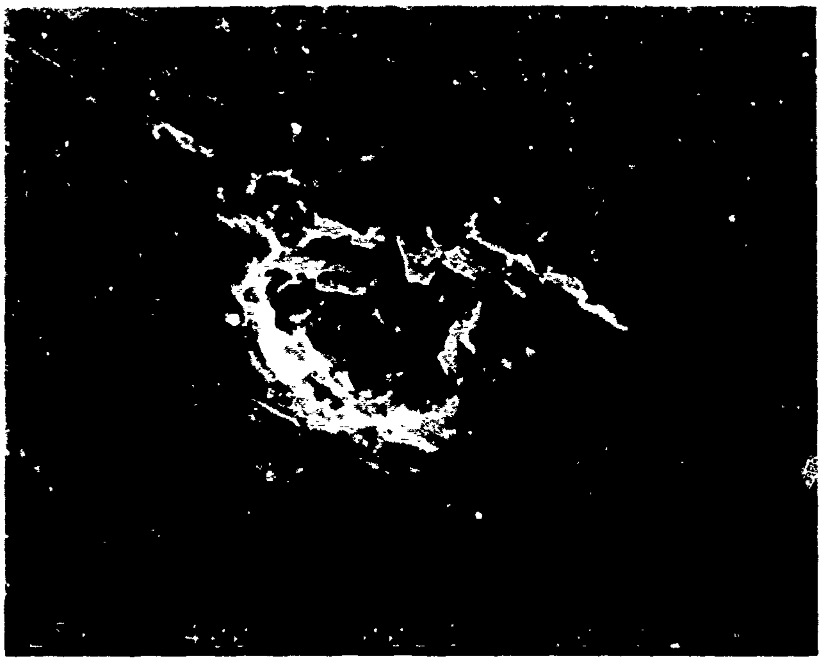

Figure 80. Stained and Pitted End Surface M50. Magnification: 400×

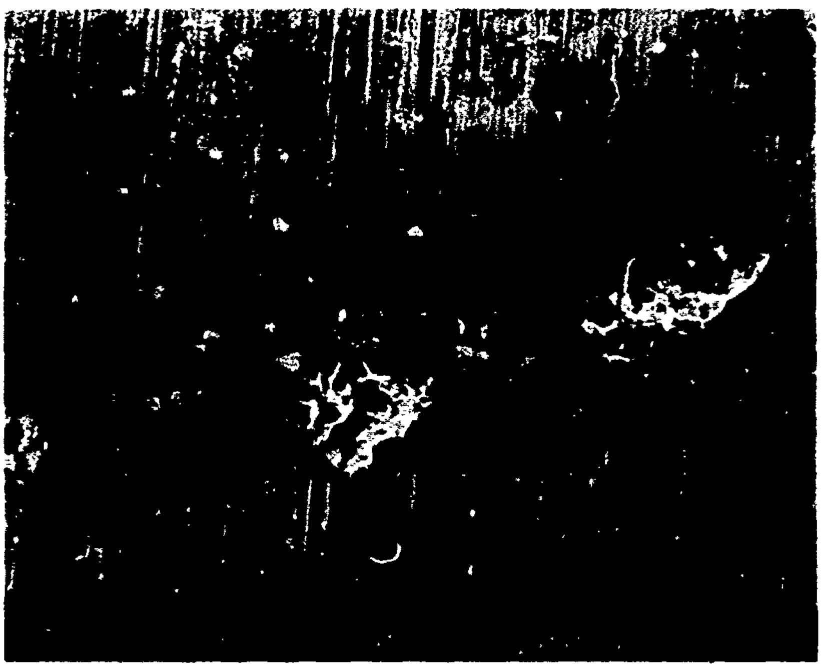

Figure 81. Stained and Pitted OD Surface M50. Magnification: 300×

4147C

Figure 82 shows corrosion in the contact meniscus area on specimen numbers 19 and 20. These specimens were chrome plated by Armoloy Corporation. Arrows point to the corrosion indications. The horizontal specimen has a large mark which is not corrosion, but relates to the plating process. Corrosion data are presented in Tables 15 through 21.

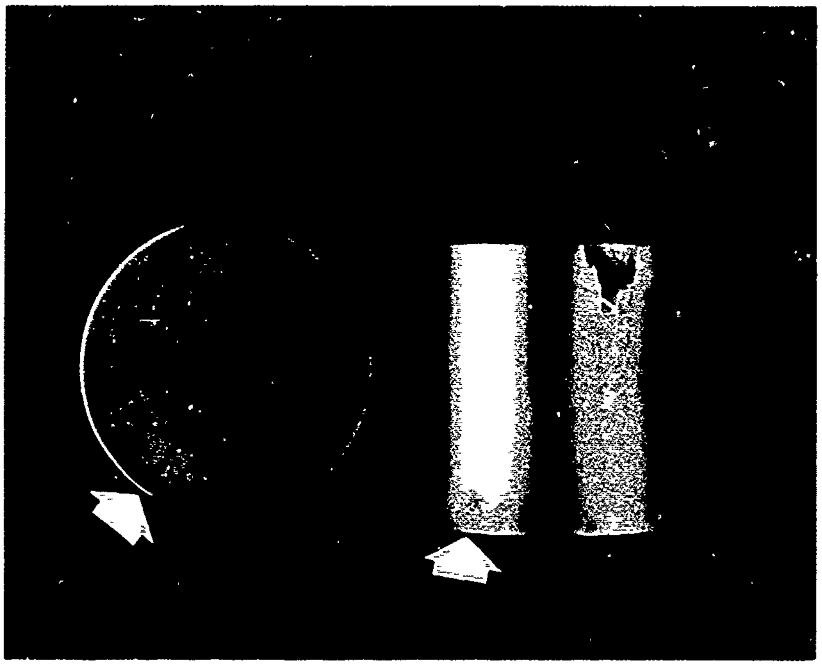

Figure 82. Chrome-Plated Specimens 19 and 20 After Corrosion Test (Arrows Point to Corroded Areas)

TABLE 15. VIM-VAR M50 CORROSION TEST DATA

Serial Number	*Material*	*Orientation*	*Corrosion in Miniscus Area (Square Inch)*	*Weight Change*	*Corrosion in Other Areas*
1	M50	Vertical	0.0100	+0.00016	Severe
2	M50	Horizontal	0.0090	+0.00008	Severe
3	M50	Vertical	0.0135	−0.00003	Severe
4	M50	Horizontal	0.0115	+0.00011	Severe
5	M50	Vertical	0.0225	−0.00003	Severe
6	M50	Horizontal	0.0200	+0.00005	Incidental
51	M50	Vertical	0.000009	−0.00008	Severe
52	M50	Horizontal	0.000007	−0.00003	Severe
53	M50	Vertical	0.000009	+0.00003	Severe
54	M50	Horizontal	0.000007	+0.00010	Severe
55	M50	Vertical	0.000009	−0.00010	Severe
56	M50	Horizontal	None	+0.00022	Incidental
		AVERAGE	0.0072	+0.00004	

4146C

TABLE 16. NICKEL SPUTTER-COATED M50 CORROSION TEST DATA

Serial Number	*Material*	*Orientation*	*Corrosion in Miniscus Area (Square Inch)*	*Weight Change*	*Corrosion in Other Areas*
7	Nickel-Sputtered	Vertical	None	−0.00002	None
8	Nickel-Sputtered	Horizontal	None	0.00000	None
9	Nickel-Sputtered	Vertical	None	+0.00011	Incidental
10	Nickel-Sputtered	Horizontal	None	+0.00004	None
11	Nickel-Sputtered	Vertical	None	+0.00003	None
12	Nickel-Sputtered	Horizontal	None	0.00000	Incidental
57	Nickel-Sputtered	Vertical	None	+0.00012	Slight
58	Nickel-Sputtered	Horizontal	None	+0.00014	None
59	Nickel-Sputtered	Vertical	None	+0.00022	Slight
60	Nickel-Sputtered	Horizontal	None	+0.00026	Slight
61	Nickel-Sputtered	Vertical	None	+0.00028	None
62	Nickel-Sputtered	Horizontal	None	−0.00002	Severe
		AVERAGE	None	+.00010	

TABLE 17. ARMOLOY-COATED M50 CORROSION TEST DATA

Serial Number	*Material*	*Orientation*	*Corrosion in Miniscus Area (Square Inch)*	*Weight Change*	*Corrosion in Other Areas*
19	Chr. Pl.	Vertical	0.0005	+0.00004	Slight
20	Chr. Pl.	Horizontal	0.0015	+0.00010	None
21	Chr. Pl.	Vertical	None	+0.00016	Incidental
22	Chr. Pl.	Horizontal	None	+0.00008	Slight
23	Chr. Pl. Polished	Vertical	None	+0.00002	Slight
24	Chr. Pl. Polished	Horizontal	None	+0.00008	Slight
71	Chr. Pl.	Vertical	None	+0.00036	None
72	Chr. Pl.	Horizontal	None	+0.00035	None
73	Chr. Pl.	Vertical	None	+0.00042	None
74	Chr. Pl.	Horizontal	None	+0.00035	Slight
75	Chr. Pl. Polished	Horizontal	+0.00032	None	
76	Chr. Pl. Polished	Vertical	None	+0.00039	None
		AVERAGE	0.00017	+0.00022	

TABLE 18. CRB7 CORROSION TEST DATA

Serial Number	*Material*	*Orientation*	*Corrosion in Miniscus Area (Square Inch)*	*Weight Change*	*Corrosion in Other Areas*
25	CRB7	Vertical	None	−0.00008	Incidental
26	CRB7	Horizontal	None	+0.00004	None
27	CRB7	Vertical	None	−0.00006	Slight
28	CRB7	Horizontal	None	+0.00002	Slight
29	CRB7	Vertical	None	+0.00004	Slight
30	CRB7	Horizontal	None	−0.00008	None
77	CRB7	Vertical	None	+0.00012	None
78	CRB7	Horizontal	None	+0.00010	Slight
79	CRB7	Vertical	None	+0.00026	None
80	CRB7	Horizontal	None	+0.00026	Slight
81	CRB7	Vertical	None	+0.00036	Slight
82	CRB7	Horizontal	None	+0.00026	None
		AVERAGE	None	+0.00010	

4146C

TABLE 19. RSR565 CORROSION TEST DATA

Serial Number	Material	Orientation	Corrosion in Miniscus Area (Square Inch)	Weight Change	Corrosion in Other Areas
31	RSR565	Vertical	None	−0.00021	Incidental
32	RSR565	Horizontal	None	−0.00006	Severe
33	RSR565	Vertical	None	0.00000	Slight
34	RSR565	Horizontal	None	−0.00006	Incidental
35	RSR565	Vertical	None	0.00000	Slight
36	RSR565	Horizontal	None	0.00000	Incidental
83	RSR565	Vertical	None	+0.00013	Incidental
84	RSR565	Horizontal	None	+0.00005	None
85	RSR565	Vertical	None	+0.00010	None
86	RSR565	Horizontal	None	+0.00010	Slight
		AVERAGE	None	+0.00000	

TABLE 20. MRC2001 CORROSION TEST DATA

Serial Number	Material	Orientation	Corrosion in Miniscus Area (Square Inch)	Weight Change	Corrosion in Other Areas
37	2001-Hipped	Vertical	None	−0.00004	Incidental
38	2001-Hipped	Horizontal	None	−0.00002	None
39	2001-Hipped	Vertical	None	−0.00013	Incidental
40	2001-Hipped	Horizontal	None	−0.00008	Slight
41	2001-Hipped	Vertical	None	−0.00014	Incidental
42	2001-Hipped	Horizontal	None	−0.00022	None
87	2001-Hipped	Vertical	None	+0.00035	Slight
88	2001-Hipped	Horizontal	None	+0.00030	None
89	2001-Hipped	Vertical	None	+0.00034	Incidental
90	2001-Hipped	Horizontal	None	+0.00025	Slight
		AVERAGE	None	+0.00005	
43	2001-Extruded	Vertical	None	−0.00034	Incidental
44	2001-Extruded	Horizontal	None	0.00000	None
45	2001-Extruded	Vertical	None	−0.00027	Severe
46	2001-Extruded	Horizontal	None	−0.00007	Incidental
91	2001-Extruded	Vertical	None	+0.00042	Incidental
92	2001-Extruded	Horizontal	None	+0.00046	Incidental
		AVERAGE	None	+0.00002	

TABLE 21. RSR113 CORROSION TEST DATA

Serial Number	Material	Orientation	Corrosion in Miniscus Area (Square Inch)	Weight Change	Corrosion in Other Areas
47	RSR113	Vertical	None	−0.00042	Slight
48	RSR113	Horizontal	None	−0.00034	None
93	RSR113	Vertical	None	+0.00026	Slight
94	RSR113	Horizontal	None	+0.00026	Slight
95	RSR113	Vertical	None	+0.00024	None
96	RSR113	Horizontal	None	+0.00018	Slight
97	RSR113	Vertical	None	+0.00026	Slight
98	RSR113	Horizontal	None	+0.00036	None
		AVERAGE	None	+0.00007	

3) *Selection of the Three Candidates for Hot Hardness and Wear Testing*

(a) Selection Criteria

At the conclusion of the RCF and corrosion testing, all candidates were ranked according to the following criteria.

(1) Corrosion resistance

(2) Rolling contact fatigue

(3) Hot hardness

(4) Wear resistance

(5) Mechanical properties, i.e., strength, HCF, etc.

(6) Adhesion (coatings only)

(7) Ability for application without affecting substrate properties (coatings and surface treatments only)

(8) Suitability for production incorporation in 3 to 5 years

(9) Cost

(10) Frugal use of strategic elements

(11) Environmental impact.

(b) Candidate Ranking

A point value was assigned to each criteria based on the criteria's relative importance with respect to a state of the art turbine engine bearing application. The candidate ranked best received the maximum point value. The 2nd, 3rd, 4th and 5th ranked candidates received 80%, 60% 40% and 20% respectively. Where rank between candidates could not be established the candidates were awarded the same point value. Failure to demonstrate superiority in corrosion resistance and at least equivalence in rolling contact fatigue life, hot hardness and wear resistance to the M50 baseline was cause to eliminate a candidate from further consideration. Additionally, a coated candidate was eliminated from further consideration if either the coating or coating process was found to be deleterious to the M50 substrate mechanical properties or if a coating failed to adhere during property testing.

(1) Rolling Contact Fatigue — 15 Points Maximum

No significant differences between candidates or between candidates and the M50 baseline. Points were not awarded for this criteria.

(2) Corrosion Resistance — 15 Points Maximum

All candidates were judged superior to M50. MRC2001, RSR565, CRB7 and the nickel sputter-coating had virtually no corrosion and were judged equal. Armoloy-coated M50, while superior to M50, was slightly less corrosion resistant than the other four candidates as follows:

- MRC2001 — 15 points
- RSR565 — 15 points
- CRB7 — 15 points
- Nickel sputter-coated M50 — 15 points
- Armoloy-coated M50 — 12 points.

(3) Hot Hardness — 15 Points Maximum

(4) Wear Resistance — 15 Points Maximum

Points were not awarded pending hot hardness and wear resistance test results

(5) Coating Adhesion — 15 Points Maximum

All alloy candidates were awarded maximum points. The Armoloy-coated candidate did not exhibit any sign of cracking or peeling under rolling contact. The nickel sputter-coated candidate was eliminated from further consideration because it failed to adhere under rolling contact as follows:

- RSR565 — 15 points
- MRC2001 — 15 points
- CRB7 — 15 points
- Armoloy-coated M50 — 15 points
- Nickel sputter-coated M50 — 0 points.

(6) Coating Application Without Affecting Substrate Properties — 15 Points Maximum

All alloy candidates were awarded the maximum points. Both coating processes expose the substrate to conditions which, while not demonstrated in this program, could be deleterious to the substrate material properties, i.e., Armoloy-hydrogen embrittlement; nickel sputtering — elevated substrate temperatures as follows:

- CRB7 — 15 points
- MRC2001 — 15 points
- RSR565 — 15 points
- Armoloy-coated M50 — 12 points
- Nickel sputter-coated M50 — 12 points.

(7) Other Mechanical Properties (High Cycle Fatigue, Strength, Fracture Toughness, etc.) — 10 Points Maximum

Lacking data to the contrary all candidates were judged equivalent to M50 and points were not awarded for this criteria.

(8) Three- to Five- Year Production Incorporation — 10 Points Maximum Candidates Were Ranked in the Following Order:

CRB7 — 10 Points

Wrought CRB7 is an existing commercially available bearing alloy.

Armoloy-coated M50 — 8 Points

Armoloy is an existing commercially available plating process. However before being qualified for production turbine engine bearing applications, the process would require some development to ensure process uniformity.

MRC2001 — 6 Points

MRC2001 is fabricated using a commercially available powder processing technique, however the powder consolidation processes will require development.

RSR565 — 4 Points

Both the powder fabrication and consolidation processes will require development and the powder fabrication capacity would limit early usage.

Nickel Sputter-Coated M50 — 2 Points

The sputter coating process would require considerable development. The processing capacity is very limited and the impact of the process on substrate properties is not defined.

(9) Cost — 10 Points Maximum

Candidates were ranked in the following order:

Armoloy-Coated M50 — 10 Points

The Armoloy-coated candidate was considered the least costly of the candidates. The plating process and associated process controls would result in a modest increase in cost compared to uncoated M50 material.

CRB7 — 8 Points

CRB7 has a higher chrome content and a lower machinability compared to M50.

MRC2001 — 6 Points

The powder fabrication and consolidation processes as well as higher chrome and alloy content would increase costs over the above candidates.

RSR565 — 4 Points

RSR565 contains 4% Cobalt and has a higher chrome content than M50. The RSR powder fabrication process is also somewhat more costly than other powder fabrication techniques.

Nickel Sputter-Coated M50 — 2 Points

The coating process and associated quality control would require added costly manual operations.

(10) Frugal Use of Strategic Elements — 5 Points Maximum

Nickel Sputter-Coated M50 — 5 Points

(4.25Cr, 0.8C, 1.0V, 4.25 Mo, 0.24 Mn, Fe)

Armoloy-Coated M50 — 4 Points

(4.25Cr, 0.8C, 1.0V, 4.25Mo, 0.24Mn, Fe)

CRB7 — 3 Points

(14.0Cr, 1.11C, 1.06V, 2.07Mo, 0.43Mn, 0.29Si, Fe)

MRC2001 — 2 Points

(15.2Cr, 1.51C, 1.81V, 6.74Mo, 0.32Mn, 0.1Si, Fe)

RSR565 — 1 Point

(9Cr, 1C, 1V, 2Mo, 4Co)

(11) Environmental Impact — 5 Points Maximum

The Armoloy-coated M50 candidate was rated fifth because of the attendant treatment and disposal of the chrome plating baths. The first four candidates are rated in order of their anticipated energy consumption as follows:

Nickel Sputter-Coated M50 — 5 Points
CRB7 — 4 points
MRC2001 — 3 points
RSR565 — 2 points
Armoloy-Coated M50 — 1 point.

Based on the above evaluations MRC2001, Armoloy-coated M50 and CRB7 were selected as the three most promising candidates for wear resistance and hot hardness testing. A summary of the ranking criteria results is presented in Table 22.

4) Wear Resistance Testing

Rolling contact bearings are subject to some sliding contacts which promote wear. A ball rolling on a raceway under angular contact, a roller contacting the flanges of the guiding race, balls or rollers pushing against cage pockets, and raceway shoulders contacting cage bores or O.D.'s are all examples of sliding action. Thus, a bearing material must accept sliding with minimum wear.

To evaluate wear resistance of candidate materials, a cross cylinder wear apparatus was used. Figure 83 shows the rig schematically, while Figure 84 is a photograph of the rig. Essentially, a half-inch diameter cylinder was rotated against a fixed half-inch diameter rod, with axes inclined 90 degrees to each other. In representing the sliding effect of a ball on a race, or a roller against raceway flanges, cylinders of the same material were run against each other. In representing the action of bearing steel against cage material, a silver plated AMS6415 bar was rotated against a bar of the candidate material. Because aircraft bearing contacts are lubricated, wear tests were conducted in the presence of MIL-L-7808 oil.

TABLE 22. TASK 3 RANKING SUMMARY

	Task 3		Task 4		Tasks 3 & 4							
	RCF	Corrosion	Hot Hardness	Wear	Mechanical Properties	Adhesion	Appl. W/O Affecting Properties	3-5 Years Production Incorporation	Cost	Strategic Elements	Environmental Impact	Total
Maximum Points	15	15	15	15	10	15	15	10	10	5	5	
CRB7	*	15			*	15	15	10	8	3	4	Task 3 Total - 70
MRC2001	*	15			*	15	15	6	6	2	3	Task 3 Total - 62
RSR 565	*	15			*	15	15	4	4	1	2	Eliminated in Task 3 Candidate Selection Based on Point Rank (Task 3 Total - 56)
Armoloy	*	12			*	15	12	8	10	4	1	Task 3 Total - 62
Sputtered N_1	*	15			*	0	12	2	2	5	5	Eliminated; Coating Failed During Task 3 RCF Tests

*No Significant Difference

FD 270304

4146C

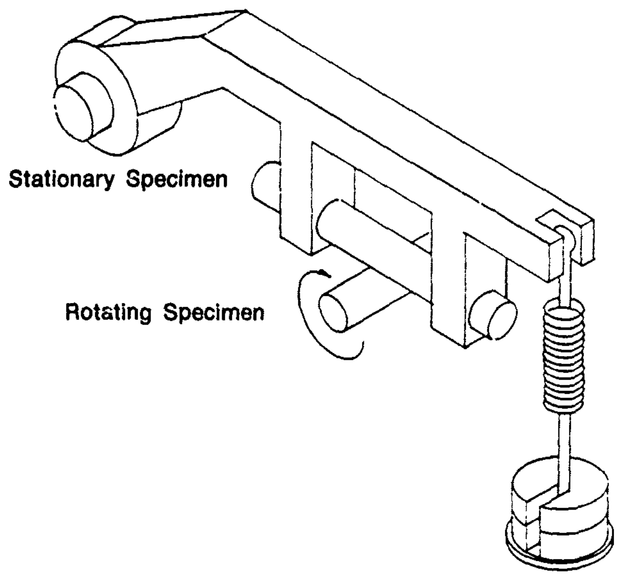

FD 216726

Figure 83. Schematic of Wear Test Apparatus

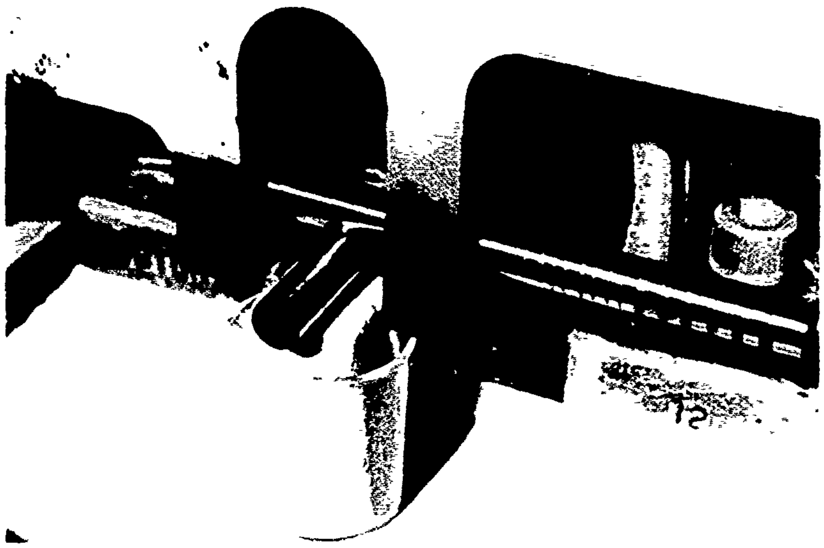

Figure 84. Photograph of Wear Test Rig Showing Wick Lubrication

4146C

Test conditions may be summarized as follows:

- Specimen size — 0.500 + 0.0015 inch diameter × 3 inches long
- Surface finish — 4 to 6 micro inch, except Armoloy-coated M50*
- Rotating speed — 1200 rpm
- Applied load — 25 pounds on load arm
- Lubrication — MIL-L-7808 oil, applied by contacting wick
- Duration — 5 minutes per test.

The effective load on the contact was 53 pounds, due to mechanical advantage of the rig and weight of the load arm. This resulted in a maximum Hertz stress at the start of a test of 340,000 psi. Stress reduced rapidly, but at an indeterminate rate as wear increased the contact area.

The rotating bar produced an elliptical wear scar on the stationary bar. When like materials were run together, this scar became practically round. When silver plated bars were run against test bars, the scars on the test bars were very small and elliptical in shape. Before and after each test, both rotating and stationary bars were weighed, to the nearest 0.0001 gram, to determine change in mass.

An accelerometer was mounted on the load arm, directly above the contact between the two bars. The output of the accelerometer, as charted by a Brush recorder, produced a measure of the stick-slip behavior of the materials (Figures 85 and 86).

Wear test changes in mass are presented in Table 23 and summarized in Table 24. The most significant changes were those of the stationary specimens when like materials were run against each other; the changes in stationary specimen mass are shown graphically in Figure 87.

Based on this weight loss data, materials may be ranked in the following order:

- MRC2001 (best, with least material loss)
- M50 Baseline
- Armoloy-coated M50
- CRB7
- RSR565.

The difference in performance between the M50 reference material and the Armoloy-coated M50 is believed to be the slightly rougher, pebbly surface of the Armoloy coating; the chrome surface of the rotating bar cut through the chrome surface of the stationary bar and then tended to abrade the M50 base material.

Changes in mass of rotating bars were all small, with little difference between materials. When silver plated AMS6415 bars were run against test materials, mass changes in test bars and silver plated bars were very small, but with generally greater changes occurring in the rotating, silver plated bars than in the stationary bars. Silver plate had been applied to the AMS6415 steel 0.0005 to 0.0015 inch thick per AMS2412, corresponding to the normal processing of steel cages. While these data provide little means of contrasting wear resistance in the test materials, they demonstrate that silver plate is an effective boundary lubricant.

*Reference Section II, C.3.1), paragraph 3

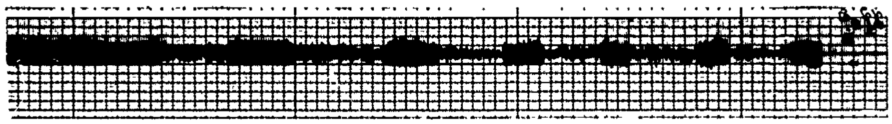

M50 vs M50 Run 5

Armoloy Coated M50 vs Armoloy Coated M50 Run 3

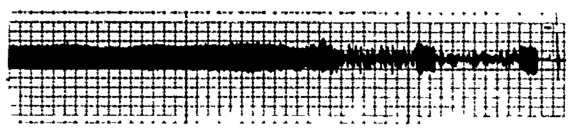

MRC2001 vs MRC2001 Run 4

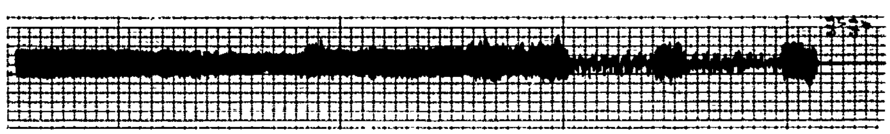

CRB7 vs CRB7 Run 3

RSR565 vs RSR565 Run 2

FD 270308

Figure 85. Sample Traces of Vibration Data From Wear Tests

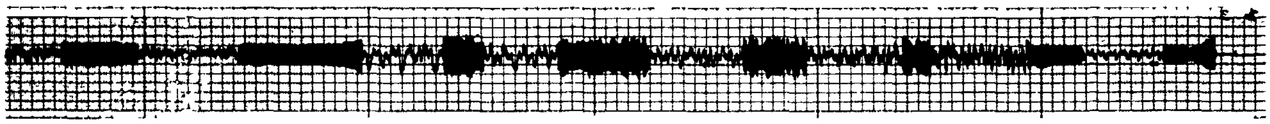

M50 vs Ag-Plated AMS 6415 Run 2

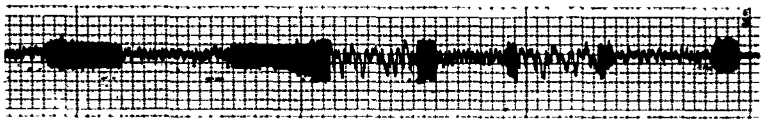

Armoloy Coated M50 vs Ag-Plated AMS 6415 Run 5

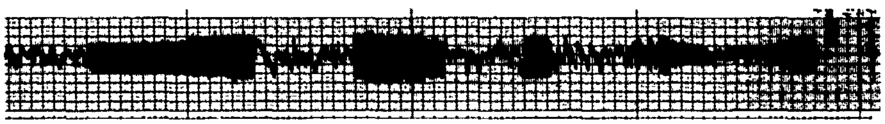

MRC 2001 vs Ag-Plated AMS 6415 Run 2

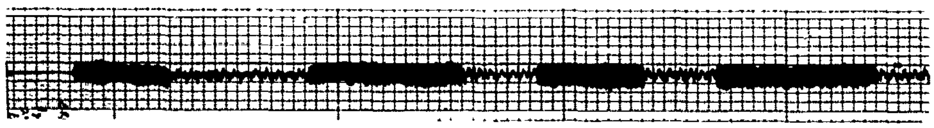

CRB7 vs Ag-Plated AMS 6415 Run 2

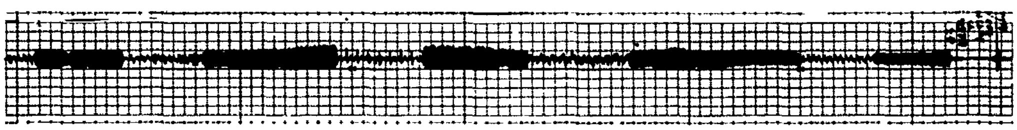

RSR 565 vs Ag-Plated AMS 6415 Run 3

FD 270309

Figure 86. Sample Traces of Vibration Data From Wear Tests

TABLE 23. WEAR TEST DATA

	M50 vs M50		*M50 vs Silver Plated AMS 6415*	
Test No.	*Wt. Loss Stationary*	*Wt. Loss Rotating*	*Wt. Loss Stationary*	*Wt. Loss Rotating*
1	0.0040 gm	0.0020 gm (gain)	0.0007 gm (gain)	0.0029 gm
2	0.0049	0.0008 (gain)	0.0010	0.0026
3	0.0055	0.0003	0.0002	0.0031
4	0.0112	0.0020	0.0001	0.0012
5	0.0087	0.0007	0.0002	0.0045
6	0.0112	0.0006 (gain)	0.0002	0.0024

	Armoloyed M50 vs Armoloyed M50		*Armoloyed M50 vs Silver Plated AMS 6415*	
Test No.	*Wt. Loss Stationary*	*Wt. Loss Rotating*	*Wt. Loss Stationary*	*Wt. Loss Rotating*
1	0.0121 gm	0.0008 gm	0.0003 gm	0.0027 gm
2	0.0193	0.0050	0.0001	0.0037
3	0.0142	0.0002	0.0001	0.0028
4	0.0174	0.0022	0.0009	0.0040
5	0.0135	0.0062	0.0005	0.0034
6	0.0161	0.0046	0.0009 (gain)	0.0026

	CRB7 vs CRB7		*CRB7 vs Silver Plated AMS 6415*	
Test No.	*Wt. Loss Stationary*	*Wt. Loss Rotating*	*Wt. Loss Stationary*	*Wt. Loss Rotating*
1	0.0415 gm	0.0034 gm	0.0002 gm	0.0012 gm
2	0.0317	0.0017 (gain)	0.0001 (gain)	0.0006
3	0.0407	0.0031	0.0005	0.0015
4	0.0314	0.0004 (gain)	0.0003	0.0033
5	0.0400	0.0046	0.0003 (gain)	0.0002
6	0.0508	0.0019 (gain)	0.0011	0.0027

	MRC2001 vs MRC2001		*MRC2001 vs Silver Plated AMS 6415*	
Test No.	*Wt. Loss Stationary*	*Wt. Loss Rotating*	*Wt. Loss Stationary*	*Wt. Loss Rotating*
1	0.0062 gm	0.0028 gm	0.0006 gm	0.0026 gm
2	0.0011 (gain)	0.0008 (gain)	0.0001 (gain)	0.0030
3	0.0038	0.0011 (gain)	0.0002	0.0020
4	0.0040	0.0038 (gain)	0.0011 (gain)	0.0007
5	0.0043	0.0023	0.0023	0.0027
6	0.0001 (gain)	0.0009 (gain)	0.0012	0.0049
7	0.0047	0.0023		
8	0.0034	0.0017		

	RSR565 vs RSR565		*RSR565 vs Silver Plated AMS 6415*	
Test No.	*Wt. Loss Stationary*	*Wt. Loss Rotating*	*Wt. Loss Stationary*	*Wt. Loss Rotating*
1	0.0438 gm	0.0004 gm	0.0003 gm	0.0003 gm (gain)
2	0.0346	0.0008 (gain)	0.0009	0.0037
3	0.0684	0.0046 (gain)	0.0005 (gain)	0.0034
4	0.0535	0.0010 (gain)	0.0015	0.0002
5	0.0532	0.0023 (gain)	0.0002	0.0020
6	0.0527	0.0001 (gain)	0.0013 (gain)	0.0034

4146C

TABLE 24. WEAR TEST RESULTS SUMMARY

Candidate	Weight Loss Stationary Element	Weight Loss Rotating Element
Candidate vs Candidate		
MRC2001	0.0032 Gram Average	(–) 0.0003 Average
M50	0.0076 Gram Average	(+) 0.0001 Average
Armoloy-Coated M50	0.0154 Gram Average	(–) 0.0032 Average
CRB7	0.0394 Gram Average	(–) 0.0012 Average
RSR565	0.0510 Gram Average	(+) 0.0014 Average
Candidate vs Silverplated 4340		
MRC2001	0.0005 Gram Average	0.0026
M50	0.0002 Gram Average	0.0028
Armoloy-Coated M50	0.0002 Gram Average	0.0032
CRB7	0.0003 Gram Average	0.0016
RSR565	0.0002 Gram Average	0.0021

Figures 88 and 89 are photographs of wear test bars, or sections of wear bars, showing representative wear scars on the stationary specimens. It was necessary to use some of the bars for hot hardness tests following completion of wear tests. The Armoloy-coated specimen and the RSR565 specimen in Figure 89 were sectioned from the original bars and heated; thus the wear scars are somewhat darkened. The M50 reference bar, as shown in Figure 89, was sectioned to permit insertion into our Scanning Electron Microscope. These photos demonstrate the difference in size of wear scars on the several materials.

Figures 90 and 91 are photographs of rotating wear test bars, showing difference in width of the tracks. These widths correspond to diameters of the wear scars on the stationary bars with which they were associated.

Figures 92, 93 and 94 are SEM photographs of representative wear scars on the stationary bars of M50, MRC2001 and CRB7, respectively.

Figure 95 is a photograph of representative wear scars on M50, Armoloy-coated M50, CRB7 and RSR565, run against rotating silver plated AMS6415 bars. All scars are very small, as would be indicated by weight loss data on Table 23. Wear scars on MRC2001 from this test were apparently destroyed when the bar was sectioned to make hot hardness test specimens. Discoloration of the RSR565 bar was caused by a hot hardness test.

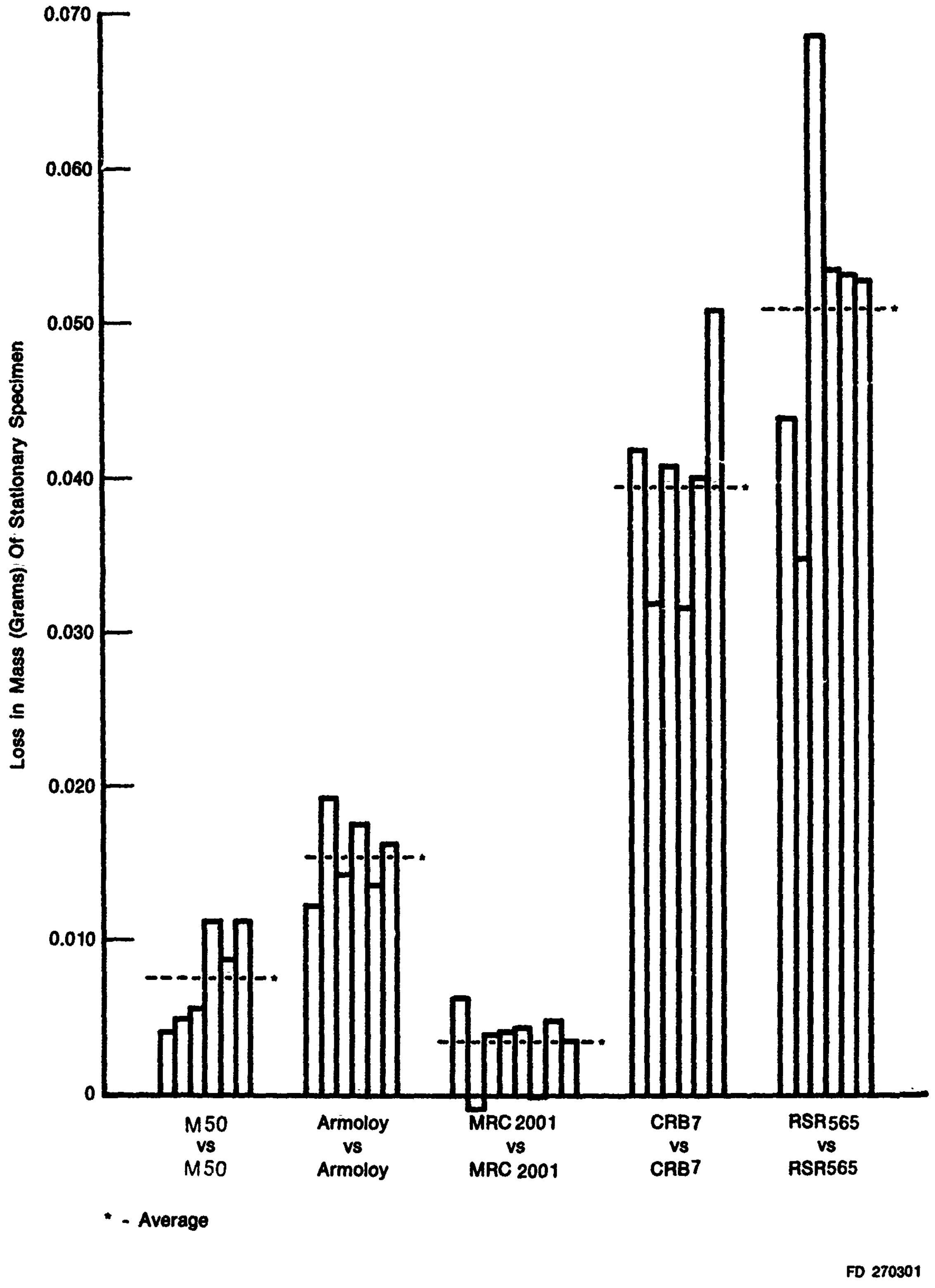

Figure 87. Bar Chart Showing Mass Change of Stationary Specimens Used in Candidate Versus Candidate Wear Tests

4146C

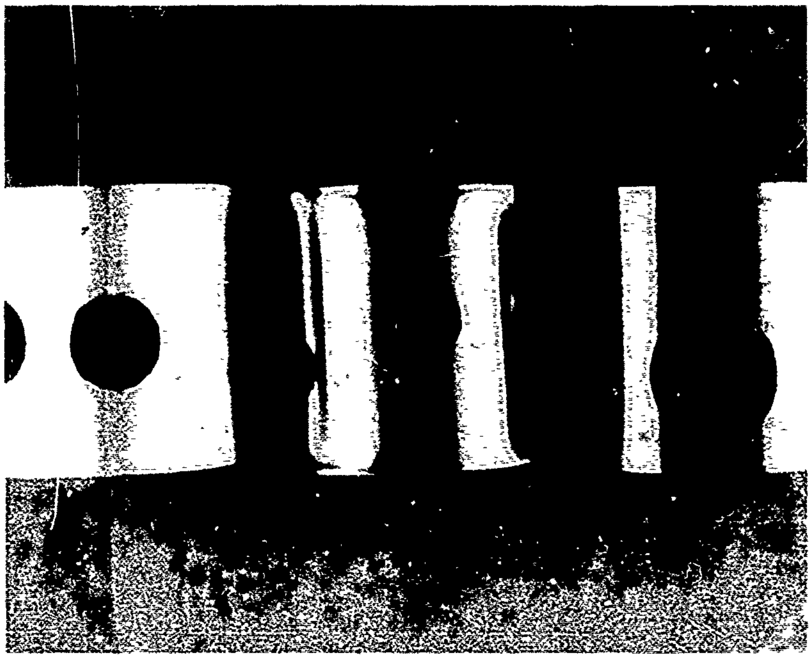

Figure 88. Wear Test Bars Showing Representative Scars on MRC2001, CRB7, and M50 Material (Scale Magnification Approximately 2.5×)

Figure 89. Sections of Wear Test Bars Showing Representative Scars on M50, Armoloy-Coated M50 and RSR565 Material. (Latter Two Bars Were Also Subjected to Hot Hardness Tests)

Figure 90. Rotating Wear Test Bars Showing Representative Tracks on M50 and MRC2001 Specimens (Scale Magnification Approximately 3X)

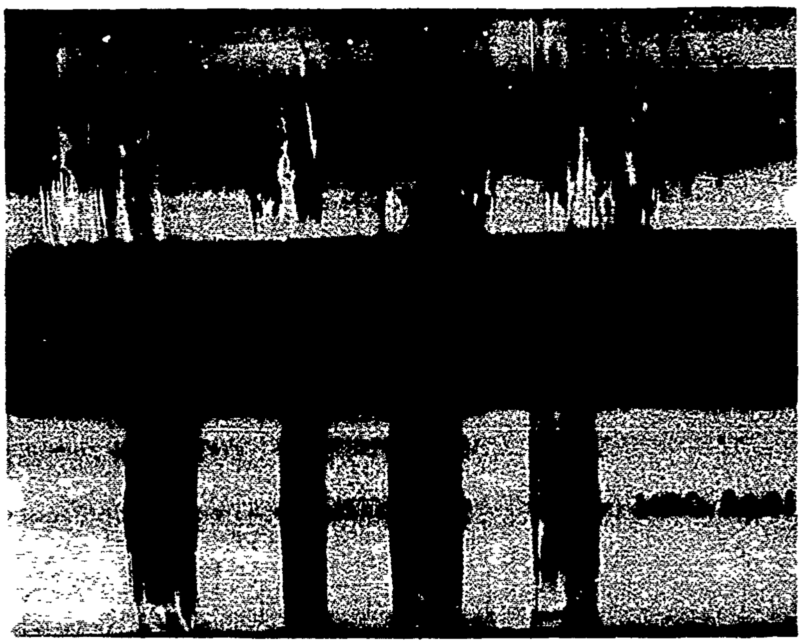

Figure 91. Rotating Wear Test Bars Showing Representative Tracks on MRC2001 and CRB7 Specimens (Scale Magnification Approximately 3X)

4146C

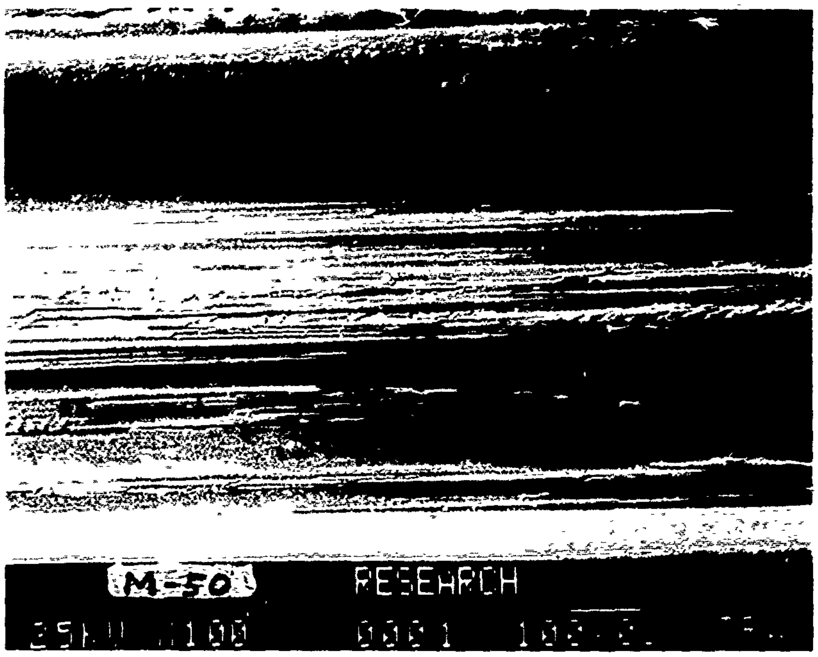

Figure 92. SEM Photograph of the Bottom of a Typical Wear Scar on an M50 Stationary Bar. Magnification: 100×

Figure 93. SEM Photograph of the Bottom of a Typical Wear Scar on an MRC2001 Stationary Bar. Magnification: 100×

Figure 94. SEM Photograph of the Bottom of a Typical Wear Scar on a CRB7 Stationary Bar. Magnification: 100×

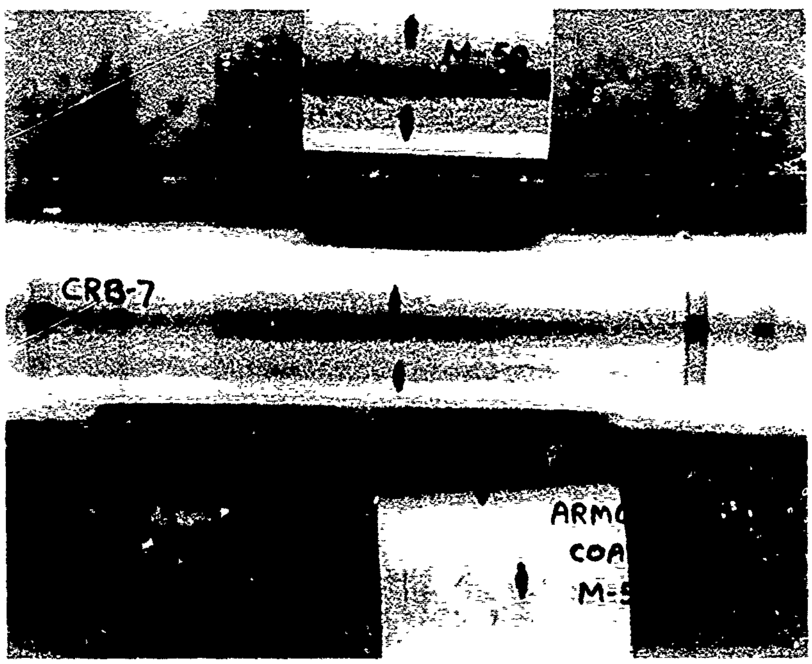

Figure 95. Wear Scars on M50, Armoloy-Coated M50, CRB7 and RSR565 Run Against Silver-Plated Steel. (The RSR565 Specimen Was Discolored Subsequent to the Wear Test)

Figure 96 is a photograph of two representative silver-plated bars used in the wear test. One of these bars was sectioned and the wear track was examined metallographically. Figure 97 shows a section across the wear track; there are still traces of silver in the bottom of the track.

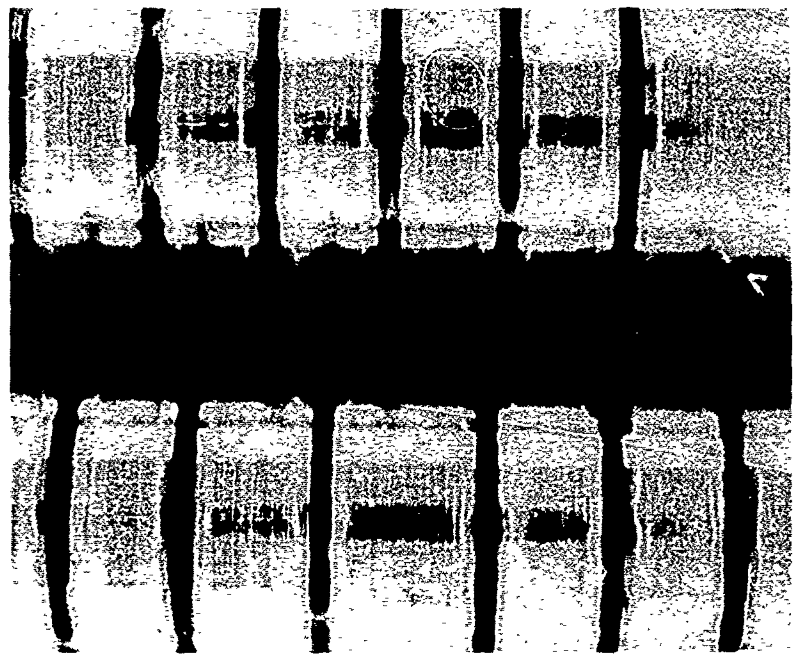

Figure 96. Rotating Wear Test Bars, Silver-Plated AMS 6515 Steel, Showing Representative Wear Tracks. Scale Magnification Approximately 3×

Recordings of vibration data from the early part of one run from each of the ten sets of runs were shown previously on Figures 85 and 86. These recordings, which include some variations in chart speed and recorder attenuation, do not demonstrate the wide divergence which is found in the weight loss data. The fact that contacts were lubricated probably minimizes the effect of stick-slip.

5) Hot Hardness Testing

Hardnesses of the five test materials, VIM-VAR M50, Armoloy-coated VIM-VAR M50, MRC2001, CRB7 and RSR565 were determined at room temperature, 400°F, 500°F, 600°F and 800°F, in a standard Detroit Testing Brinell machine set up for hot hardness testing. Details of the equipment are shown schematically in Figure 98. The furnace is insulated to minimize heat transfer away from the test zone. The controller holds specimen temperature to within 5°F.

Hardness test specimens were 0.5 inch diameter cylinders, 0.5 inch long with ends ground flat and parallel. These specimens were prepared from wear test bars. Care was taken in preparing specimens to prevent overheating or cold working of the surfaces.

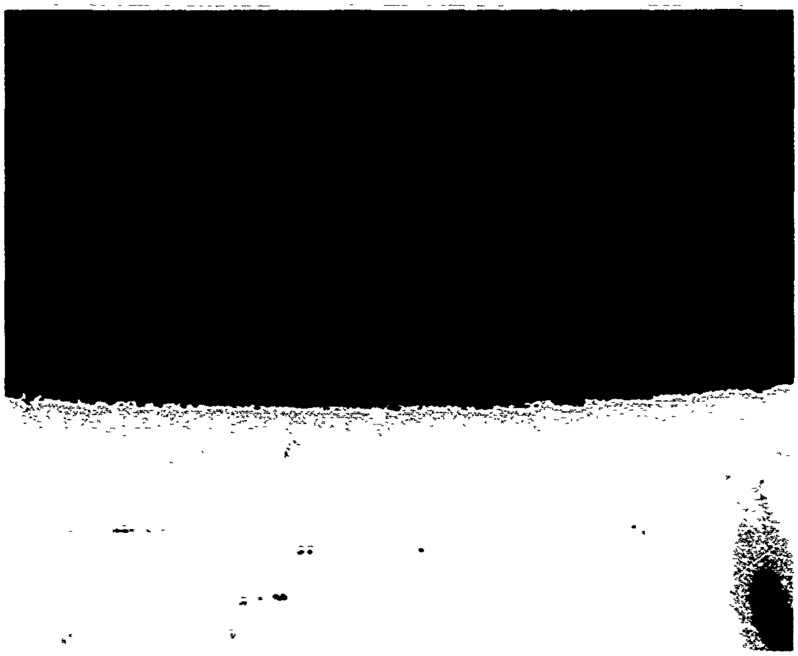

Figure 97. Metallographic Examination of Cross Section of Wear Track on a Silver-Plated Steel Bar. Magnification: 400×

In performing a hot hardness test, a specimen and the 5 mm diameter chromium carbide indenter were installed in the preheated furnace and held at test temperature for 20 minutes. During this stabilization of conditions, the indenter was positioned adjacent to, but not contacting, the upper end of the specimen. Then a 750 kilogram load was applied for precisely 20 seconds, forcing the 5 mm diameter indenter into the end of the test specimen. After removal of load, the specimen was removed from the oven and allowed to air cool.

The impression of the indenter was then measured to the nearest 0.025mm with a standard Brinell Microscope. Two measurements were made, at 90 degrees to each other, and the average taken. Brinell hardness was then calculated by the formula:

$$BHN = \frac{P}{\frac{\pi D}{2}\left(D - \sqrt{D^2 - d^2}\right)}$$

where: P = Load in kilograms
D = Diameter of ball in millimeters
d = Diameter of impression in millimeters.

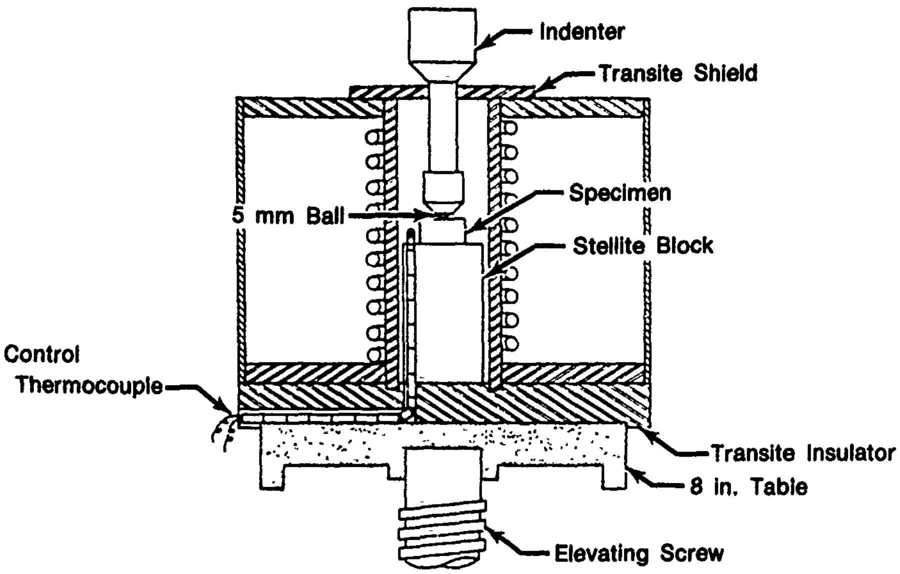

Figure 98. Schematic of Hot Hardness Test Apparatus

Four hot hardness tests were made with each material at each temperature. Results are presented in Table 25 and summarized in Table 26. A normalized plot of average hardness values converted to approximate Rockwell "C" equivalents, is presented in Figure 99. Figure 100 is a photograph of two representative test specimens, showing indentations.

Bearing hardnesses are usually presented as readings on the Rockwell "C" scale. A Rockwell Hardness Tester is not able to function at high temperature, so it is necessary to convert Brinell hardness readings to Rockwell "C" values by approximate methods. In presenting Rockwell "C" values in Table 25 and Figure 99 we have used the table, "Approximate Equivalent Hardness Numbers for Brinell Hardness Numbers for Steel", from ASM's Metals Handbook, Volume 1. The room temperature hardness values obtained in this test are slightly, but consistently, lower than hardnesses reported earlier using a Rockwell Hardness Tester.

Performance of all materials in the hot hardness test was quite comparable, with much of the small scatter probably due to resolution of the indentation measurement. We should expect M50 and Armoloy-coated M50 to produce identical readings, for instance, but we see variations of up to 1.0 on the Rockwell "C" scale. Both MRC2001 and RSR565 have as high or higher hardness values than M50 over the entire temperature range. CRB7 exhibited lower hardness values than M50 at some temperatures, but these differences are small, particularly after the data is normalized to account for initial room temperature hardness.

4146C

TABLE 25. HOT HARDNESS TEST DATA

(Hardness values in BHN, with averages converted to approximate Rockwell "C" equivalents. Indentation diameters in millimeters.)

	Room Temperature		*400°F*		*500°F*		*600°F*		*800°F*	
	Dia.	*BHN*	*Dia.*	*BHN*	*Dia.*	*BHN*	*Dia.*	*BHN*	*Dia.*	*BHN*
M50	1.20	653	1.20	653	1.25	601	1.25	601	1.30	555
(Reference)	1.20	653	1.20	653	1.225	626	1.225	626	1.30	555
	1.15	712	1.20	653	1.20	653	1.20	653	1.275	578
	1.20	653	1.20	653	1.225	626	1.25	601	1.30	555
		668		653		627		620		561
		(60.9) Rc)		(60.0 Rc)		(58.7 Rc)		58.3 Rc)		55.1 Rc)
Armoloy	1.20	653	1.20	653	1.20	653	1.25	601	1.275	578
Coated	1.20	653	1.20	653	1.225	626	1.25	601	1.30	555
M50	1.20	653	1.20	653	1.20	653	1.20	653	1.30	555
	1.20	653	1.20	653	1.20	653	1.25	601	1.30	555
		653		653		646		614		561
		(60.0 Rc)		(60.0 Rc)		(59.7 Rc)		(58.0 Rc)		(55.1 Rc)
MRC2001	1.175	682	1.20	653	1.20	653	1.225	626	1.275	578
	1.15	712	1.20	653	1.20	653	1.225	626	1.275	578
	1.20	653	1.20	653	1.20	653	1.20	653	1.275	578
	1.15	712	1.20	653	1.20	653	1.225	626	1.275	578
		690		653		653		633		578
		(62.1 Rc)		(60.0 Rc)		(60.0 Rc)		59.0 Rc)		(56.0 Rc)
CRB7	1.20	653	1.225	626	1.225	626	1.25	601	1.25	601
	1.20	653	1.225	626	1.225	626	1.275	578	1.25	601
	1.20	653	1.20	653	1.20	653	1.25	601	1.25	601
	1.20	653	1.20	653	1.25	601	1.25	601	1.275	578
		653		640		627		595		595
		(60.0 Rc)		(59.3 Rc)		(58.7 Rc)		(57.0 Rc)		(57.0 Rc)
RSR565	1.20	653	1.20	653	1.20	653	1.225	626	1.275	578
	1.15	712	1.20	653	1.225	626	1.225	626	1.300	555
	1.175	682	1.20	653	1.20	653	1.225	626	1.275	578
	1.20	653	1.20	653	1.20	653	1.225	626	1.275	578
Average		675		653		646		626		572
		(61.3 Rc)		(60.0 Rc)		(59.7 Rc)		(58.6 Rc)		(55.7 Rc)

TABLE 26. SUMMARY OF HOT HARDNESS TEST RESULTS

Brinell Hardness (Brinell 650 $\approx$ Rc 60)

Candidate	*RM Temp.*	*400°F*	*500°F*	*600°F*	*800°F*
M50 (Ref)	668	653	627	620	561
Armoloy-Coated M50	653	653	646	614	561
MRC2001	690	653	653	633	578
CRB7	653	640	627	595	595
RSR565	675	653	646	626	572

4146C

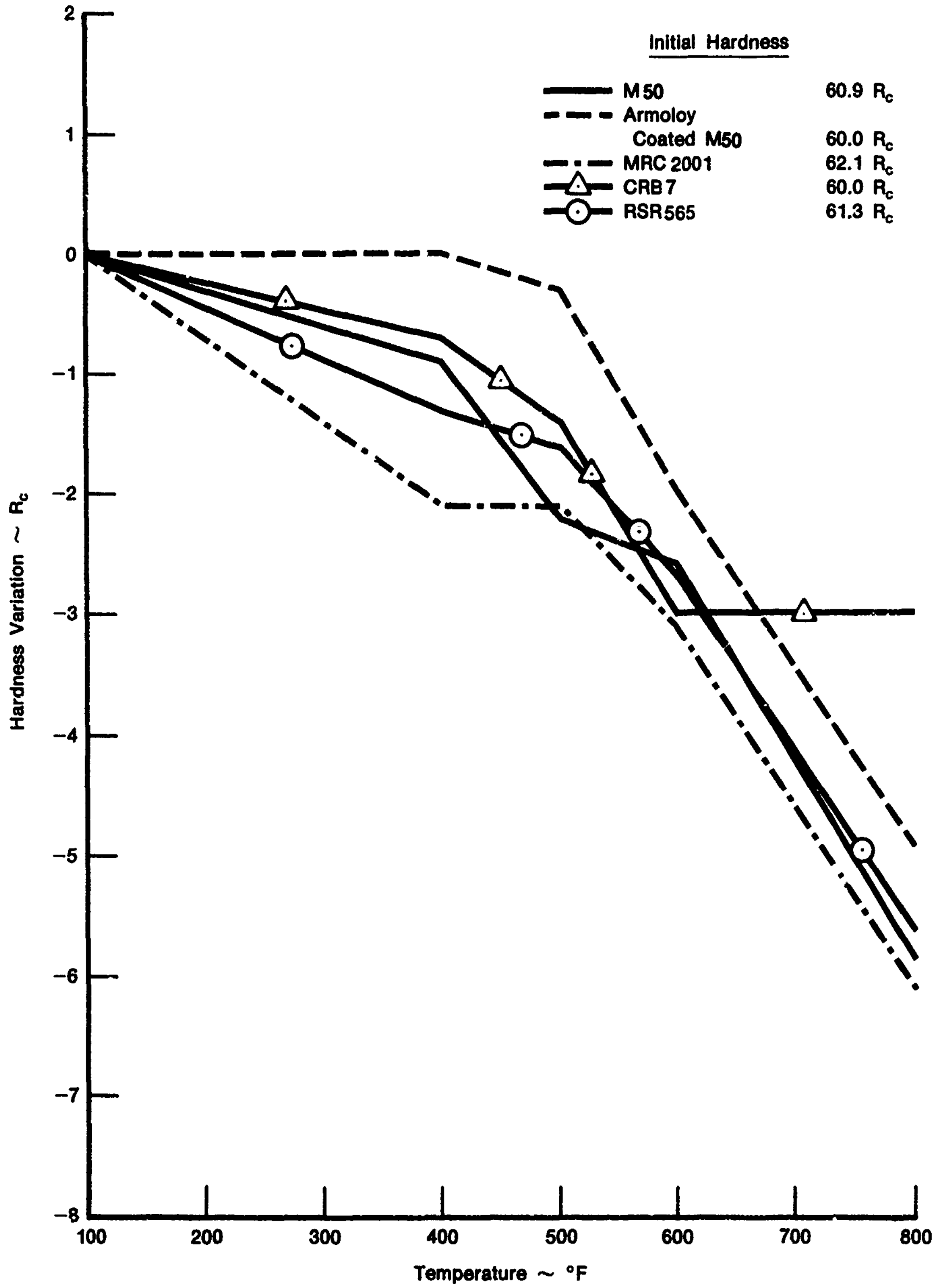

FD 270300

Figure 99. Plot of Normalized Hardness Versus Temperature for Candidates and VIM-VAR M50 Baseline Material

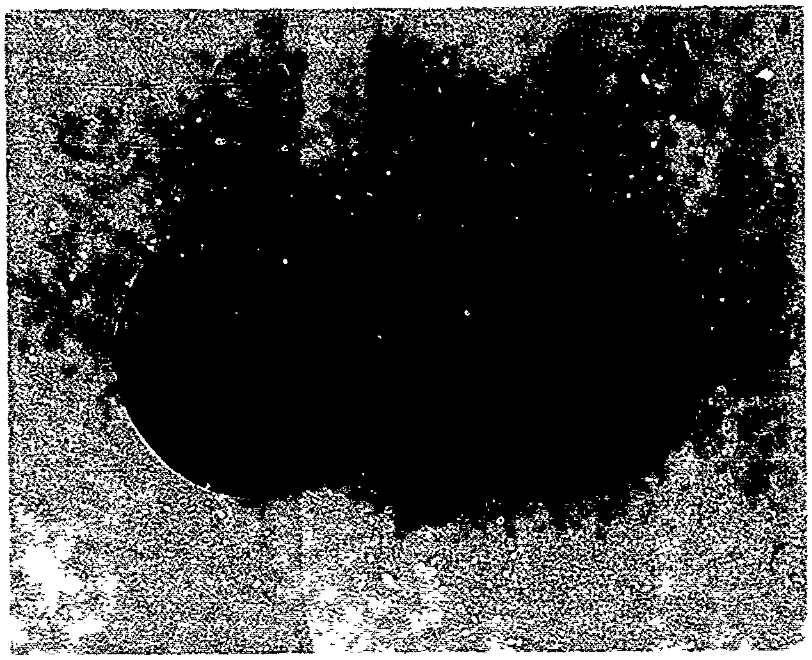

Figure 100. Typical Indentations on Hot Hardness Test Specimens

6) Selection of the single best candidate for Phase II evaluation.

In order to be considered for Phase II evaluation a candidate, as a minimum, had to demonstrate equivalence to M50 in hot hardness and wear resistance.

(a) Hot Hardness — 15 points maximum.

CRB7 demonstrated superior hot hardness compared to M50. All other candidates were judged equal to M50.

(b) Wear Resistance — 15 points maximum.

The only candidate to demonstrate wear resistance equal to or better than the M50 baseline was MRC2001.

Table 27 summarizes candidate ranking at the conclusion of Phase I property testing.

Based on the above results, the USAF program office was requested to and did approve MRC2001 as the single best candidate to be carried into Phase II full-scale bearing development and testing.

4146C

TABLE 27. TASK 4 RANKING SUMMARY

	Task 3		Task 4		Tasks 3 & 4							
	RCF	Corrosion	Hot Hardness	Wear	Mechanical Properties	Adhesion	Appl. W/O Affecting Properties	3-5 Years Production Incorporation	Cost	Strategic Elements	Environmental Impact	Total
Maximum Points	15	15	15	15	10	15	15	10	10	5	5	
CRB7	*	15	*	0	*	15	15	10	8	3	4	Eliminated; Failed Task 4 Wear Resistance Criteria. Task 3 Total - 70
MRC2001	*	15	*	15	*	15	15	6	6	2	3	77 (Task 3 Total - 62)
RSR 565	*	15	** (*)	** (0)	*	15	15	4	4	1	2	Eliminated in Task 3 Candidate Selection Based on Point Rank (Task 3 Total - 56)
Armoloy	*	12	*	0	*	15	12	8	10	4	1	Eliminated Failed Task 4 Wear Resistance Criteria (Task 3 Total - 62)
Sputtered N_1	*	15			*	0	12	2	2	5	5	Eliminated; Coating Failed During Task 3 RCF Tests

*No Significant Difference
**Tested (But Not Officially Ranked) for Task 4 Wear and Hot Hardness as Part of P&WA's Planned and On-going Bearing Material Improvement Programs

FD 270303

SECTION III

FUTURE WORK

In Phase II, full scale bearing life, performance and corrosion resistance demonstrations will be performed to substantiate the MRC2001 candidate selection.

A. ENDURANCE TESTS

Twenty each MRC2001 and M50 baseline MRC2075 ball bearings will be fabricated and endurance tested. The MRC2075 bearing design has a 35 mm bore and a 72 mm outside diameter. The bearings will conform to ABEC Grade 5 standards and will be assembled with a molded Nylon snap-in cage.

The twenty bearing MRC2001 lot and twenty bearing VIM-VAR M50 Lot will be concurrently tested to provide a direct life comparison.

Bearings will be tested for fatigue endurance in Model A machines, as shown schematically in Figure 101. Test conditions will be:

- Speed — 5500 rpm
- Load — 1975 lb Radial
- Lubrication — MIL-L-7808
- Temperature — No heat added

Each lot of bearings will be tested until at least ten inner rings have failed and unfailed bearings have run at least as long as the 10th failure. Loading has been selected to provide approximately 450,000 psi maximum Hertz stress at the inner race contact. Fatigue endurance life at the L_{10} level, as calculated by the AFBMA method without multiplying factors, is 39 hr. We estimate that testing can be suspended at approximately 2000 hr, representing an estimate of L_{50}.

Temperatures of outer rings, oil-in, and scavenge oil will be measured by chromel-alumel thermocouples and recorded on a multiple point recorder. A chip detector is incorporated in each test head and automatically stops testing when there is a spall.

B. PERFORMANCE TEST

One performance bearing will be fabricated from MRC2001. The bearing selected for the performance demonstration test is the TF30 No. 4 ball bearing; it is also used to support the high rotor of an advanced demonstrator engine. This bearing is a 110 mm bore by 175 mm outside diameter split inner ring angular contact ball bearing.

The MRC2001 performance bearing will be tested for 100 hr, or failure, at 16,000 rpm (1.76×10^6 DN) with load varying from 2500 lb to 5000 lb. The rig to be used for the performance test is shown schematically in Figure 102.

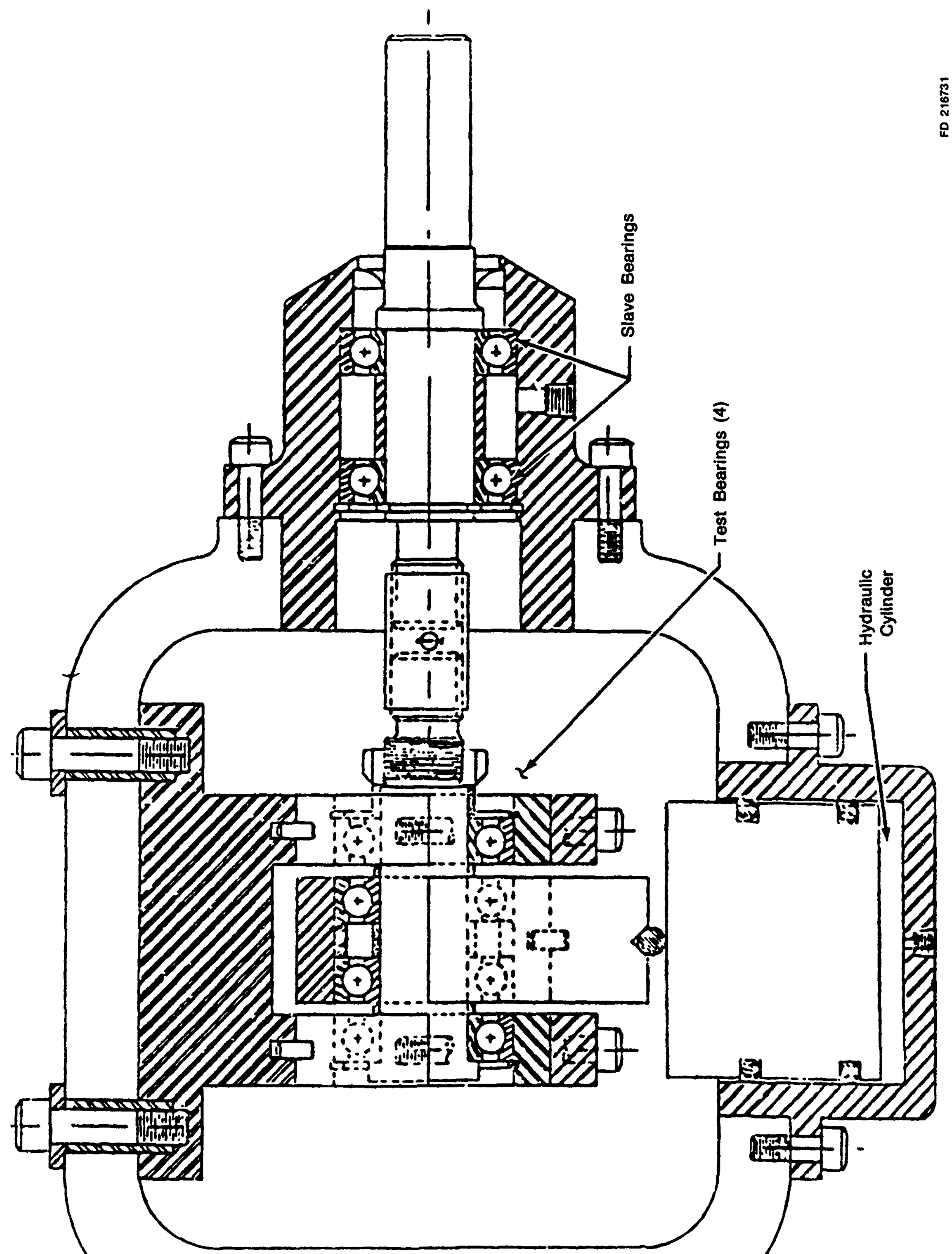

Figure 101. Schematic of TRW's Model A Test Rig

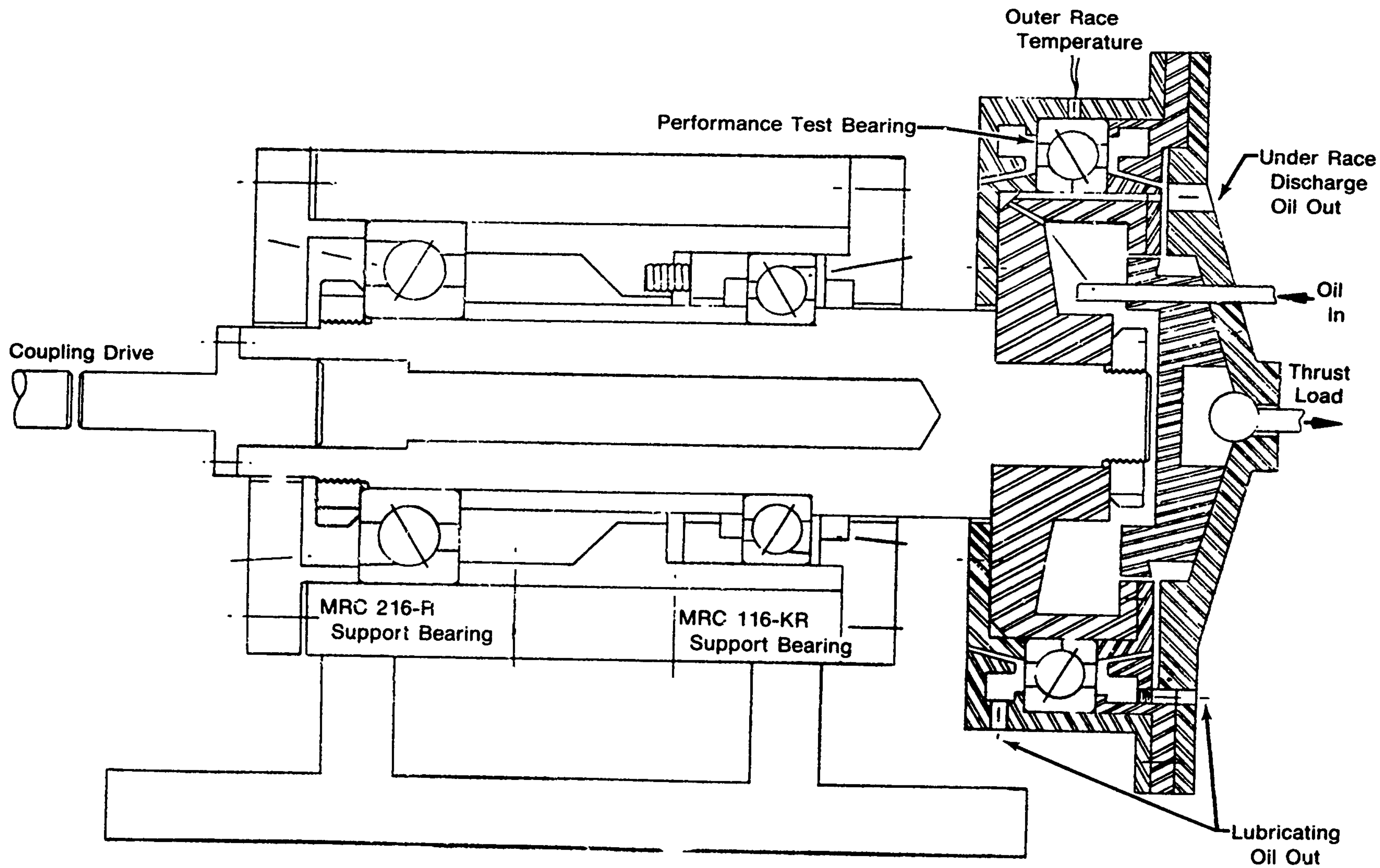

Figure 102. Schematic of Test Rig for Performance Testing Aircraft Turbine Engine Thrust Bearings

The test bearing shall be subjected to a performance test under the following conditions:

Speed	— 16,000 rpm
Load	— Variable, 2500 to 5000 lb Axial
Lubricant	— MIL-L-7808G
Lubricant Quantity	— 1.25 ± 0.12 gal per min delivered under the inner race
Lubricant Temperature	— 240 to 260°F oil-in
Duration	— Failure or 100 hr, whichever comes first.

Test monitoring will include outer race temperature, oil-in temperature, oil out temperature, rig vibration and scavenge oil chip detectors.

Post-test evaluation will include photographic documentation of overall appearance and condition. Scanning electron and optical microscopy will be used as required for specific areas. Post-test measurement of guide land clearance, internal diametral clearance and contact angle, ball and race finish and ball diameter will be made for comparison with pretest measurements to identify wear if any occurs.

C. CORROSION RESISTANCE VERIFICATION TESTS

Twenty spalled endurance test bearings, 10 MRC2001 bearings and 10 M50 bearings, will be corrosion tested with five different, Government supplied, test oils. There will be two tests per test oil. Use of an endurance bearing design with a snap-in cage facilitates this type of test program by allowing repeated assembly and disassembly for inspection at various stages of test. Thus, the raceways and balls can be readily inspected and documented after endurance testing and prior to the final corrosion test and again after the corrosion test.

The full-scale corrosion resistance verification tests will follow the same procedure used in the candidate screening tests.

The back-to-back MRC2001 and M50 corrosion test results will be quantified and documented photographically.

SECTION IV

SUMMARY OF PRINCIPAL PHASE I RESULTS

A. CORROSION MECHANISM INVESTIGATION

Analyses of bearing materials subjected to corrosive attack both by service and storage environments indicate that once corrosion of the steel is initiated, it proceeds by a common mechanism, i.e., autocatalytic pitting corrosion, in both environments. Bearing operation can mechanically remove the corrosion products, thus changing the visual appearance. Superficially, therefore, there appears to be different mechanisms for storage and service bearing corrosion. Corrosive attack of new steel bearing surfaces during storage probably initiates at or is more rapid along grain boundaries due to stress concentrations at these interfaces. The corrosive attack then progresses to autocatalytic pitting corrosion, characterized by *mudcracking* morphology and typically exhibiting higher X-ray emission spectroscopy (XES) intensities for the alloying elements. By contrast, corrosive attack of steel surfaces of bearings exposed to a service environment is probably initiated directly by autocatalytic pitting corrosion at sites of physical damage. These areas usually appear rough and pitted especially in locations of bearing functioning, and are characterized by more normal XES spectra.

Silver-plated bearing components seem more susceptible to initial attack by reactive species present in storage and service environments, particularly sulfur. The possibility of accelerated attack due to galvanic potential between silver-plated materials and bearing steels has also been shown.

The presence of reactive species in sufficient concentration to cause corrosion of bearing components has been confirmed in preservatives and is suspected in engine oils.

B. INITIAL CANDIDATE SCREENING

Using literature searches, material supplier contacts and available experience, 17 candidates were identified which had potential application to aircraft bearings. These candidates were ranked using all available data and perceived material properties. The five most promising candidates were:

1. Armoloy-coated VIM-VAR M50
2. CRB7 in wrought form
3. MRC2001 conventional powder process material
4. RSR565 rapid solidification powder process material
5. Nickel sputter-coated VIM-VAR M50.

C. INITIAL TESTING

The five selected candidates were evaluated in rolling contact fatigue and corrosion resistance. Rolling contact fatigue results indicated no significant difference existed between the selected candidates and VIM-VAR (vacuum induction melt, vacuum arc remelt) M50. Post RCF inspection indicates that the nickel sputter-coated VIM-VAR M50 candidate coating failed to adhere during RCF testing.

Compared to the VIM-VAR M50 baseline, all candidates showed superior corrosion resistance with CRB7, MRC2001, RSR565 and sputter nickel-coated VIM-VAR M50 having virtually no corrosion. Based on criteria established in Task 2 and RCF and corrosion test results, three candidates were selected for further evaluation. These were:

1. Armoloy-coated VIM-VAR M50
2. CRB7
3. MRC2001.

D. MECHANICAL PROPERTY EVALUATION

The three selected candidates were tested for wear resistance and hot hardness. All were considered equivalent to VIM-VAR M50 in hot hardness. Only MRC2001 was considered equal to or better than VIM-VAR M50 in wear resistance.

E. SELECTION OF ONE CANDIDATE

Using established criteria, MRC2001 was evaluated as the single most promising candidate to be carried into Phase II, full-scale bearing development and testing.

REFERENCES

1. Cunningham, Jr., J. S. and M. A. Morgan, "Review of Aircraft Bearing Rejection Criteria and Causes," *Lubrication Engineering,* Vol. 35, 8, pp 435-441, Aug. 1979

2. P&WA Internal Correspondence, Memo, H. L. Hess to L. M. Mazer, "Bearing Design System" 21 April 1980

3. Warner, P. A., G. C. Brown, R. J. Meehan, and W. J. Purvis, "Corrosion Inhibiting Engine Oils" AFWAL TR-81-4028

4. Brown, C. and F. Feinberg, "Development of Corrosion Inhibited Lubricants for Gas Turbine Engines and Helicopter Transmissions," ASLE 80-AM-6C-3

5. Valori, R., G. K. Hubler, and D. Popgoshev, "Ion Implanting Bearing Surfaces for Corrosion Resistance," ASME Paper 82-LUB-23

6. Parker, R. J. and R. S. Hodder, "Rolling Element Fatigue Life of AMS 5749 Corrosion Resistant High Temperature Bearing Steel," ASME paper 77-Lub-3

7. Brown, P. F. and J. R. Potts, "Evaluation of Powder Processed Turbine Engine Ball Bearings," AFAPL-TR-77-26

8. Philip, T. V. "A New Bearing Steel; A New Hot Work Die Steel," *Metal Progress,* Feb. 1980

9. Johnson, B. L., "A Stainless High Speed Steel for Aerospace Applications," *Metal Progress,* Sept 1964

10. Nimos, N. J., D. E. Hahn, and R. E. Maurer, "Research Report on Functional Testing of Armoloy, Nobilizing and Electroless Nickel Coating in Rolling Contact," SKF Industries, Inc., Report AL76M001

11. Wensel, R. G., "Testing of Unlubricated Water Immersed Carbon-Steel Ball Bearings," Atomic Energy of Canada Limited, AECL-5824

12. Parker, T. D. "14%Cr-4%Mo the Stainless Bearing and Tool Steel," Climax Molybdenum Co., 1962

13. Johnson, L. G. "The Statistical Treatment of Fatigue Experiments," Elsivier Publishing Co., 1964